ORNL/SUB--88-07685/03

DE93 004064

EVALUATION OF HAZ LIQUATION CRACKING SUSCEPTIBILITY AND HAZ SOFTENING BEHAVIOR IN MODIFIED 800H

Research sponsored by the U.S. Department of Energy,
Fossil Energy
Advanced Research and Technology Development Materials Program

Report prepared by
C.D. Lundin and C.Y.P. Qiao

Materials Joining Research Group
Materials Science and Engineering Department
The University of Tennessee, Knoxville, TN 37996-2200
under
ORNL/Sub/88-07685C, WBS Element UTN-2, REL U24

for

OAK RIDGE NATIONAL LABORATORY
Oak Ridge, Tennessee 37831
managed by
MARTIN MARIETTA ENERGY SYSTEMS, INC.
for the
U.S. DEPARTMENT OF ENERGY
under Contract No. 41B-07685C

PREFACE

A modified 800H alloy, developed at Oak Ridge National Laboratory (ORNL), is one of the candidate materials designed for high temperature applications. Extensive mechanical and corrosion investigations have been completed and it has been proven that modified 800 has excellent high temperature mechanical and metallurgical behavior. Weldability studies of modified 800H are being carried out at the University of Tennessee, Knoxville. A series of modified 800H alloys and two similar commercial high temperature materials (310Ta and HR3C) were used to conduct this investigation. A preliminary weldability evaluation has been accomplished and the major part of the results (HAZ liquation cracking resistance and HAZ softening behavior in modified 800H) is addressed in this report. The basic conclusion of this investigation is that modified 800H material possesses good resistance to HAZ liquation cracking especially with a grain size control (thermo-mechanical treatment). The information from this study is important to the further modification of the material in order to extended its applications.

I. LITERATURE REVIEW

HAZ liquation and Liquation Cracking Mechanisms

Most base metal HAZ hot cracking theories are derived from fusion zone solidification cracking theories in which solid-liquid reactions are involved. For austenitic

Research sponsored by the U.S. Department of Energy, Fossil Energy AR&TD Materials Program, DOE/FE AA 15 10 10 0, Work Breakdown Structure Elements UT-2

stainless steels and high nickel alloys HAZ hot cracking is primarily related to grain boundary liquation. HAZ hot cracking related to solid-state embrittlement mechanisms is not a significant for most of the common austenitic stainless steels and high nickel alloys.

Three different mechanisms have been proposed for producing liquid films:

(1) Preferential grain boundary melting,

(2) Low-melting temperature segregates,

(3) Adsorption of alloy elements from the molten-weld pool and lower the melting temperature of grain boundary.

Cracks can initiate as a result of the liquid films under the thermal stresses resulting from welding.

Mechanisms of Liquid-Film Formation

Preferential melting of large angle (>20°) boundaries in pure metals has been reported to occur at essentially the equilibrium melting point [9]. The Gibb's free energy of a grain boundary in a pure metal is usually higher than the grain matrix. Therefore, thermodynamically, the grain boundary will melt preferentially at temperature slightly below the bulk melting temperature. Kinetically, the rate of grain boundary melting increases with applied stress, impurity content, and increased heating rate. The presence of low melting segregates in an alloy provides a further potential for preferential melting at temperatures considerably lower than the bulk solidus of the alloy. An eutectic reaction between the grain boundary and the matrix can also enhance the grain boundary liquation tendency. For example, the melting point of Fe is about 2800°F (1538°C), while that of FeS is about 2170°F (1188°C) and the Fe-S eutectic temperature is 1746°F (988°C).

In Borland's generalized theory [6], the distribution of a liquid is controlled by the ratio of the liquid-solid and solid-solid interfacial energies (τ). When τ is less than 0.5, the liquid weld metal can penetrate grain boundaries in the adjacent HAZ. Medovar and Rehbinder [9] suggested a mechanism of HAZ grain boundary liquation induced by fusion zone liquid at elevated temperature. They postulated [9] that certain elements in the liquid enhanced penetration intergranularly into the HAZ since these same elements lower the surface energy of the matrix. If such elements are present in the weld pool, a liquid may penetrate into the HAZ and cause base metal HAZ cracking. This mechanisms is more important for materials which are basically free of segregates.

In the early 1950's, Pepe and Savage et al. [60] studied the HAZ liquation phenomenon and proposed a constitutional liquation theory. According this theory, liquid will form during a welding thermal cycle if the melting point of a localized region is lower than the effective solidus temperature or a reaction involving a liquid occurs at elevated temperature. Constitutional liquation can also occur by reaction between intermetallic compounds and the matrix at elevated temperature.

Recent research in the Materials Joining Group of The University of Tennessee [28] indicated that there are four basic types of HAZ grain boundary liquation in fully austenitic stainless steels and high nickel alloys. Based on this work, the different modes of grain boundary liquation result in different HAZ liquation cracking potentials. It is evident that additional more studies should be carried out in order to precisely correlate the type of HAZ grain boundary liquation and the HAZ liquation cracking tendency.

HAZ Liquation Cracking Mechanisms

Unlike weld metal solidification theories which have been successfully applied to cracking phenomena, the HAZ liquation cracking theories available are far from practical application although many mechanisms have been proposed to explain HAZ liquation cracking/ductility dip cracking behavior in a particular material. Therefore, a generalized HAZ hot cracking theory needs to be developed in order to derive sophisticated and generally acceptable concepts.

Although the Strain theory was proposed for fusion zone/weld metal solidification cracking, the basic concept has been adopted to explain base metal HAZ cracking by Kammer et al. [9]. Figure 1 shows a schematic representation of the formation of HAZ liquation cracks (after Kammer). The top figure illustrates that grain boundary melting occurs over the distance for which the temperature gradient corresponds to the solidus temperature of the segregate film. At this stage, the HAZ zone is in a state of compression due to thermal expansion of the hot metal near the fusion line. During the on-cooling portion of welding thermal cycle, the grain boundaries (in all three dimensions) in the HAZ adjacent to fusion zone are essentially in a tensile strain zone. At this point, if grain boundaries in the HAZ are at a liquid film stage, HAZ cracking may occur.

Owczarski et al. [40] proposed a model for HAZ cracking in nickel base superalloys. In their model, grain boundary liquation is the primary cause of HAZ hot cracking. For the materials (Udimet 700, Udimet 500, Udimet 630, Inconel 718, Hastelloy X and Waspaloy) they used, liquation initiates in the vicinity of primary MC-type carbides and appears to be due to the abrupt decomposition of these particles during rapid heating (constitutional liquation). They suggested redefining the HAZ to include a partially melted region.

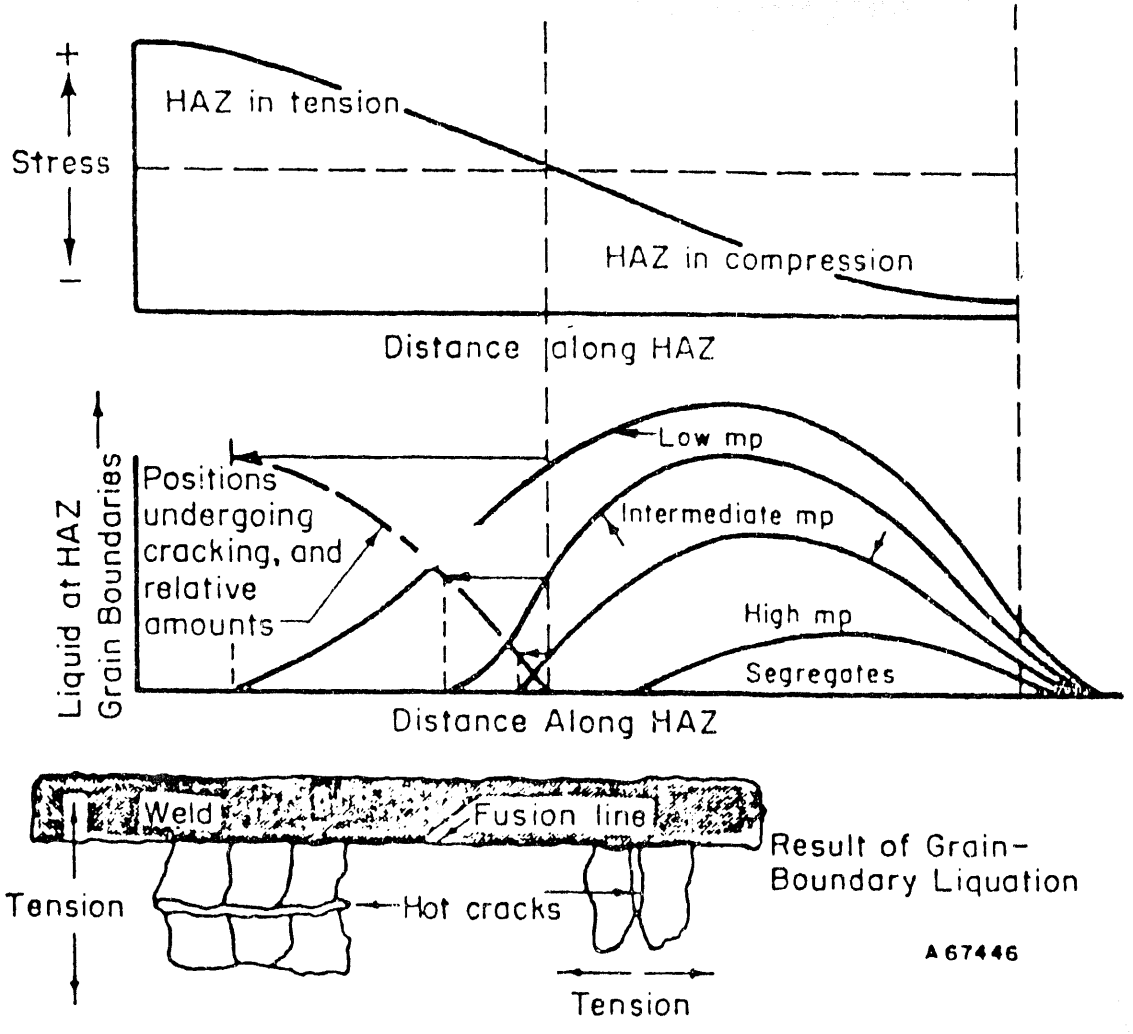

Figure 1. Schematic Representation of Strain Theory.

This important concept has been widely accepted and the occurrence of this region in high alloy materials may govern weldability.

Lundin et al. [2, 10, 28, 36 and 38] proposed a HAZ liquation cracking mechanism based upon their investigations on conventional austenitic stainless steels and modified 316 alloys. The mechanism of HAZ liquation cracking provides a relatively integrated consideration concerning HAZ liquation. Three major parts included in this mechanism are (1) enhancement of segregation of alloying and trace elements along the grain boundary in the HAZ adjacent to the fusion zone; (2) liquation along the grain boundaries and wetting between the intergranular liquid and grain matrix and; (3) welding thermal strain.

A summary of the mechanism proposed is addressed as follows:

(1) Grain boundary segregation of alloying and trace elements and the existence of second phases provided a primary condition for HAZ grain boundary liquation. Segregation is mainly enhanced by a so-called "sweeping up" phenomenon generated by grain growth during welding and precipitate dissolution.

(2) Segregated containing grain boundaries in the HAZ may preferentially melt at elevated temperatures. Wetting between the intergranular liquid and grain matrix affects the formation of intergranular separations. If a liquid covers all of the liquated grain boundaries (extensive wetting) then, the liquation cracking tendency is great. If the wetting between liquid and grain matrix is (minimal liquid distributed discontinuously), the liquation cracking tendency is low.

(3) The formation of grain boundary liquation is the only necessary condition for HAZ liquation cracking. However, a sufficient condition for occurrence of HAZ

liquation cracking should including the sufficient tensile strain acting on the liquated grain boundary.

Many investigators [47 and 48] realized that grain size has a significant influence on HAZ liquation cracking tendency. However, only few have systematically investigated the phenomena. Thompson et al. [47] claimed that the HAZ microfissuring susceptibility in alloy 718 is linearly dependent on the grain size. They explained that the effect of grain size on microfissuring is related to both the liquid distribution and grain boundary sliding. A large grain size would lead to a thicker liquid layer than a small grain size if the same volume of liquid is present in both cases. A larger volume fraction of intergranular liquid could increase the temperature range and time duration during which the liquid wets the grain boundary faces under nonequilibrium freezing conditions.

Effect of Composition on Hot Cracking Susceptibility

The weld metal composition of austenitic filler alloys affects solidification cracking in two ways. The first, is the compositional effect on the solidification sequence and ferrite potential. It is well accepted that austenitic stainless steels which have a primary ferritic solidification mode show a higher solidification cracking resistance even if at room temperature the microstructure is fully austenitic. Thus, when an alloy system composition possess high ferrite potential it has a higher hot cracking resistance. Secondarily, is the effect of individual elements which can form low melting point constituents or can segregate along the cellular and/or grain boundaries, therefore, degrading the cellular and/or grain boundary ductility at elevated temperature and therefore reduce hot cracking resistance. The most significant trace and alloying elements which

influence hot cracking tendency are: S, P, B, Nb, Ti, N, C, Si, O and Mo in Fe-Ni-Cr alloy systems.

Base metal HAZ liquation cracking tendency is mainly dependent on base metal composition from the metallurgical viewpoint. The effects of alloying elements and/or trace elements on HAZ liquation cracking is same as that of a filler metals response to solidification cracking.

As mentioned previously, hot cracking tendency is related to many factors. To interpret the hot cracking results solely by analyzing chemical composition is difficult. Therefore, when discussing hot cracking resistance of an alloy, all metallurgical factors (such as microstructure, fabrication conditions and chemical composition) and mechanical factors (such as residual stress and hot ductility) should be considered. Some general observations in the literature concerning the effects of composition are summarized below.

Nitrogen

It is well known that nitrogen alloyed austenitic stainless steels have improved austenitic stability, mechanical properties and corrosion resistance. Nitrogen can increase the risk of hot cracking due to the strong austenitizing effect. On the other hand, however, an increase in nitrogen can partly replace carbon in modified 316 stainless steel and modified 800H alloys. Therefore, it is expected to decrease the base metal hot cracking susceptibility since the eutectic temperatures of Nb and Ti nitrides and carbo-nitrides are appreciably higher than NbC and TiC. In 1960, Borland and Younger [49] summarized the effect of N on hot cracking and indicated nitrogen does not exert a harmful influence on the cracking resistance of 18Cr-8Ni type stainless steel weld in the range of 0.05 to 0.06%

and free of Nb. When niobium is present, nitrogen in amounts less than about 0.05% intensifies the hot cracking tendency. If niobium is absent, the effect of increasing the nitrogen content from 0.02% to about 0.06% is beneficial, and may even eliminate cracking if the austenite/ferrite structure is changed from orientated to random by the grain refining action of the nitrogen.

Ogawa and Tsunetomi [48] also found that nitrogen has a differing effect on hot cracking susceptibility, depending on whether or not niobium is presented. They claimed that increasing the nitrogen content improved the hot cracking resistance of fully austenitic stainless steel (25%Cr-20%Ni) which contained no niobium as shown in Figure 2. The beneficial effect of nitrogen is stated as the attribution of nitrogen inhibiting the enrichment of silicon at grain boundaries. The results of hot cracking tests for the Nb-containing (0.25%Nb) stainless steel obtained by Ogawa and Tsunetomi [48] are indicated in Figure 3. As shown in the figure, within the nitrogen range of 0.02 to 0.13%, the hot cracking susceptibility of the low Nb (0.25) fully austenitic weld metal did not vary significantly with nitrogen content whether or not heat treatment was applied prior to welding. In another study by Ogawa et al. [55], they further emphasized that additional nitrogen can have a detrimental effect on weld metal cracking of (γ + δ) dual phase weld metal (δ-phase being unstable when transformation to austenite occurs). However, if nitrogen is added to the weld metal while still maintaining the (γ + δ) dual phase, there is no deterioration in the resistance to hot cracking. Nitrogen can substantially improve the resistance to weld cracking in fully austenitic weld metals.

A beneficial effect of nitrogen on hot cracking resistance in austenitic stainless steels can be seen from the work done by Cullen and Freeman [34] who studied the

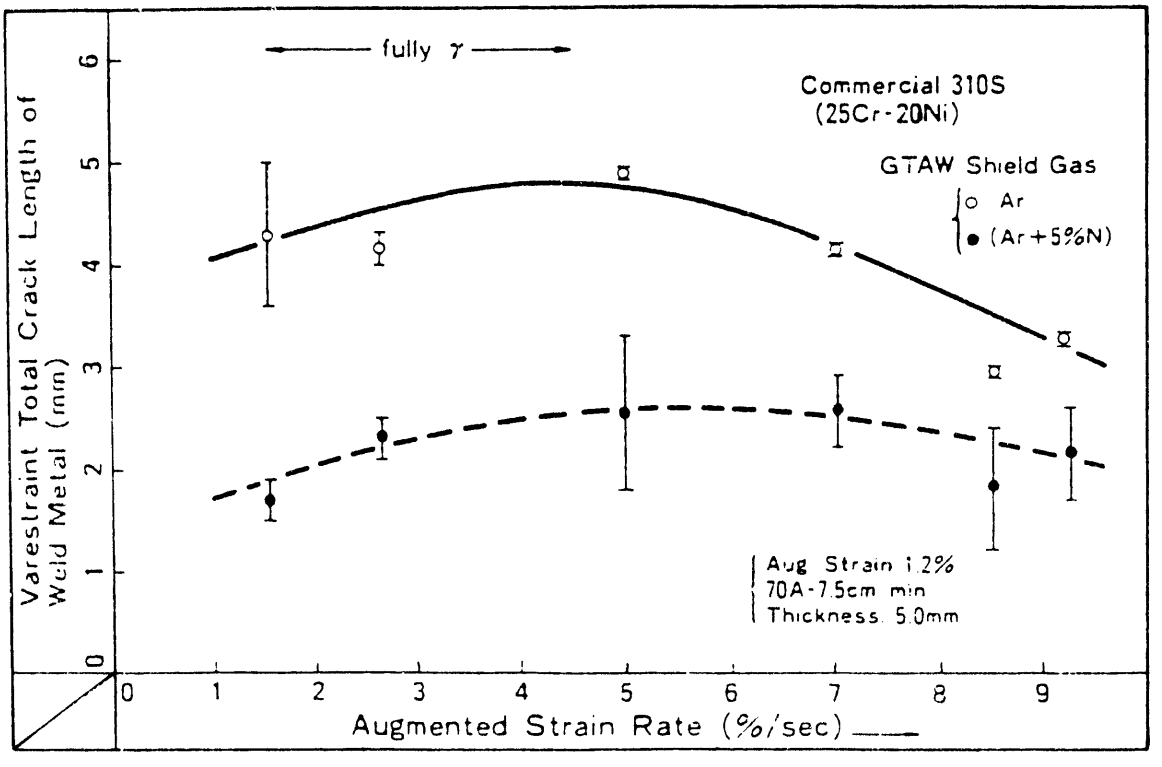

Figure 2. Effect of N on Hot Cracking Susceptibility in Fully Austenitic Stainless Steels without Nb.

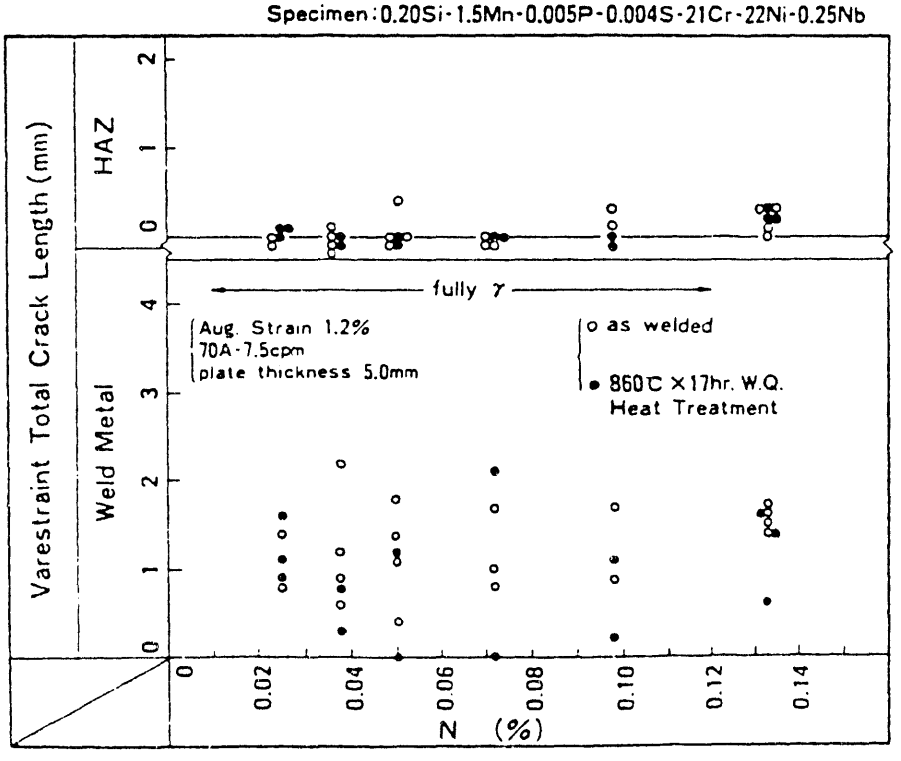

Figure 3. Effect of N on Hot Cracking Susceptibility in Fully Austenitic Stainless Steels Containing Nb.

effect of nitrogen on HAZ intergranular type liquation cracking due to formation of the Nb(C,N) type eutectic in type 347 steel under welding thermal exposures, as shown Figure 4. It is evident that the liquation temperature of the Nb(C,N) eutectic increases with an increase in nitrogen content. This prediction has been proven by Lundin et al. [10-11]. Lundin et al. [11] investigated relationship between 0.5Nb/(30C+50Nb) (Cullen and Freeman's (C&F) parameter) and hot cracking/hot ductility behavior in nuclear grade 347 steels. The results they obtained indicated that reducing the 0.5%Nb/(30%C+50%N) parameter significantly increases HAZ liquation cracking resistance. They [10] further proposed a criterion for calculating the optimum Nb content in 347 steel concerning both sensitization and weldability.

Boron

Many investigators [12,15] have studied the effect of boron additions to stainless steels on solidification and HAZ liquation cracking. According to Brooks [12], the presence of boron at about 0.05% seems to introduce brittleness, and, in larger amounts can cause hot shortness. Ductility of the weld metal was significantly reduced as the boron content exceeded 0.05%. However, no weldability testing was conducted. Further, Hull [13-14] confirmed the detrimental effects of boron on weldability in austenitic alloys. Tamura [48] noted that $M_{23}(C,B)_6$, M_3B_2 and Ni_4B_3 can liquate at grain boundaries and cause HAZ cracking in stainless steels. Brooks [12] found the reduction of boron from 0.006 to 0.001 greatly reduced HAZ cracking in alloy A286. Donati et al. [16] observed an increase in liquation cracking when B exceeded 0.001% in Type 321 stainless steel. A safe upper limit for B in stainless steels appears to be 0.003% which is

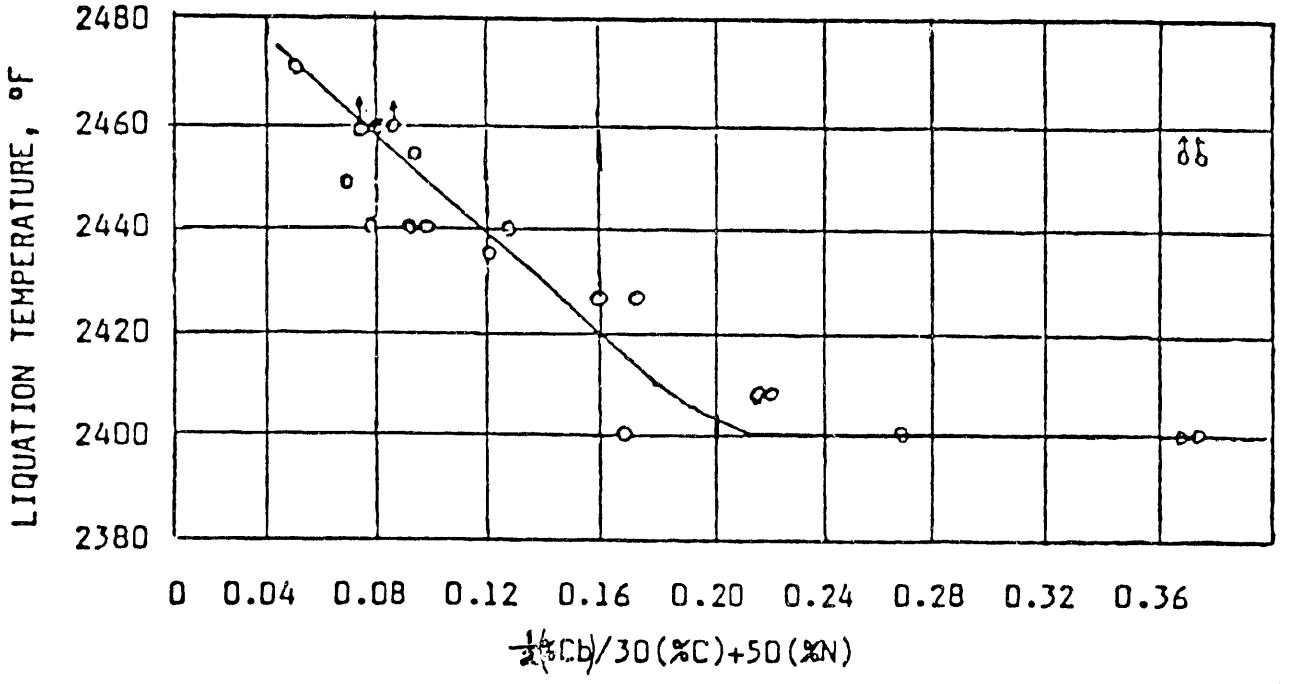

Figure 4. Liquation Formation Due to Nb(CN) Type Eutectic in 347 Stainless Steel as a Function of Cullen and Freeman Parameter.

the amount of boron which can remain in solution after annealing.

Phosphorus and Sulphur

The degree of cracking susceptibility in fully austenitic weld metal as well as the base metal HAZ is strongly dependent on P and S content. That hot cracking tendency decreases with reductions in P and S is basically correlated with a decrease in phosphides and sulphides. P and S are known to segregate to HAZ grain boundaries during a weld thermal cycle and lower the melting point of the grain boundaries thus promoting liquation at the boundaries. Lippold, [33] while investigating the weldability of alloy 800, found a considerable increase in the grain boundary phosphorus content over the matrix content of 0.01%. In a recent study at ORNL [50] it was observed that the amount of S at HAZ grain boundaries in fully austenitic 310 stainless steel was about 2000 times greater than the bulk composition (0.009%). The authors did not, however, determine the segregation of P to HAZ grain boundaries. The P content in the 310 stainless steel studied was 0.019%. The presence of S and P in such large amounts can the grain boundary melting point significantly. Matsuda et al. [51] measured the lower temperatures where lowest melting point phases were liquid in 25/20 Cr-Ni fully austenitic stainless steels and determined the following:

Phosphorous (wt%)	Lower Temperature Limit (°C)
0.003	1300
0.013	1270
0.022	1240
0.032	1200

Recently [63] the variation in the extent of HAZ cracking in Nb containing stainless steels with P content has been studied by Japanese researchers and the results are

shown in Figure 5. If the P content is below 0.005% no HAZ cracking was observed even in fully austenitic stainless steels containing 0.20 to 0.60% Nb.

Kujanpaa et al. [50] pointed out the interrelationship between the solidification mode and (P+S) content, and hot cracking susceptibility in the stainless steel alloys. The most susceptible alloys had Cr_{eq}/Ni_{eq} ratios less than about 1.50 and if P+S content is kept below 0.01% no HAZ liquation cracking should be observed even in the fully austenitic alloys. Cieslak and Savage [52] studied the influence of P on the hot cracking sensitivity in cast austenitic stainless steels and found that the effect of P content on hot cracking was considerably greater for a material with a primary austenitic solidification mode as opposed to a ferritic material with primary ferritic solidification.

The relationship between Cr_{eq}/Ni_{eq} ratio with P+S and hot cracking susceptibility from Kujanpaa's work [50] is shown in Figure 6. When the data from type 347 (Nb content ranging from 0.23 to 0.74) from a recently completed study at the University of Tennessee are plotted in Figure 7, it is noticed that the boundary separating susceptible and not-susceptible regions is shifted towards greater Cr_{eq}/Ni_{eq} ratio (>1.6). This could be due to Nb enhancing the tendency towards liquation cracking.

Rare Earth Materials (REM) [43,72,204]

It is believed that La combines with P and S in iron-chromium-nickel alloys to form LaP and/or LaS which have a higher melting temperature than the γ-M_3P type phosphide eutectics. The optimum amount of La, suggested by Matsuda et al. [27], to improve fusion zone hot cracking in type 310 ss is give by Equation 1.

$$La=4.5P+8.7S \quad (1)$$

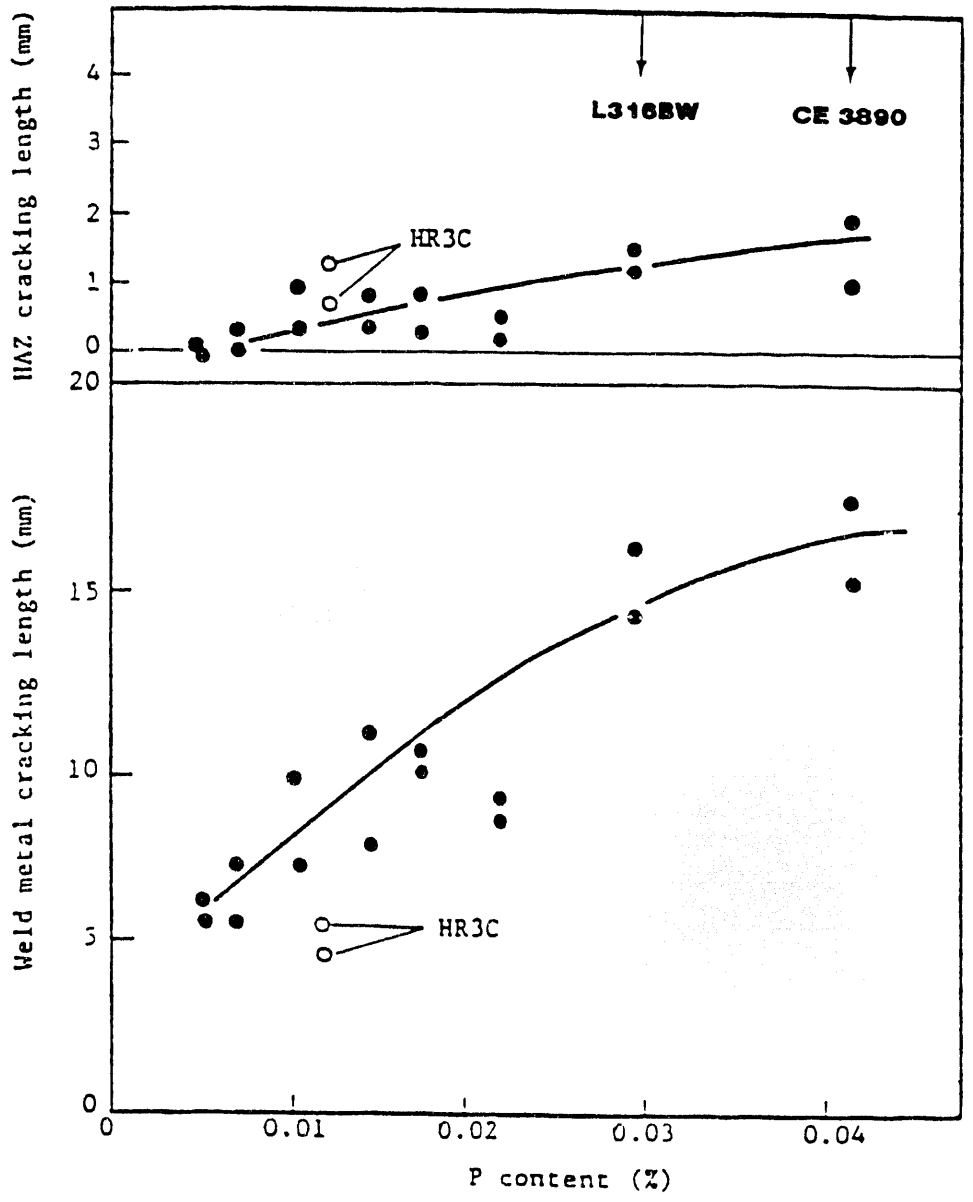

Figure 5. Crack Length of 20Ni-25Cr-0.45Nb Steel in Varestraint Tested Sample.

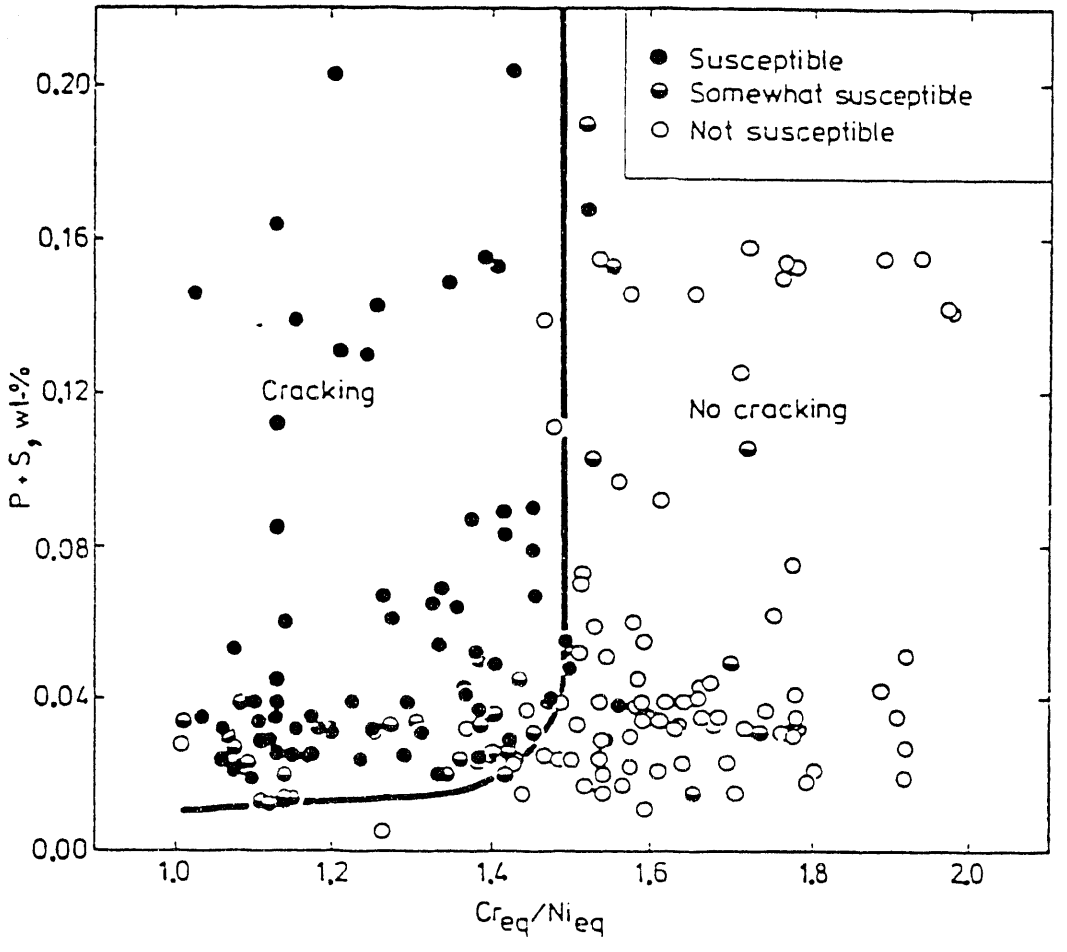

Figure 6. Relationship Between Solidification Mode and Weld Cracking Susceptibility.

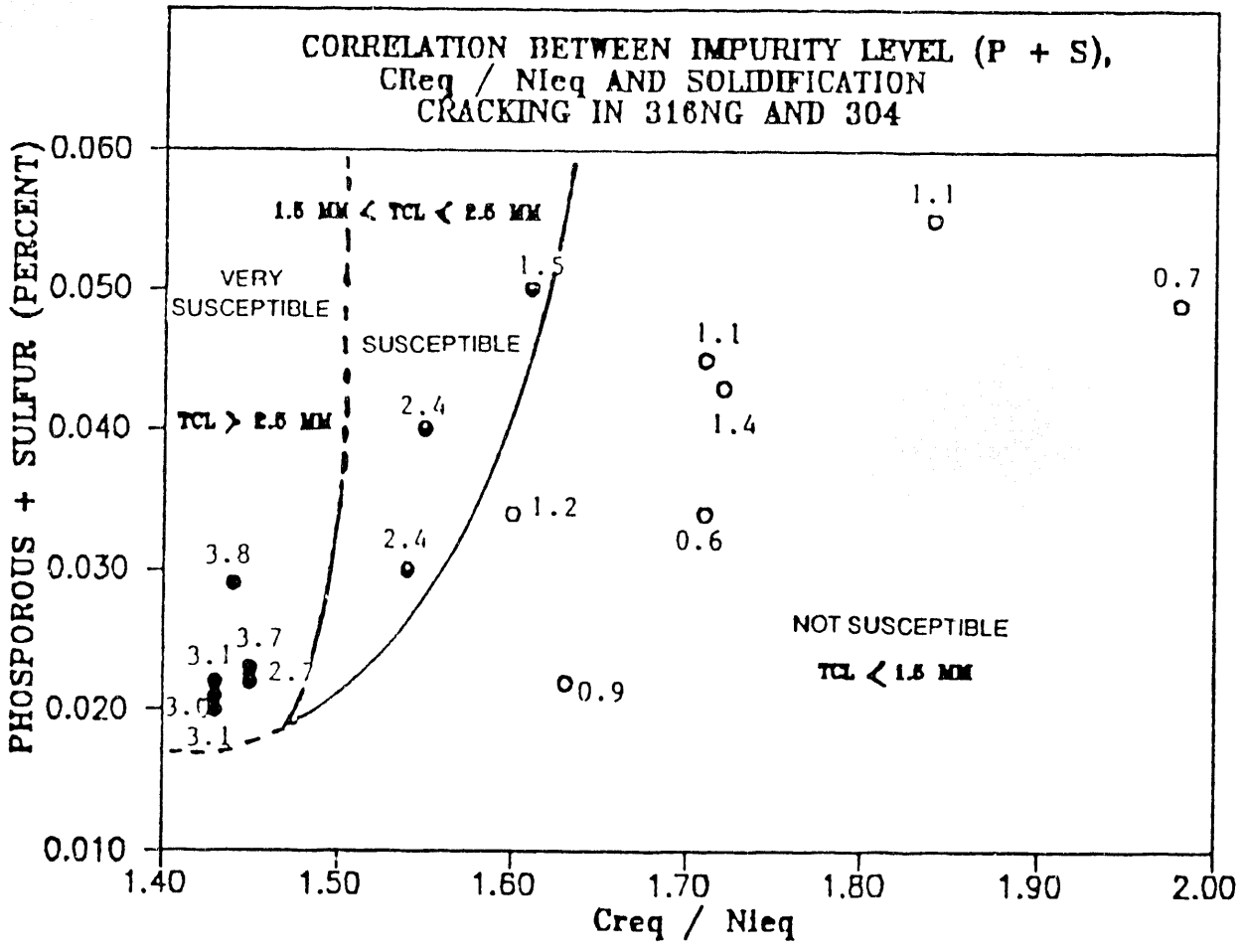

Figure 7. Correlation among the P+S Content, Cr_{eq}/Ni_{eq} and Extent of Solidification Cracking in 316NG and 316.

Morishige [24] in a statistical analysis of 40 heats of austenitic stainless steels suggested the following equation (Equation 2) to estimate the liquation cracking susceptibility as measured by hot ductility tests.

$$\Delta H=-700C+17Cr-37Ni-117Nb+29Mo+188 \quad (2)$$

Morishige further modified [24], the above equation to include the effect of REM on HAZ liquation. The modified form is indicated by Equation 15.

$$\Delta H_m=-700C+17Cr-37Ni-117Nb+29Mo++3000REM+170 \quad (3)$$

The materials with $\Delta H > 60$ are considered to show greater resistance to HAZ hot cracking. This equation is derived from data on 347 stainless steels with REM<0.02%.

Morishige's modified equation, however, should be used with caution as it is based on two heats of REM treated 347 out of a total of 36 heats studied. Nevertheless, the increase in the ΔH value after a REM addition indicates a strong positive influence on HAZ liquation cracking resistance.

Silicon

Many researchers have studied the effect of silicon on hot cracking resistance of stainless steels and nickel base alloys [67-70]. Kihlgren and Lacy [22] evaluated the hot cracking resistance of nickel-chromium-iron alloys employing an X-groove test. A detrimental effect of silicon on hot cracking resistance was defined in their work. They also found that an addition of niobium counteracts the deleterious effect of silicon and made possible the production of crack free welds. Arata et al. [20] assessed the effect of Si on hot cracking behavior of 310 steel using the BTR criterion they developed. They reported that increasing Si from 0.1 to 1% only slightly decreased the hot cracking resistance in 310 steel. Rundell [21] investigated effects of minor elements

on the weldability of a nickel base heat resistant alloy (nickel: 44.1-45.8%, chromium: 24.7-25.6%) using the so-called Circular Patch Test and found that a increase in silicon content from about 1.2 to 1.7% had an effect on hot cracking susceptibility similar to that of phosphorus. However, it was found that additions of molybdenum and tungsten can reduce the silicon influence.

Carbon

In general, it is believed that increasing carbon enhances hot cracking susceptibility in stainless steels and high nickel alloys. However, depending on the alloy system the effect of carbon on hot cracking susceptibility may vary.

A study on the influence of silicon content on hot cracking in austenitic stainless steel weld metal with particular reference to 18Cr-8Ni steel was carried out by Polgary [23]. As Polgary quoted that the unfavorable influence of silicon can be effectively compensated for by increasing the carbon content, at least within certain limits. The explanation for this phenomenon was provided by Polary as follows:

"The pick-up of carbon in molten fully austenitic stainless steel weld metals shows, however, a clear connection with the C-Si-O balance in the molten pool:

$$[C].[O]/[Si]=K'.P_{CO}.a_{SiO_2} \qquad (4)$$

where [C], [Si] = concentration of C, Si in the melt,
P_{CO} = pressure of C_O in the arc atmosphere,
a_{SiO_2} = activity of SiO_2 in the slag,
K' = constant".

Consequently, at constant P_{CO} the silica activity also decreases with an increase in the [C]/[Si] ratio in the weld metal. Most probably incomplete equilibrium can be considered one of the reasons for the favorable effect of

carbon. At quite high C contents, a carbide eutectic appears in the grain boundaries, causing the crack tendency to decrease somewhat due to the phenomenon known as eutectic healing: the eutectic phase occurs during the period of weld metal solidification.

According to their experimental results, when the filler metal electrode was 25Cr-20Ni and the weld metal had a ratio, [C]/[Si] = 0.16, that cracking occasionally could occur. When the electrode composition adjusted so that it gave a weld metal in which [C]/[Si] = 0.22 no further cracking was reported.

By using the Varestraint Test, Arata et al. [20] noted different HAZ hot cracking susceptibilities between Type 316 and 316L materials. The lower carbon content (0.026%) material (316L) showed a greater hot cracking resistance than higher carbon content (0.07%) 316 material. This result was further confirmed by Morishige et al. [24]. By analyzing the hot ductility testing results statistically, Morishige et al. derived an equation to define liquation cracking susceptibility as follows:

$$\Delta H=-700[C\%]+17[\%Cr]-37[\%Ni]-117[\%Nb]+29Mo+188 \quad (5)$$

The relationship between hot ductility parameter ΔH and reduction in area, measured at 1300°C after heating to a peak temperature of 1350°C is indicated in Figure 8. As Morishige et al. [24] pointed out when ΔH is greater than 100, "the material exhibits an excellent hot ductility". It is evident from the above hot ductility parameter calculation equation that C shows a strong negative influence on HAZ liquation cracking resistance.

Niobium

Niobium is one of the most controversial elements in terms of hot cracking susceptibility. After studying the

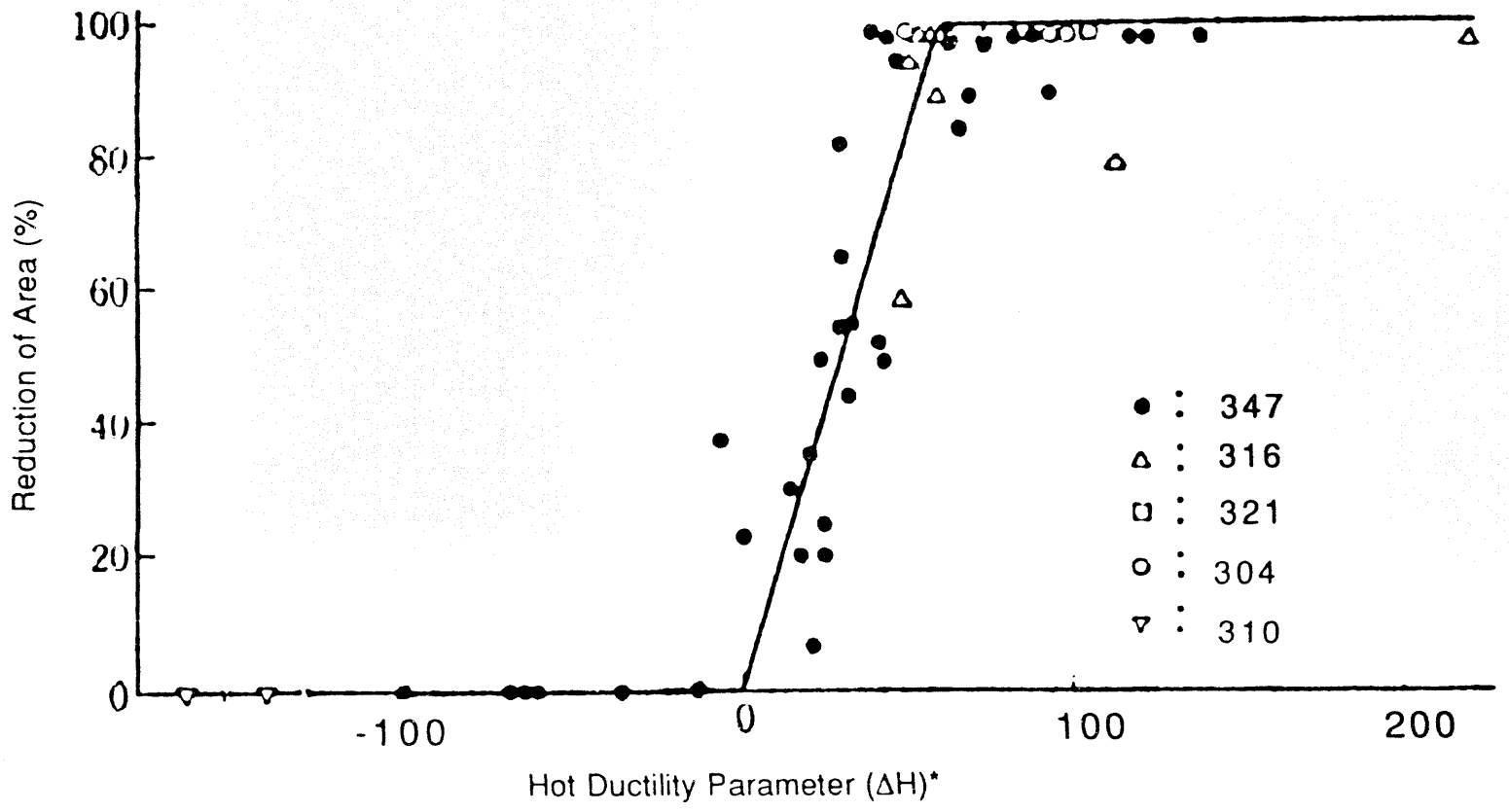

(Note) $$*\Delta H = -700[\%C] + 17[\%Cr] - 37[\%Ni] - 117[\%Nb] + 29[\%Mo] + 3{,}000[\%REM] + 170$$

Figure 8. Relationship between Hot Ductility Parameter ΔH and Reduction in Area, Measured at 1300°C.

weldability of austenitic stainless steel tubes using Y-groove and Varestraint tests, Miura [30] revealed that niobium increases solidification cracking and HAZ liquation cracking susceptibility although he did not report the HAZ liquation cracking test results.

Pease [18] claimed niobium has a beneficial effect on hot cracking resistance in nickel base alloys and can reduce the harmful effect of silicon. It was also mentioned by Borland and Younger [49] that niobium increases the ferrite potential of fully austenitic stainless steel, therefore, it tends to prevent hot cracking. However, in general, niobium increases hot cracking susceptibility by segregating at grain boundaries during welding. This has been confirmed by examination of the surfaces of solidification cracks as well as HAZ liquation cracks. Lundin et al. [11] showed the influence of the combination of Nb, N and C on hot cracking tendency using many heats of nuclear grade 316 and 347. Their results for nuclear grade 347 are plotted (see Figure 9) using the hot ductility criteria (RDR, DRR and NDR) and hot cracking test criterion (CHL) versus the C&F parameter.

Titanium

Titanium is strong MC type carbide, TiN type nitride and Ti(CN) type carbonitride former in austenitic stainless steels and nickel based alloys. Adding titanium can significantly increase creep strength and elevated temperature tensile strength in these materials. Matsuda et al. [51] concluded that a small amount of titanium had a beneficial effect in reducing solidification cracking in 310 steel. For the case of 0.024% P and 0.002% S, the effective Ti content was in the range of 0.04 to 0.12% and the optimum Ti content is about 0.05%. The beneficial effect of titanium was considered due to the attribution of the raised

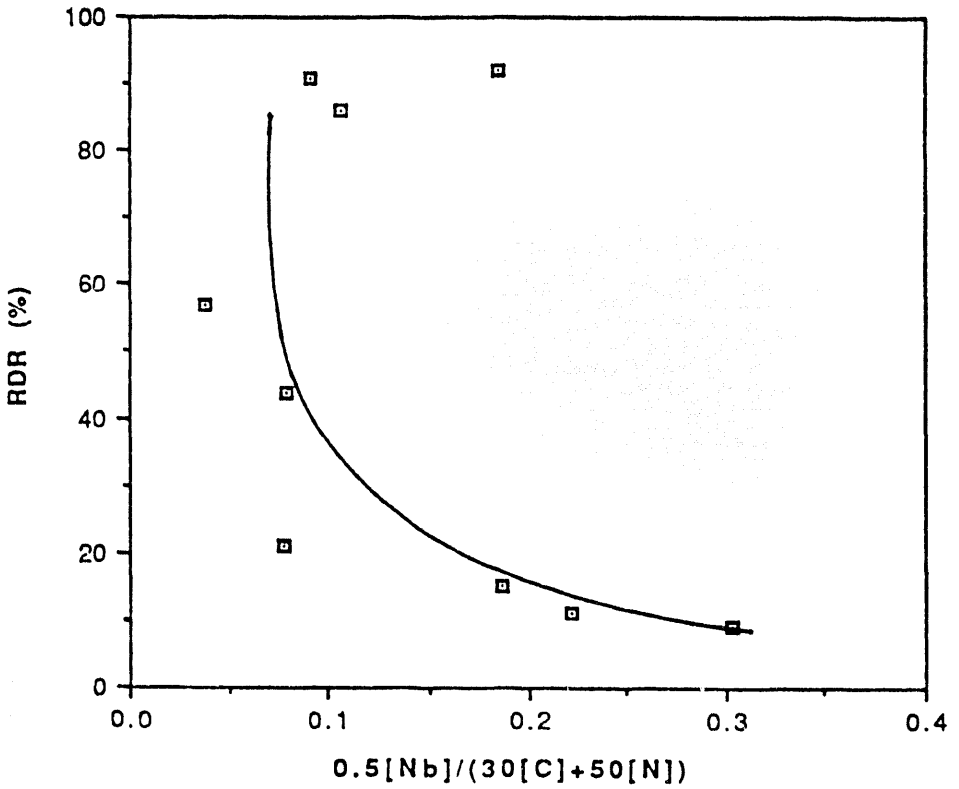

Figure 9. The Gleeble Hot Ductility Testing Criteria RDR, DRR, and NDR and Hot Cracking Testing Criterion CHL as Function of the C&F Parameters. (a) RDR vs. C&F; (b) DRR vs. C&F; (c) NDR vs. C&F and (d) CHL vs. C&F.

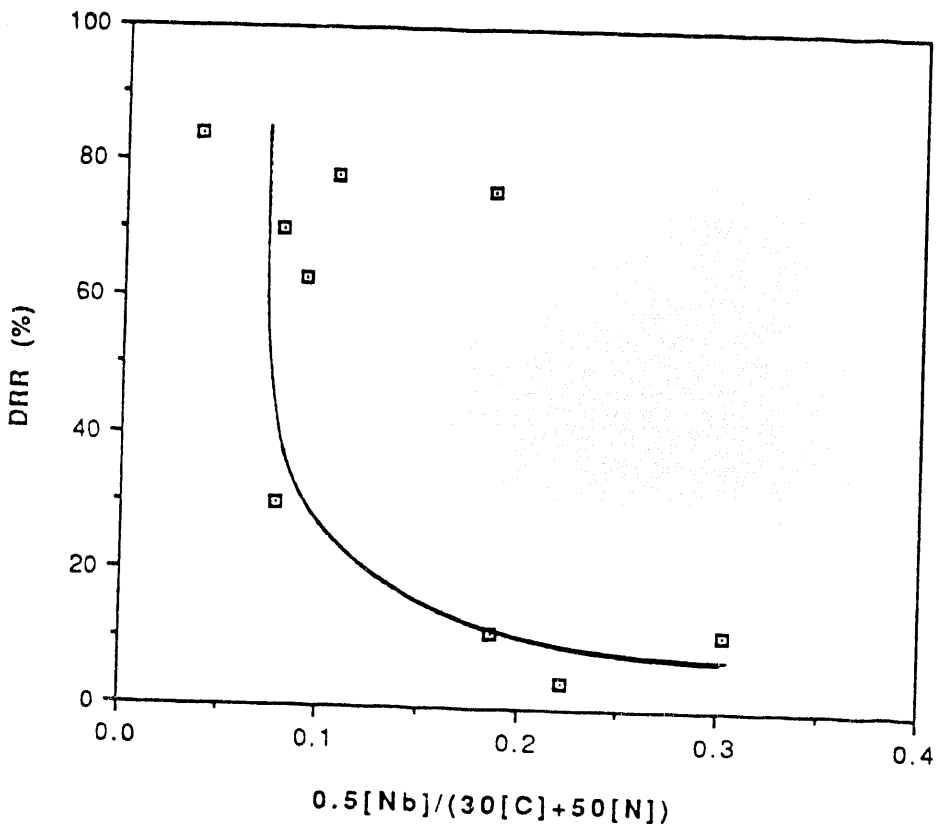

(b)

Figure 9. (Continued)

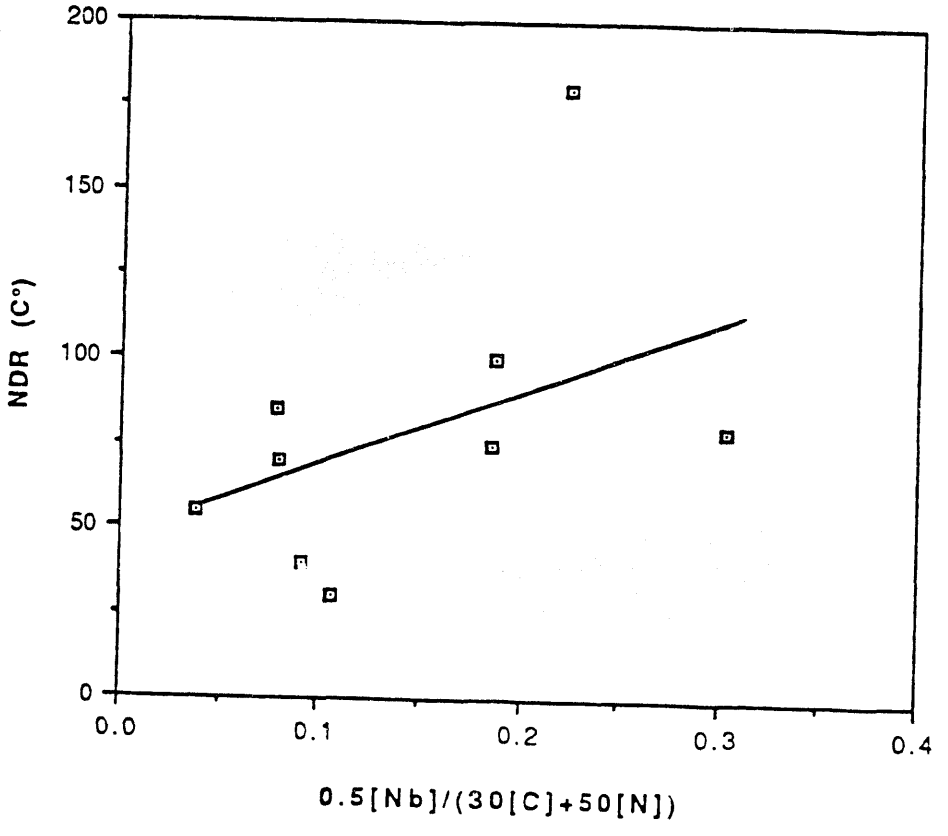

(C)

Figure 9. (Continued)

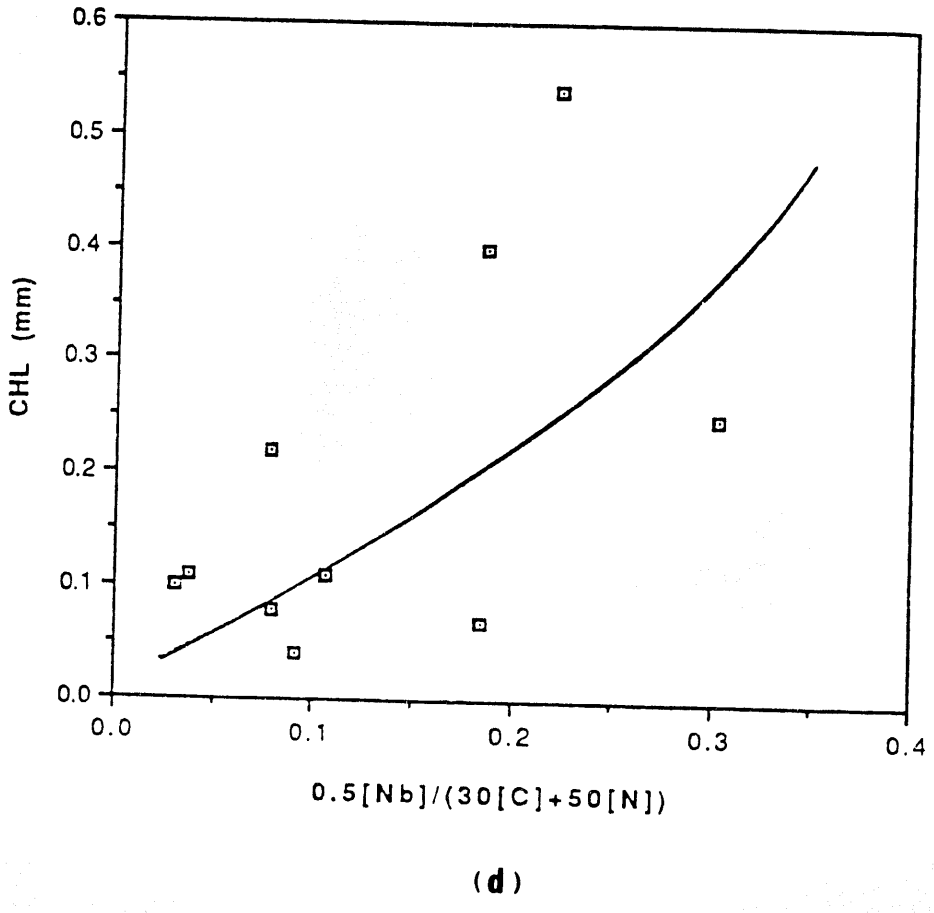

(d)

Figure 9. (Continued)

solidification temperature of the phosphide eutectic. An excess titanium addition, however, was judged to be harmful to solidification cracking. The detrimental effect was postulated to result from the increased amount of low melting eutectic enriched in titanium.

Both theoretical and experimental studies on hot cracking resistance of modified 800 alloy were conducted by Canonico et al. [29]. They pointed out that segregation of titanium and aluminum resulted in grain boundary embrittlement and banding which was sufficiently severe to exhibit liquation during heating. The microprobe analysis they performed indicated a strong association between sulfur and titanium in the discrete inclusions observed in the sulfur-bearing alloys. Thermodynamically, TiS and Al_2S_3 are relative easy to form in the HAZ. Agreement with the results of Canonico et al. [29] was demonstrated in work performed by Lundin et al. [2] using modified 316 and modified 800H.

Aluminum

According to both the criteria of Hull [13] and Pease [18], the effect of aluminum on hot cracking susceptibility is variable. It is manifested that the aluminum influence on the hot cracking susceptibility in fully austenitic stainless steels and nickel-base alloys and is dependent on the alloy system and amount of aluminum in the system. However, the general effect of Al on hot cracking resistance is slightly negative for fully austenitic stainless steels and Incoloy 800 alloys.

Manganese

In many respects, manganese plays an important role in austenitic stainless steels and high nickel alloys. Many

researchers recognized that the addition of manganese to fully austenitic stainless steels has a favorable effect on hot cracking resistance. It is well known that the conventional reason for applying manganese in austenitic stainless steels is deoxidation and sulfur control. Matsuda et al. [27] found that the optimum manganese content for improving solidification cracking resistance is related to the phosphorous and sulphur content. The beneficial effect of manganese is the reduction in the "harmful" effect of sulphur by forming MnS type sulphides of relatively high melting temperature.

Tungsten

Very few investigations have been carried out to study the effect of tungsten on HAZ liquation cracking in stainless steels and high nickel alloys. However, the binary equilibrium diagrams for Fe-W, Ni-W and Cr-W respectively shown in Figures 10 indicate an increase in the melting points of the alloys with the addition of tungsten. This phenomenon could aid in reducing the segregation tendency of tungsten in stainless steels and thus prove to be beneficial in mitigating the HAZ liquation cracking tendency. Additions of tungsten to nickel-base alloys has helped in reducing the hot cracking problem in weldments.

The addition of tungsten to nickel base alloys does not appear to deteriorate the elevated temperature properties. McCoy and King [54] compared the room temperature and elevated temperature properties of Inconel 617 (Ni, - 22 wt.%Cr, - 12.5 wt.%Co, - 9 wt.% Mo, - 1 wt.%Al, - 0.07 wt.%C) and Inconel 618 (Ni, - 22.5 wt.% Cr, - 15 wt.%Fe, - 6 wt.%W, - 0.04 wt.%C) and found that "short-term" tensile tests on alloy 617 showed that aging severely reduced the strain at fracture at both ambient and elevated temperatures. The

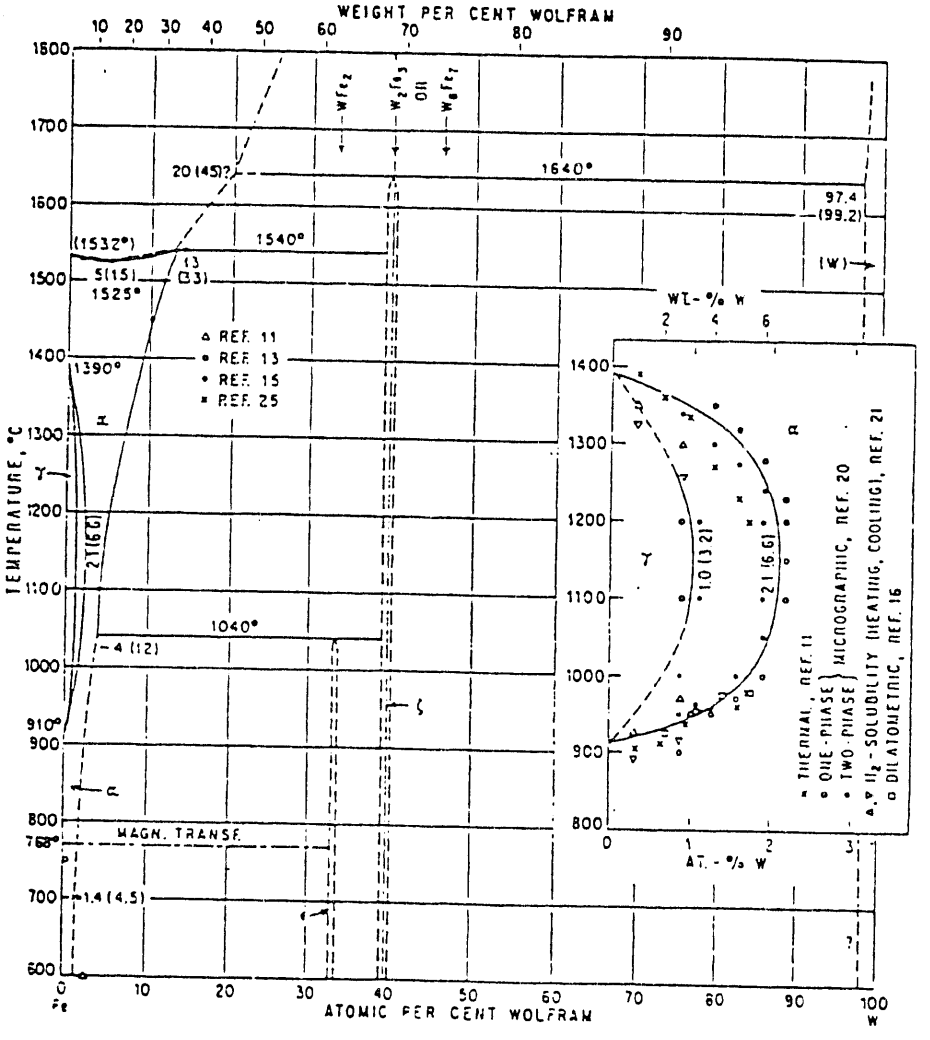

(a)

Figure 10. The Binary Equilibrium Diagrams for (a) Fe-W; (b) Cr-W, and (c) Ni-W.

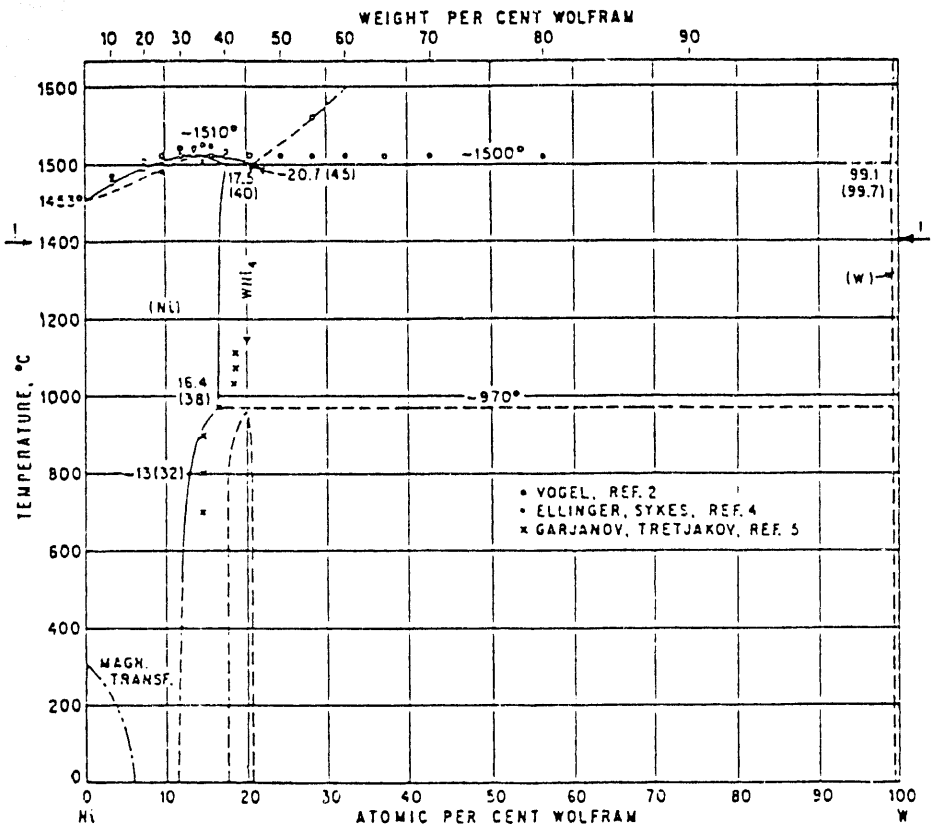

(b)

Figure 10. (Continued)

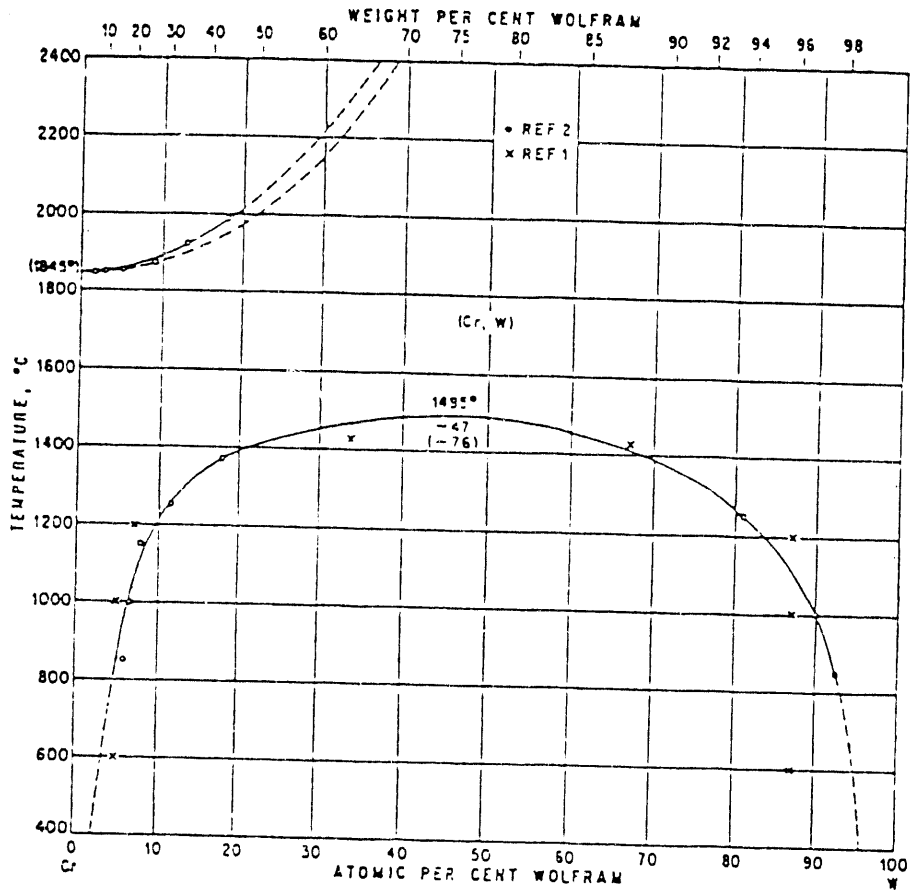

(c)

Figure 10. (Continued)

impact energy at ambient temperature was severely degraded by aging. On the contrary, Inconel alloy 618 had excellent stability during aging. Fracture strains in short-term tensile tests and impact together remained high after aging.

General

It should emphasized again that hot cracking resistance of an alloy is a function of many factors. To use only composition to predict a materials hot cracking resistance is not completely accurate, although it is the most important factor. With regard to compositional influences, the behavior of a single element is strongly dependent on the alloying system. Nevertheless, it is important to have a general idea of the possible effects of individual alloying and trace elements on solidification cracking/HAZ liquation cracking in stainless steel and high nickel superalloys as was discussed above. Reviews indicate that some elements (such as S, P, B, and Zr) promote severe reduction hot cracking resistance and some elements show a variable influence (such as Al, Nb, Mo, C, Si, and Ti). The elements which show a minor influence are Mn, Cu, Cr, Fe, Ni, and Co. Those that exhibit a beneficial influence are N, W, and La/REM. This characterization applies to the range of fully austenitic stainless steels and high nickel superalloys. Many investigation [18,24] led to a consolidated ranking of specific elements on hot cracking. The earliest guide to the compositional effects in high nickel alloys was given by Pease [18]. The ranking Pease stated is listed as follows:

Beneficial	No Major Effect	Variable	Harmful
Nb	Mn	Al	Pb
Mg	Cu	Ti	S
Cr	C	P	
Fe	Mo	Zr	
Co	Si	B	

Cancnico et al. [29] attempted to quantify some of these compositional effects with respect to the welding of alloy 800. These workers used the Borland method of estimating the 'relative potency factor' (RPF) to show that the order of potency in nickel was sulphur, boron, phosphorus, carbon, silicon with an order of magnitude lower RPF than the one before. Also estimated in this work were the RPF values for aluminum, manganese, and titanium, none of which were high. This RPF technique was also used by Wolstenholme [19] in his study of weld crater cracking in alloy 800. It is interesting to note that elements revealed in this estimation, sulphur, carbon, titanium, niobium and chromium are somewhat different that those indicated by previous workers. Wolstenholme agrees with the very high RPF of sulphur and the moderate value of carbon but, an estimate of the RPF values in iron as well as nickel shows titanium and niobium have higher values than silicon.

Varestraint Hot Cracking Test Criterion

Many hot cracking test methods [9,37,55] have been developed to evaluate susceptibility of welding related hot cracking since late 1940's. Two general types of test methods, namely, full size weld structure tests (usually self-restraint type) and laboratory type test (usually with a laboratory type specimen and augmented strain or semi-self restraint type) are available for use. Most of these tests were devised to evaluate the tendency toward one particular type of cracking such as solidification cracking, HAZ liquation cracking and reheat cracking. Many test methods developed early-on can only quantitatively rank the weldability of materials, therefore, it is difficult to use them to investigate the basic concepts and/or mechanisms of cracking. Kammer et al. [9] reviewed the cracking behavior

in high strength steel weldments and summarized the fundamental requirements for a suitable test method. The so-called "ideal" weldability test should incorporate:

(1) Ability to show a direct correlation with actual fabrication and service behavior;

(2) Reproducibility of results with freedom for variation due to the human elements;

(3) Sensitivity to small changes in a test variable;

(4) Ability to show the effects of several welding variable;

(5) Economical preparation of specimens and running of tests;

(6) Applicability to all welding processes.

It is difficult to meet the requirements for an ideal weldability test. Therefore, many researchers have tried to invent new test methods, or further develop and modify existing test methods. In the early 1960's, Savage and Lundin [57] developed a new test method, the Varestraint, and claimed it met the above requirements for an ideal test. The initial design of Varestraint test is schematically illustrated in Figure 11. Later, Lundin et al. [11,28,37-38] evaluated the weldability of more than forty heats of conventional and nuclear grade austenitic stainless steels and proposed recommended testing procedures and parameters. The use of standard procedures and testing parameters provides a way to compare the results obtained from different laboratories. A schematic of the testing device and, standardized procedures are indicated in Figure 12.

Many Varestraint criteria were proposed to assess hot cracking tendency. The most commonly employed criteria include threshold strain (SS), total crack length (TCL), maximum crack length (MCL), solidification embrittlement temperature range (BTR), ductility dip temperature range (DTR), and the recently developed cracked HAZ length (CHL).

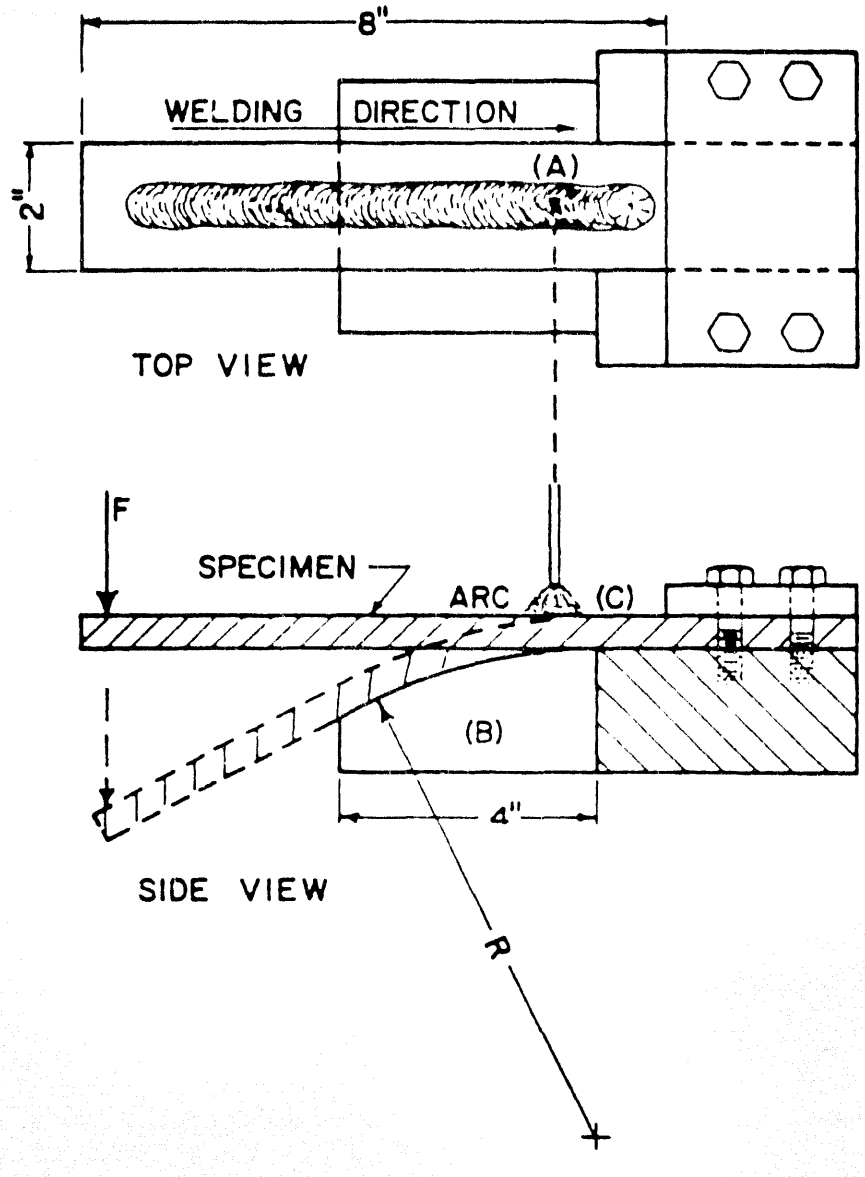

Figure 11. Simplified Sketch of the Operation of the "Varestraint" Testing Device.

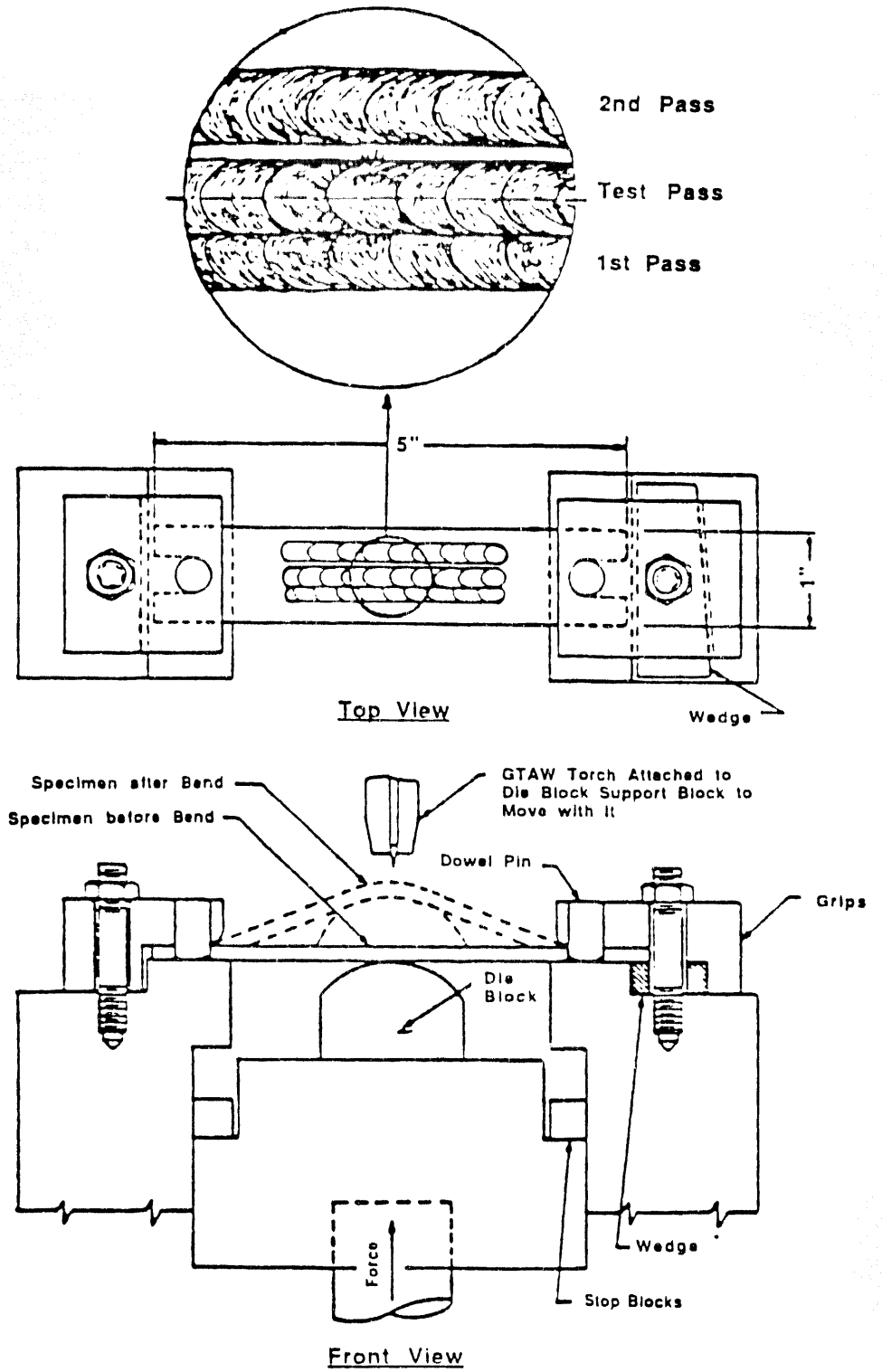

Figure 12. Schematic Drawing of the Varestraint Test Device Showing the Manner in Which a Specimen Is Tested.

All criteria can properly assess hot cracking tendency, however, MCL and CHL possess the advantage of relative simplicity and are highly precise. The BTR and DTR are actually related to MCL in principle, however, determination requires complicated experimental work compared to MCL and CHL. Each of the above criteria are discussed in detail in the following paragraphs.

Threshold Strain Criterion

Since hot cracking resistance differs for different materials, the minimum augmented strain to cause cracking varies with material. If the threshold strain is high, the hot cracking resistance is high. On the other hand, if the threshold strain is low, the hot cracking resistance is low. However, because the radius of the die block can not be continuously varied, the exact threshold strain can not be readily found. Therefore, in some situations the hot cracking resistance can not be compared by only using this criterion.

Total Crack Length Criterion

The total crack length is obtained by adding the lengths of all cracks found in the weld deposit (fusion zone TCL) and/or the heat-affected zone (HAZ TCL) for each specimen. The greater the total crack length, the lower the hot cracking resistance. The data provides a quantitative index of hot cracking sensitivity.

Maximum Crack Length Criterion

The maximum crack length is the length of the longest crack in a sample. The maximum crack length reflects the hot

cracking temperature range and is a rapid quantitative means of assessing hot cracking sensitivity. It is often used as a semi-quantitative index for preliminary and rapid screening of material behavior.

Solidification Brittleness Temperature Range Criterion

This criterion is determined using a plot of ductility verses temperature. Usually, the ductility curve is obtained by coupling the maximum crack length with the temperature distribution measured with a thermocouple (W.5%Re-W.26%Re and 0.3 mm diameter) immersed in the weld pool during welding.

Ductility-dip Temperature Range Criterion

This criterion is determined using similar procedure to the BTR criterion and can be used to evaluate ductility dip cracking propensity. The temperature range is below the solidus of a material.

Cracked HAZ Length Criterion (CHL)

Based upon the idea of a "null ductility zone" in a weld HAZ addressed by Donati et al. [16], Lundin et al. [58] developed the "cracked HAZ length criterion" (CHL). Like MCL, the CHL criterion provides both an indication of the relative hot cracking temperature range and a rapid semi-quantitative means of assessing hot cracking propensity. Previous experience with the CHL criterion proved that CHL and MCL can be used in precisely assessing HAZ liquation cracking tendency preciously. Figure 13 schematically shows the concept of the Varestraint hot cracking criteria.

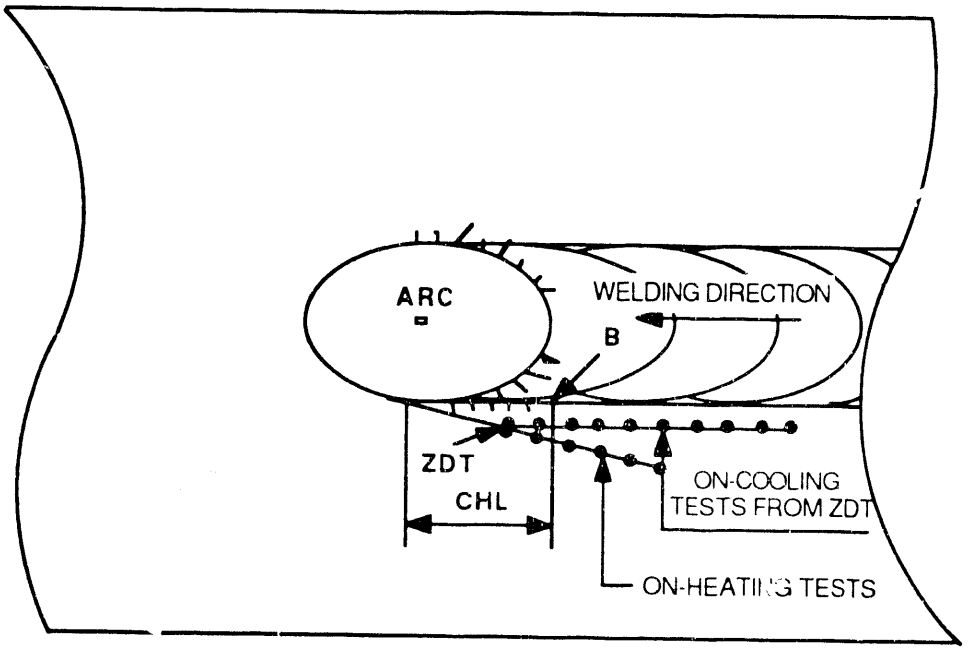

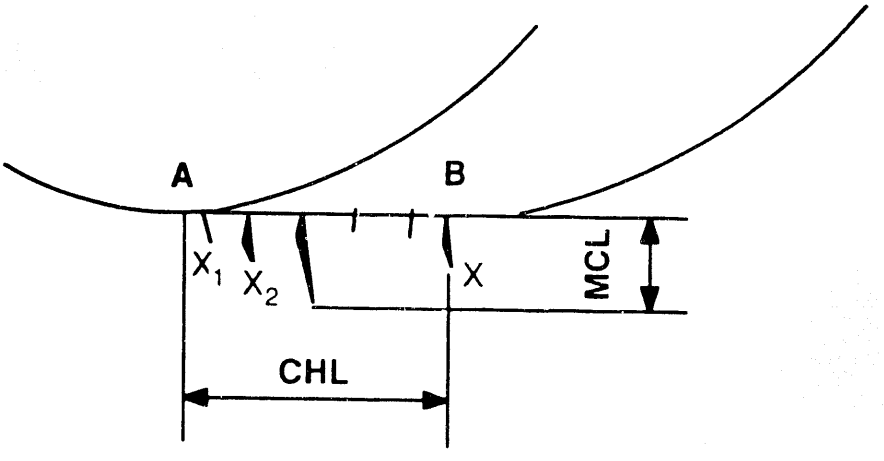

Maximum Crack Length (MCL) = Maximum of (X_1, X_2, ...X_i);

Total Crack Length (TCL) = Σ (X_1, X_2, ...X_i);

CHL = Length of A to B.

Figure 13. Schematic Illustration of the Varestraint Hot Cracking Criteria.

MATERIALS AND EXPERIMENTAL PROCEDURES

Materials

Ten small heats of modified 800H with variations in tungsten and/or nitrogen plus a low level of P and S were prepared by ORNL and tested to determine hot cracking sensitivity. One small heat and one commercial tubing heat of modified 800H prepared at Bobcock and Wilcox were also used for comparison in Varestraint hot crack testing. In addition, one heat of HR3C (commercial tubing heat) and one heat of 310Ta (small heat produced at ORNL) were employed in the evaluations. All materials were employed for the HAZ liquation/liquation cracking mechanism investigation by using a resistance spot welding technique. The tubing heat (V988-1) was used for a HAZ softening behavior investigation. The composition of the materials studied is listed in Table 1.

Experimental Procedures

The Varestraint hot cracking test method was used to evaluate hot cracking susceptibility. Testing conditions are summarized as follows:

Process	Autogenous GTAW
Current	100 Amp.
Voltage	12 V
Travel speed	4.23 mm/sec (10ipm)
Shielding gas	Argon - 0.85 m^3/hr (30 cfh)
(10 seconds pre- and post- weld purge)	
Electrode	2% thoriated tungsten
Arc length	1.6 mm (0.062 inch)
Polarity	DCEN
Interpass temperature	22°C

Table 1. Composition of Materials Studied.

	A	B	C	D	E	F	G	H	J	K	L	M+N (V988-1)	P	310Ta	HR3C-A1 (V35623)
C	0.11	0.08	0.08	0.11	0.16	0.15	0.11	0.11	0.05	0.082	0.116	0.10	0.113	0.051	0.046
S	0.009	0.009	<0.005	0.020	<0.005	<0.005	<0.005	0.008	0.011	0.012	0.006	0.006	-	0.003	0.010
P	0.013	0.013	0.013	0.013	0.013	0.014	0.013	0.014	0.014	0.008	0.006	0.022	-	-	0.018
Cr	20.50	20.37	20.33	20.96	19.83	19.97	20.26	20.13	20.20	20.87	20.27	20.13	19.49	24.87	24.23
Ni	29.33	29.26	30.23	30.17	29.63	29.93	30.03	29.47	29.83	30.56	29.15	30.09	29.95	20.21	18.68
Mo	1.97	2.01	2.03	2.05	0.58	1.09	1.09	0.09	0.09	1.90	1.05	1.89	0.97	-	0.18
Mn	1.96	1.96	2.01	2.00	0.50	0.98	0.50	0.97	0.97	2.08	1.85	2.00	2.61	1.53	1.61
Si	0.21	0.25	0.22	0.23	0.52	0.49	0.47	0.07	0.07	0.017	0.14	0.19	0.29	0.33	0.64
V	0.46	0.47	0.47	0.48	0.75	0.75	0.81	-	-	0.49	0.84	0.59	1.81	-	0.008
Al	0.04	0.03	0.04	0.04	0.93	0.05	0.87	0.44	0.43	0.090	0.079	0.01	-	-	-
W	-	-	<0.01	-	0.88	1.80	1.76	-	-	0.006	1.73	-	2.00	-	-
Ti	0.32	0.32	0.28	0.32	0.44	0.40	0.40	0.53	0.51	0.29	0.34	0.28	0.09	-	0.009
Nb	0.21	0.21	0.18	0.19	0.21	0.23	0.15	-	-	0.19	0.13	0.22	0.32	-	0.32
Ta	-	-	-	-	-	-	-	-	-	-	-	-	-	1.60	-
N	0.012	0.029	0.049	0.0088	0.028	0.027	0.026	0.0014	0.026	0.0094	0.039	0.007	0.097	-	0.202
Cu	-	-	-	-	-	-	-	-	-	0.01	0.01	0.01	-	-	0.08
B	-	-	-	-	-	-	-	-	-	0.005	0.0104	0.006	-	-	-
O	-	-	-	-	-	-	-	-	-	0.0018	0.0063	-	-	-	0.044
Co	-	-	-	-	-	-	-	-	-	-	-	-	-	-	0.12
Fe	Bal.	Bal.	Bal.	Bal.	Bal.	Bal.	Bal.	Bal.	Bal.	Bal.	Bal.	Bal.	Bal.	Bal.	Bal.

A Leco M-400-G1 type microhardness tester was utilized for conducting the hardness evaluation. The testing conditions included a 100 g load and 15 second loading time.

The Model 1500 Gleeble thermal mechanical simulator was used for simulating HAZ samples. The thermal cycle is characteristic of a SMAW weld in 38 mm (1-1/2 inch) thick stainless steel with an energy input of 2.8 kJ/mm (70 kJ/inch) at 22°C (72°) preheat. Seven peak temperatures (1001°C, 1090°C, 1145°C, 1200°C, 1260°C, 1290°C, and 1320°C) which represent different distances from the fusion line in an actual weld HAZ, were chosen for conducting the Gleeble thermal cycling.

The Gleeble thermal simulated samples were utilized to conduct electrolytic precipitate extraction. To extract the precipitates from the specimen, a known weight of sample was dissolved in a 10% HCl + 90% methanol solution at a 10 V constant potential with respect to a platinum cathode with a 2 ampere current at room temperature. Rigaku type x-ray equipment was used to analyze the extracted particles.

Metallographic and fractographic examinations were carried out using OLM, TEM (Hitachi H-600), STEM (Hitachi H-800) equipped with an EDS analytical system, and SEM (Cambridge 360) equipped with EDS and WDS chemical analytical systems. The quantitative chemical analysis programs (ZAF4/FLS and BP) were employed during EDS evaluations. Element line scanning across grain boundaries, especially in the HAZ, was undertaken. Element dot mapping of particular alloying elements was employed to evaluate the distribution of alloying and trace elements.

RESULTS AND DISCUSSIONS

Varestraint Hot Cracking Evaluation

Varestraint hot crack tests were conducted for all ten heats of the modified 800H materials (as indicated in Table 1). For the purpose of comparison, one heat of modified 310 (310Ta) and one heat of HR3C (V35623) were also used. The complete information on the hot cracking susceptibility of the materials evaluated using the Varestraint hot crack test includes fusion zone, weld metal HAZ and the base metal HAZ determinations. However, as indicated earlier, HAZ liquation cracking tendency is the major concern for these materials since non-matching filler materials will be used for actual weld. Thus, in this report, only base metal HAZ cracking results are presented.

Base Metal HAZ Liquation Cracking Results

Figure 14 shows the base metal HAZ hot cracking behavior in terms of total crack length measured in the Varestraint hot cracking test at 4% augmented strain. Heats F and G showed the greatest resistance to base metal HAZ liquation cracking resistance while Heats K and L showed the lowest hot cracking resistance among the materials evaluated. In general, most of the materials (except Heats K and L) evaluated passed the Varestraint hot crack testing total crack length criterion developed by Lundin et al. [11] and thus are generally resistant to weld cracking during good practice production welding.

Figure 15 shows the base metal HAZ hot cracking behavior in terms of the maximum crack length at 4% augmented strain. Heats F and G showed the best base metal HAZ liquation

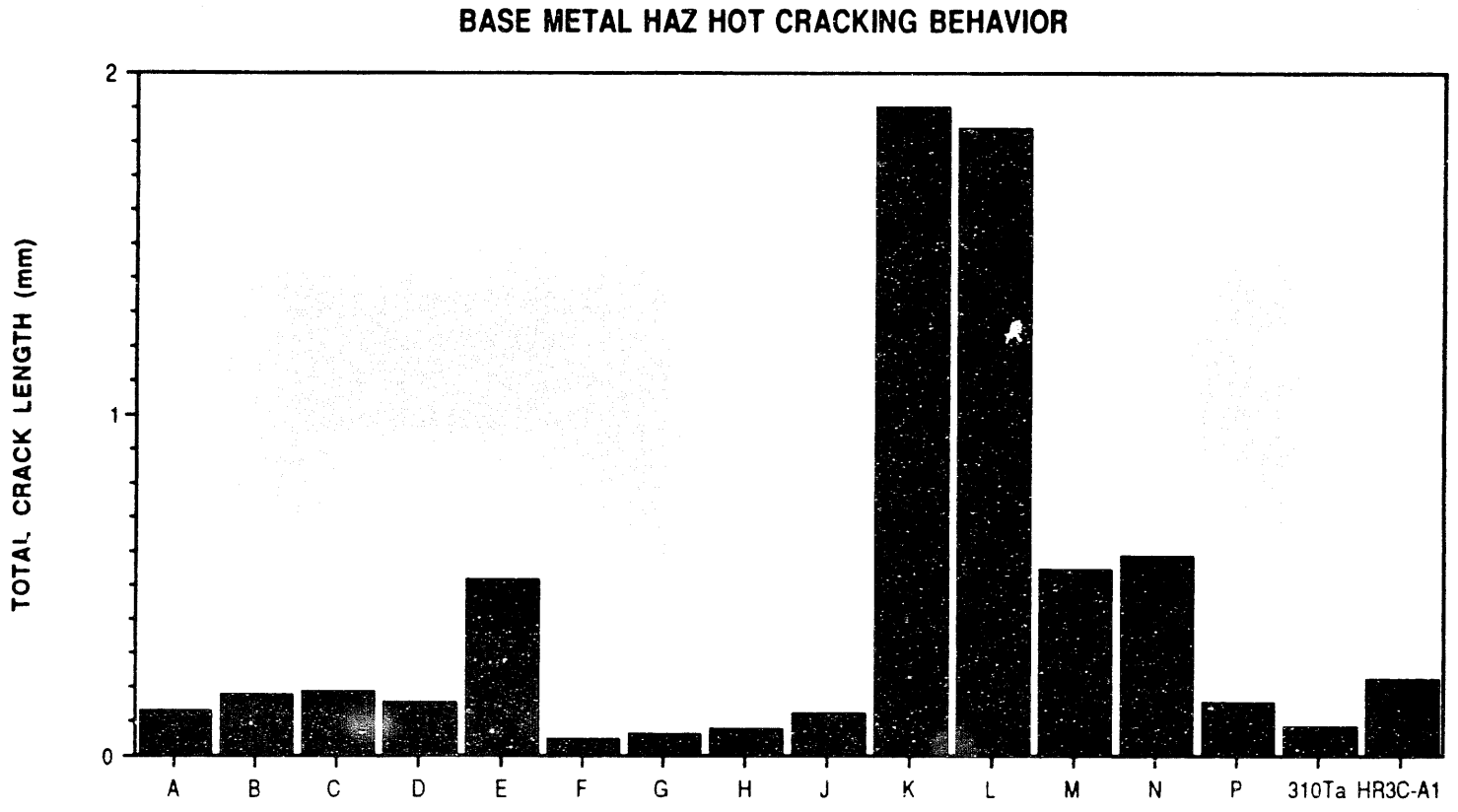

Figure 14. The Varestraint Testing Results in Terms of Total Crack Length at 4% Augmented Strain.

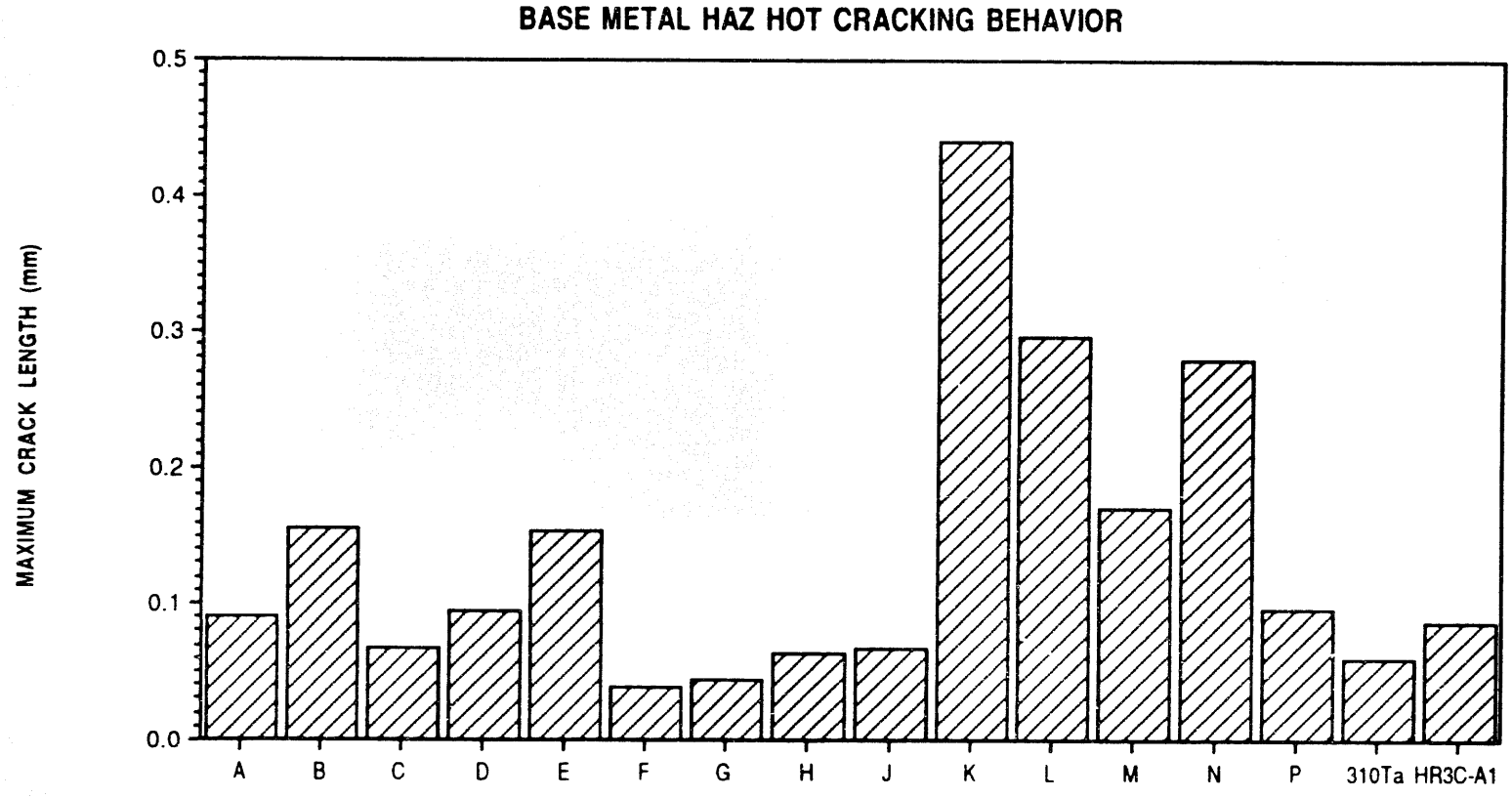

Figure 15. The Varestraint Testing Results in Terms of Maximum Crack Length at 4% Augmented Strain.

resistance and Heats K and L showed the lowest base metal HAZ liquation cracking resistance. All materials evaluated except Heats K, L, and N, passed the test according to the maximum crack length criterion developed by Lundin et al. [11].

Figure 16 shows the base metal HAZ hot cracking behavior in terms of cracked HAZ length (CHL) measured in the Varestraint samples at 4% augmented strain. Heats H and L showed the greatest HAZ liquation cracking resistance while the Heats K and L showed the lowest HAZ liquation cracking resistance. All the materials evaluated except Heats K, L, and N pass the Varestraint cracked HAZ length (CHL) criterion developed by Lundin et al. [11].

The Varestraint test results for the materials evaluated are summarized in Table 2. It is evident from Table 2 that three criteria (total crack length, maximum crack length and cracked HAZ length) exhibit good correlation. The relationship between these three criteria is shown in Figures 17 to 19. The results agree with the relationship obtained by Lundin et al. [11] during investigation on nuclear grade stainless steels. According the criteria, a material possesses a low hot cracking tendency if the total crack length (TCL) at 4% augmented strain is equal to or is less than 1 mm, the maximum crack length (MCL) at 4% augmented strain is equal to or is less than 0.2 mm and the cracked HAZ length (CHL) is equal to or is less than 1.8 mm. Heat N passed TCL criterion, however, failed the MCL and CHL criteria although the CHL value (1.95 mm) for Heat M is just slightly greater than 1.8 mm.

Comparison Between Weldability of Modified 800H and Other High Temperature Materials

Heat P of the modified 800H series was selected for a weldability comparison study. The preliminary comparison

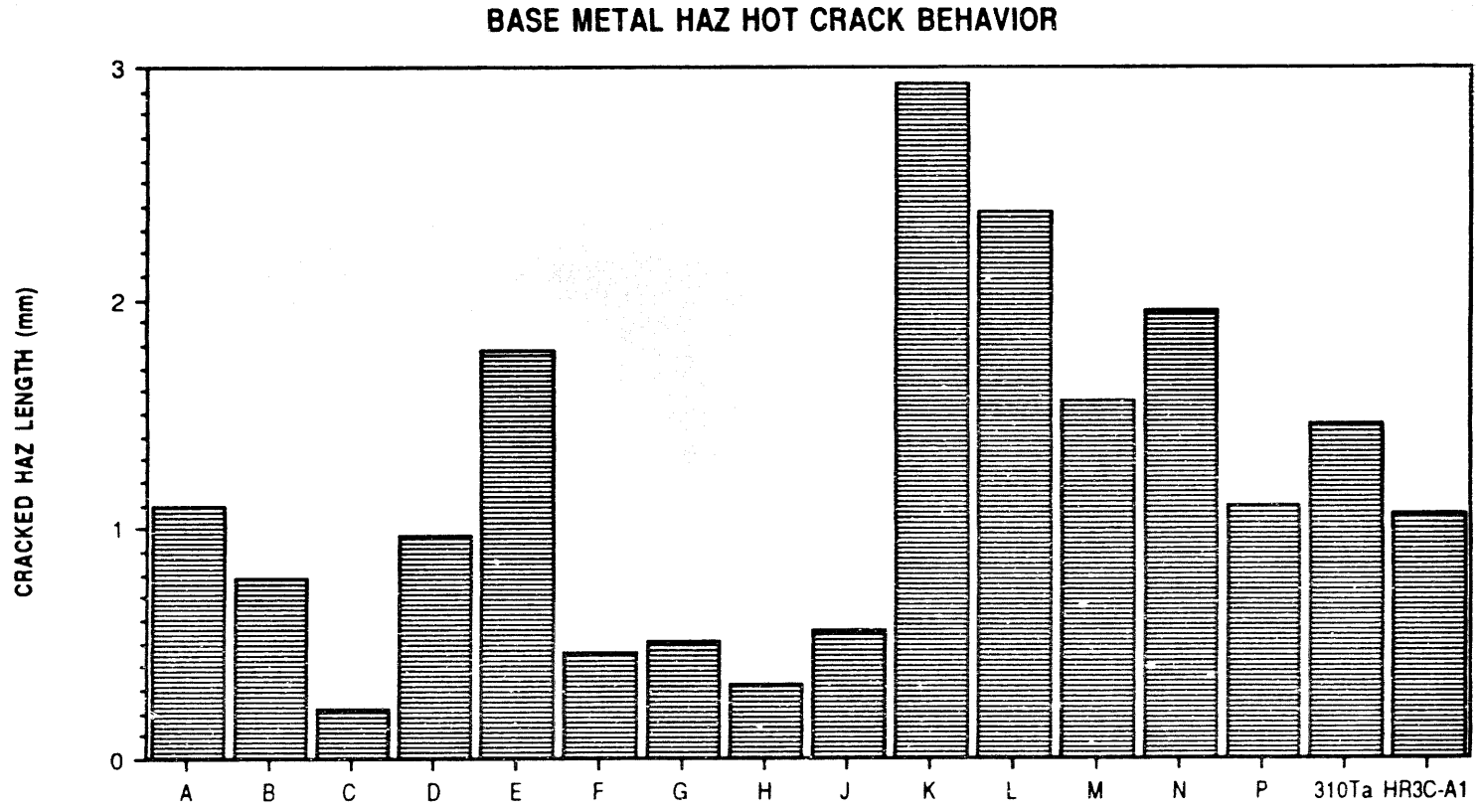

Figure 16. The Varestraint Testing Results in Terms of Cracked HAZ Length at 4% Augmented Strain.

Table 2. Summary of Base Metal Hot Cracking Behavior.

Materials Code	Base Metal HAZ Total Crack length (mm)	Base Metal Maximum Crack Length (mm)	Cracked HAZ Length (mm)
A	0.130	0.091	1.100
B	0.179	0.155	0.787
C	0.184	0.067	0.223
D	0.157	0.095	0.966
E	0.513	0.154	1.782
F	0.050	0.038	0.466
G	0.059	0.044	0.506
H	0.080	0.063	0.328
J	0.120	0.067	0.555
K	1.897	0.440	2.930
L	1.841	0.296	2.380
M	0.548	0.172	1.560
N	0.585	0.279	1.950
P	0.151	0.096	1.092
310Ta	0.081	0.060	1.449
HR3C-A1	0.223	0.086	1.056

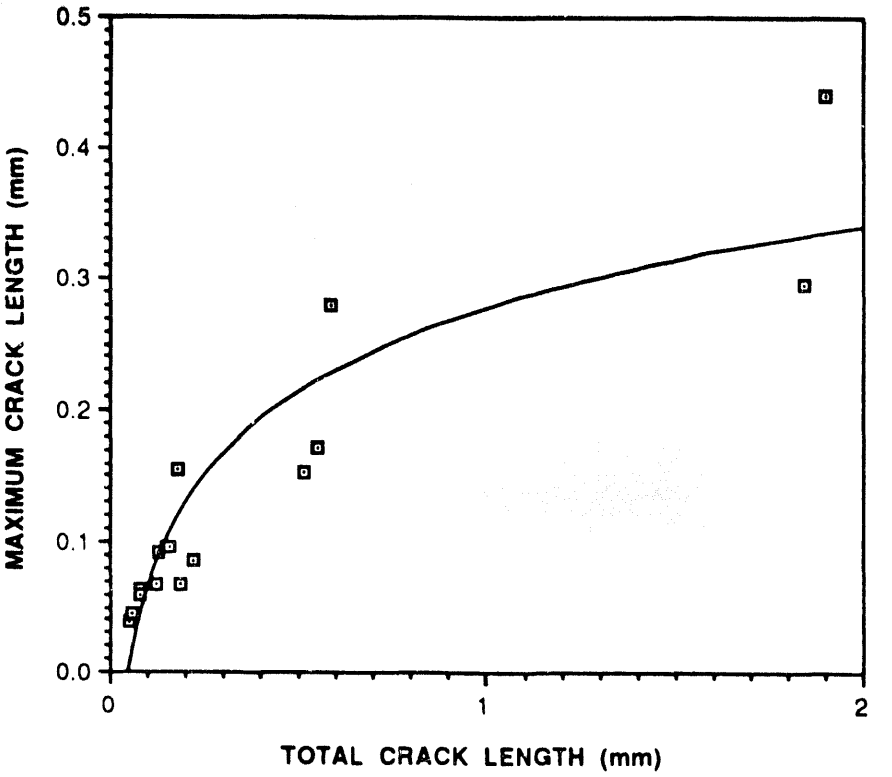

Figure 17. Relationship between Maximum Crack Length and Total Crack Length.

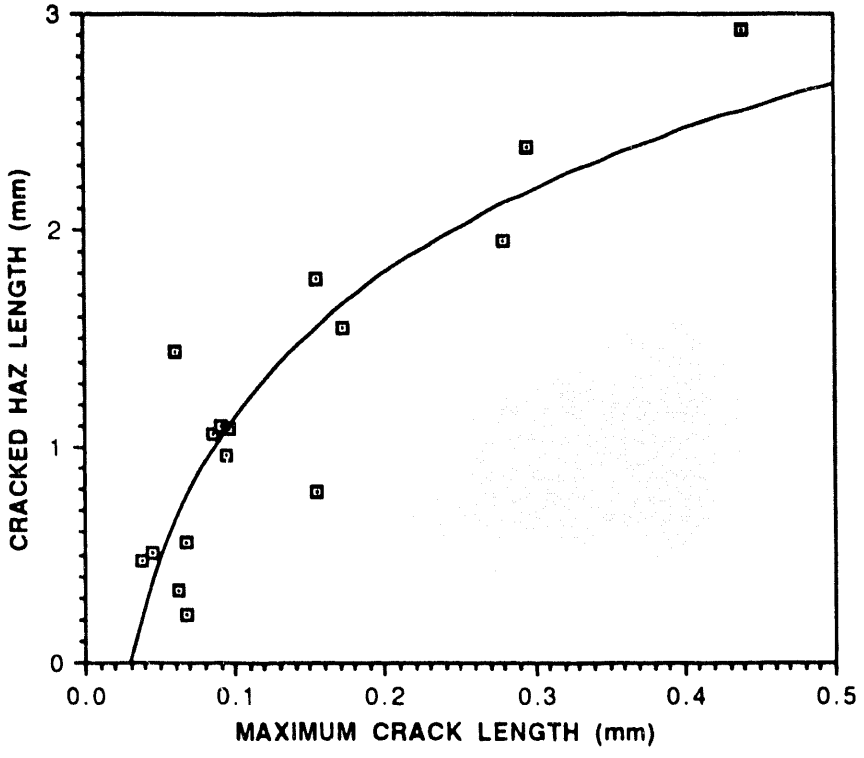

Figure 18. Base Metal HAZ Hot Cracking Behavior; Maximum Crack Length vs. Augmented Strain.

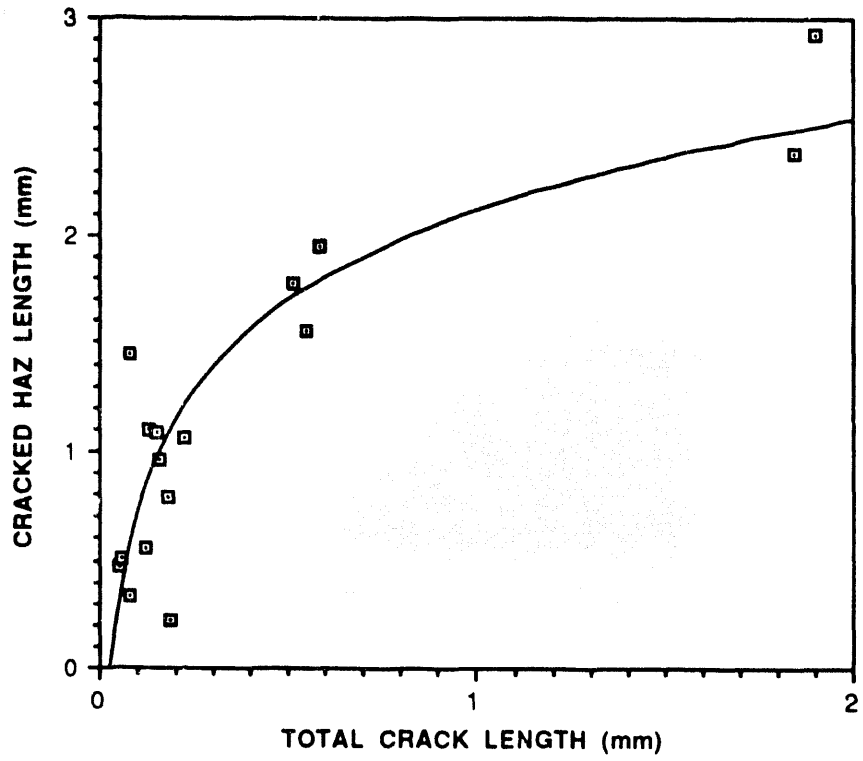

Figure 19. Base Metal HAZ Hot Cracking Behavior; Total Crack Length vs. Augmented Strain.

study includes two other high temperature materials (310Ta and HR3C-A). Figure 20 shows the HAZ liquation cracking behaviors of modified 800H (Heat P), 310Ta and HR3C-A1 in terms of TCL and MCL. All three materials exhibit good base metal HAZ liquation cracking resistance according to criteria developed by Lundin et al. [11]. Figure 21 shows in bar graph form the HAZ liquation cracking tendencies of the three materials. It is evident that modified 800H with a controlled grain size (Heat P) has an equal or better HAZ liquation cracking resistance than the commercialized tubing heat HR3C-A1 and experimental heat 310Ta. This result manifests that modified 800H materials with a controlled base metal grain size possess good weldability in terms of base metal HAZ liquation cracking.

Metallographic Examinations on the Varestraint Samples

Heats E and F were selected for SEM metallographic examination since Heat E showed a relatively high base metal HAZ hot cracking propensity while heat F showed the lowest HAZ hot cracking tendency among the ten modified small heats. The general microstructural morphologies in the HAZ and the liquation cracking morphology in modified 800H are shown in Figure 22. It can be clearly observed that a partial melted zone, grain boundary migration, grain boundary liquation, constitutional liquation and liquation induced cracking exist in the HAZ of modified 800H.

Figure 23 shows the SEM microstructural morphology of a liquation crack region from a Varestraint tested sample of Heat E. Particles of various sizes are distributed along the grain boundaries as well as in the grain matrix. Back-scattered electron imaging revealed that heavy elements (such as Mo, Nb, W) may be segregated along the crack and in adjacent regions (see arrows). The dark particles in the

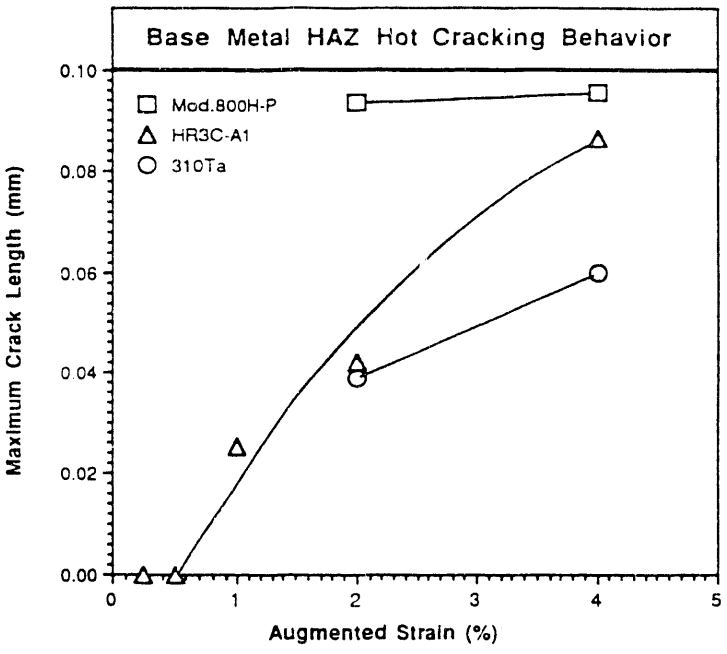

(a)

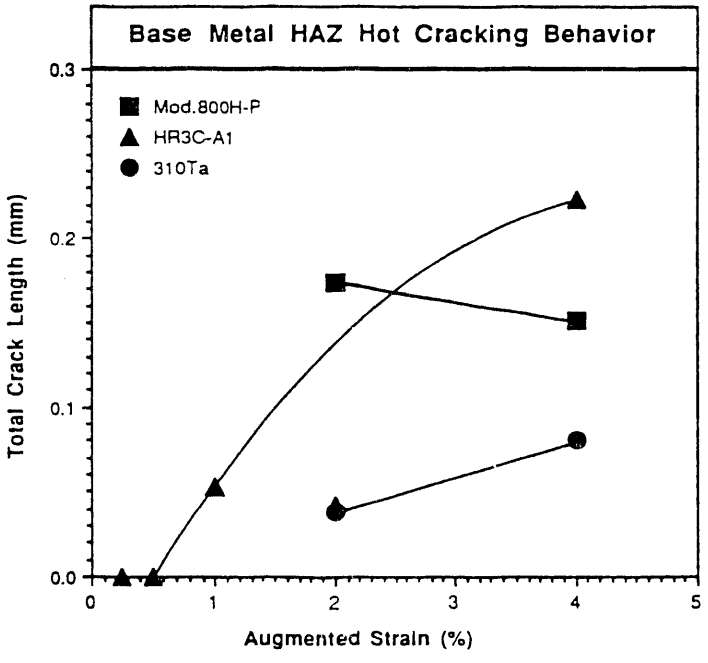

(b)

Figure 20. Comparison of the HAZ Hot Cracking Susceptibility Among the Modified 800H, 310Ta and HR3C Materials. (a) Maximum Crack Length vs. Augmented Strain; (b) Total Crack Length vs. Augmented Strain.

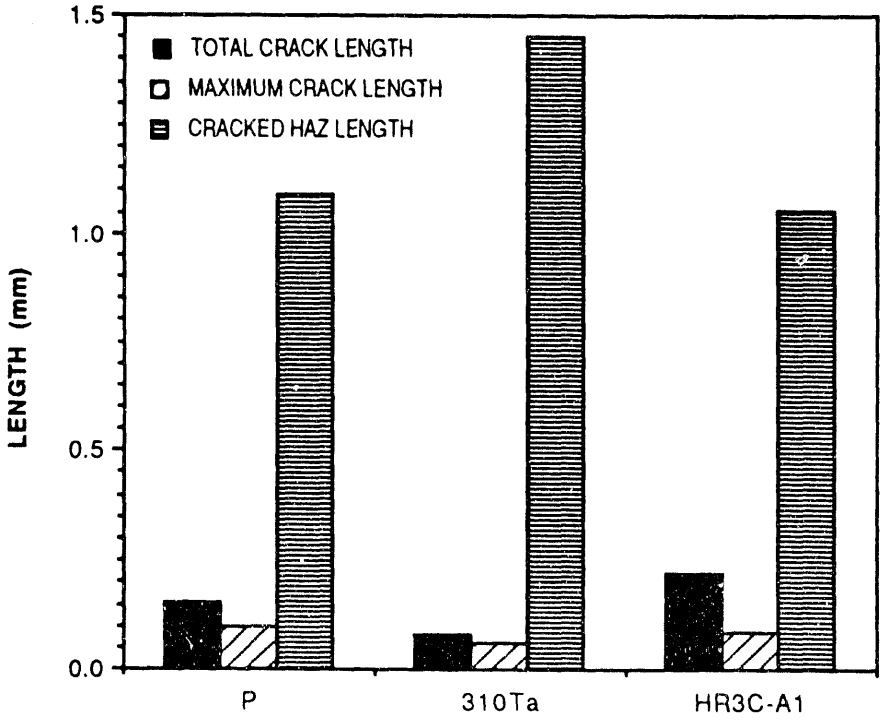

Figure 21. Bar Graphs Showing Comparison of the HAZ Cracking Behavior Among the Modified 800H, 310Ta and HR3C.

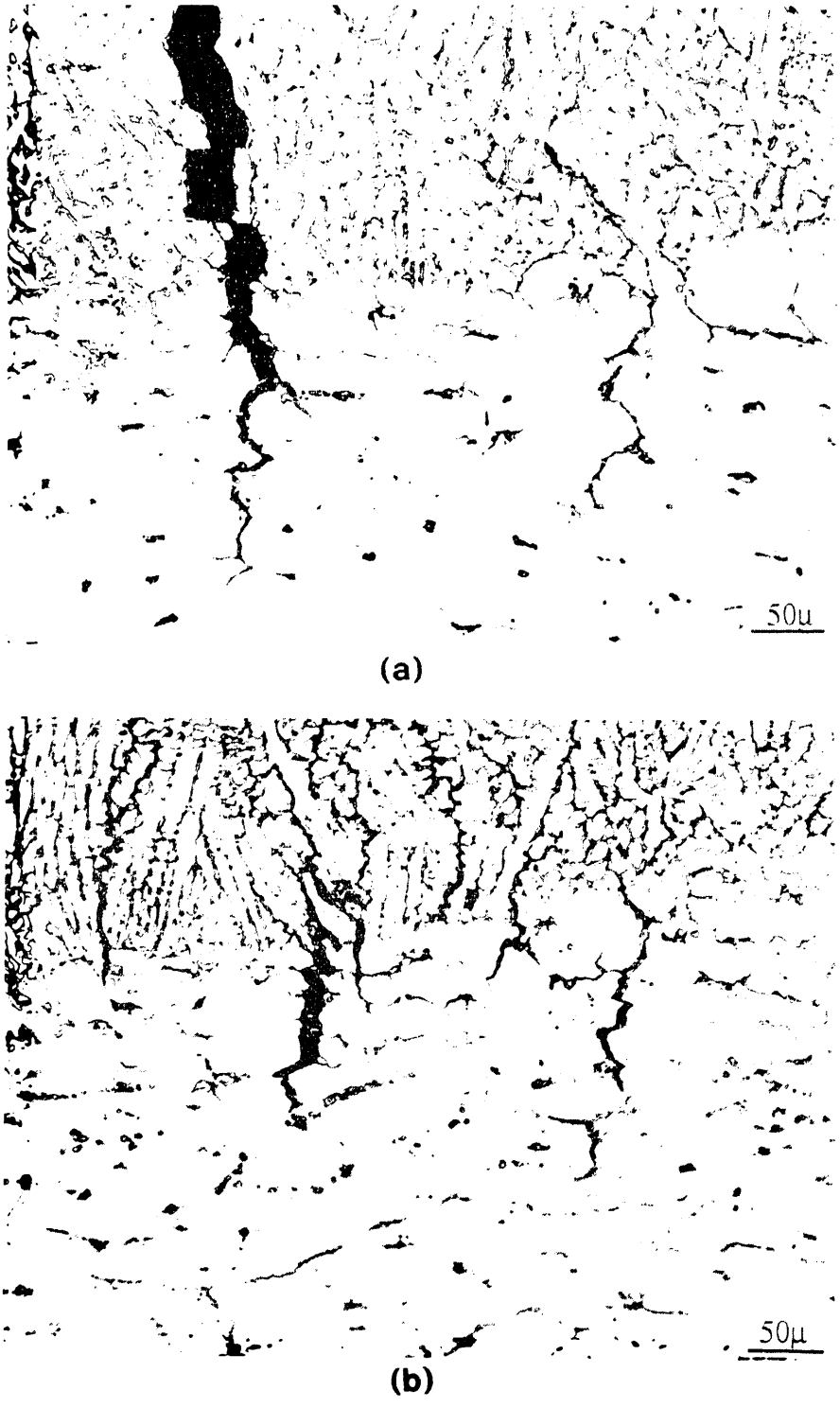

Figure 22. HAZ Morphology of the Varestraint Tested Sample in Modified 800H. (a) Heat E and (b) Heat F.

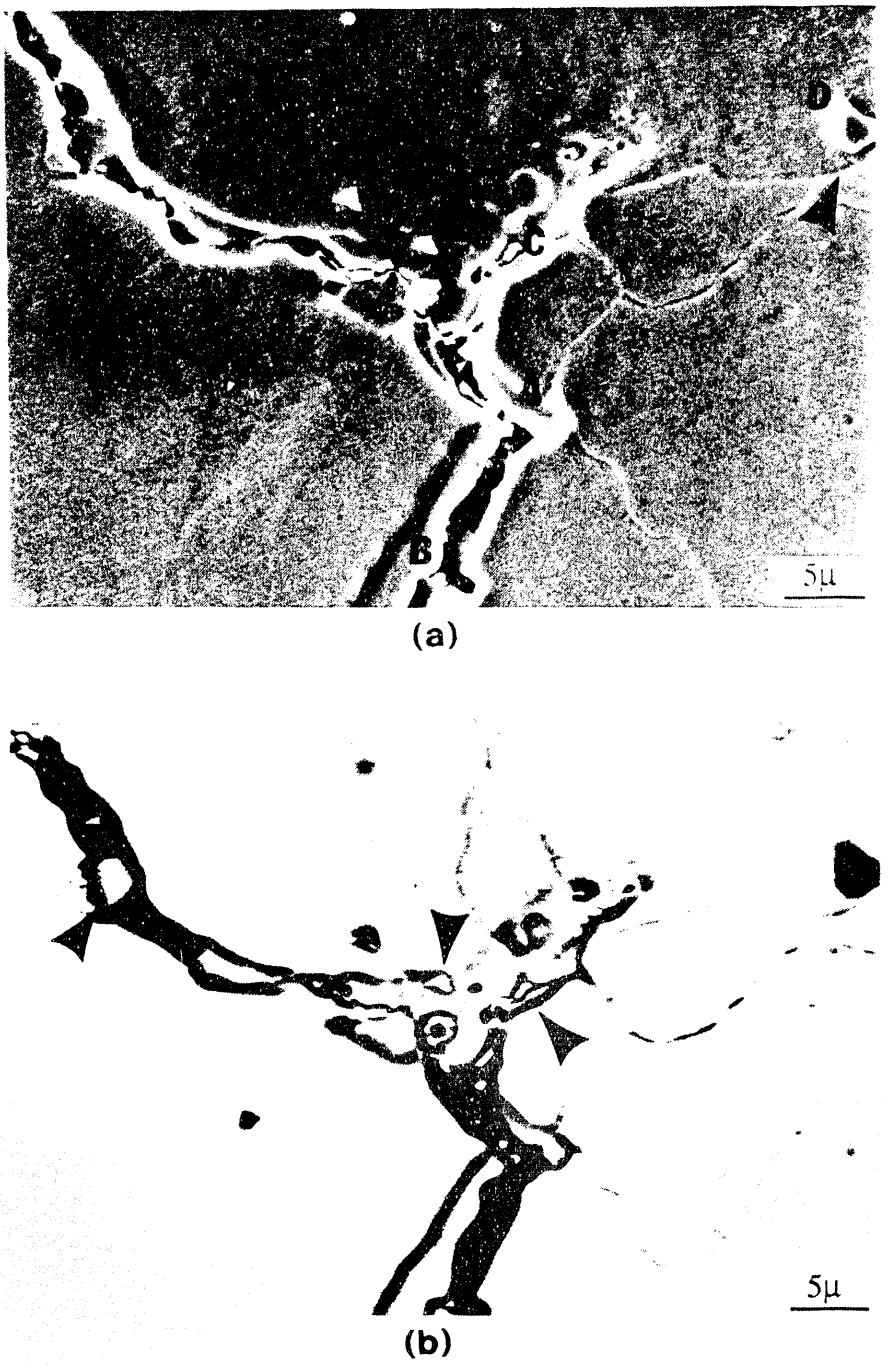

Figure 23. Microstructural Morphology of HAZ Cracking and Liquated Grain Boundaries in Heat E. (a) Secondary Electron Imaging; and (b) Back-scattered Electron Imaging.

micrograph are primarily TiC which are mainly found in the matrix. Semi-quantitative chemical analysis was performed at several locations indicated by the arrows and letter designations. The major alloying and trace elements detected at these locations are summarized in Table 3. As indicated in Table 3, S and P are concentrated in the precipitates present adjacent to the grain boundaries which were nucleated as a result of liquation (liquid reaction with the matrix). The results of element line scans and element dot mapping agree with the EDS spot analysis. The element line scan results for Ni, Cr, Ti and Nb are shown in Figure 24 while dot mapping for the same elements is shown in Figure 25. No segregation of Cr was found. Slightly increased segregation along the crack and a reduction adjacent to crack in Ni is indicated. A significant segregation of Ti and Nb is evident in the cracked region. These results again show that a higher Nb and Ti concentration plus S and P segregation occurs along the grain boundaries which have liquated and cracked in the Varestraint test.

Table 3. Composition (wt%) at locations in Figure 5

	Cr	Ni	Ti	Nb	V	Si	Al	S	P	W
A	25.49	25.10	3.2M	2.6M	1.3M	0.1M	0.5M	0.6M	0.5M	0.73
B	21.76	26.91	11M	22M	1.3M	1.5M	1.3M	1.4M	1.5M	0.96
C	22.42	29.80	1.2M	1.2M	1.2M	1.3M	1.2M	1.2M	1.2M	0.94
D	8.35	5.63	567M	9.8M	4.9M	0.4M	3.8M	1.1M	1.3M	0.69
E	15.03	16.81	218M	3.2M	2.4M	1.3M	4.3M	1.3M	1.5M	0.80
F	15.00	18.77	60M	88M	1.1M	2.1M	1.5M	1.5M	1.9M	0.85
G	20.38	30.07	M	M	M	M	M	M	M	0.88

*. "M" chemical content in matrix; Contents less than or greater than or equal to the matrix, the "M" is preceded by a multiplier.

Heat F has the greatest liquation cracking resistance among the ten small heats. Figure 26 shows the SEM microstructural morphology on HAZ region in Heat F. Chemical

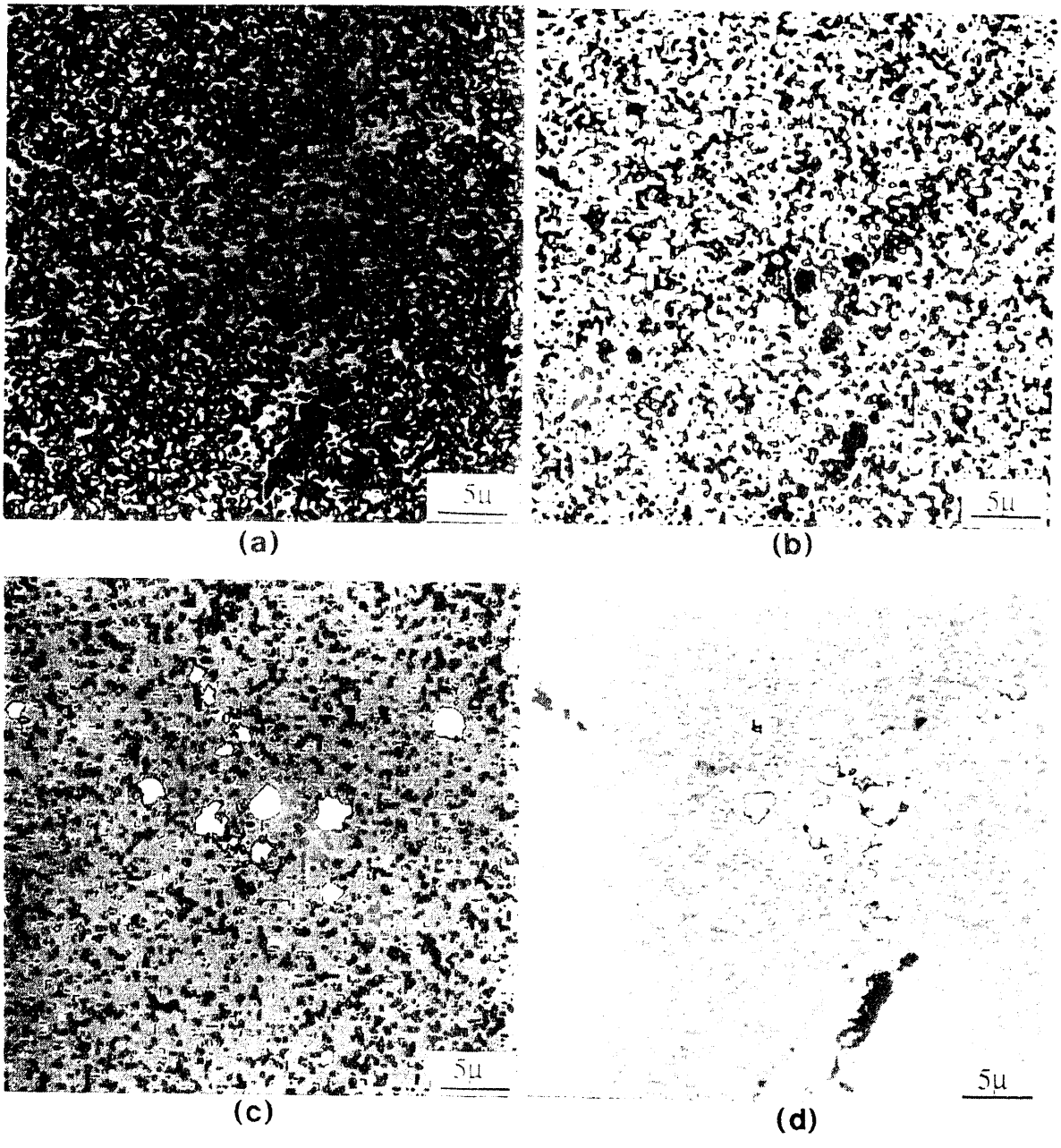

Figure 24. Element Dot Mapping of HAZ Region in Heat E. (a) Dot Mapping for Ni; (b) Dot Mapping for Cr; (c) Dot Mapping for Ti, and (d) Dot Mapping for Nb.

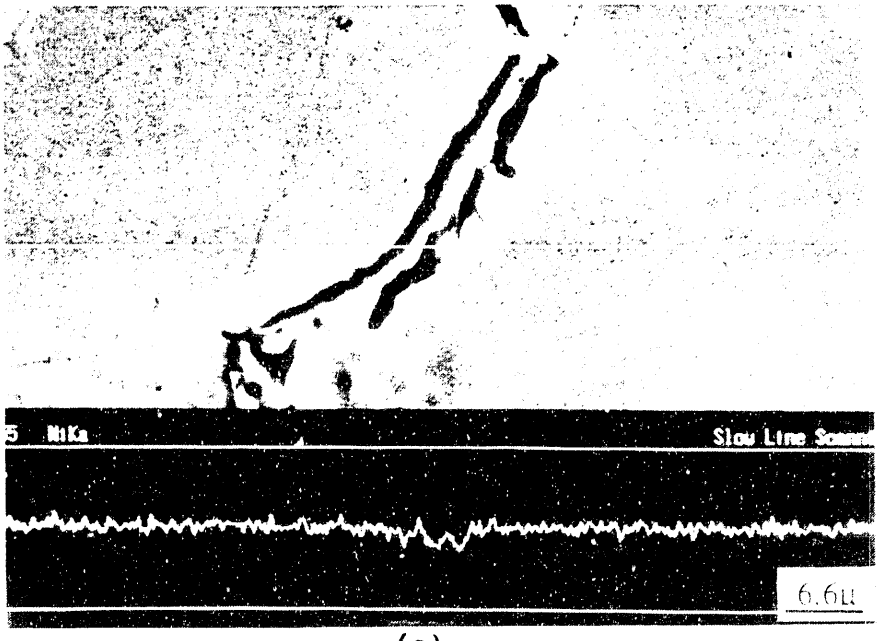

(a)

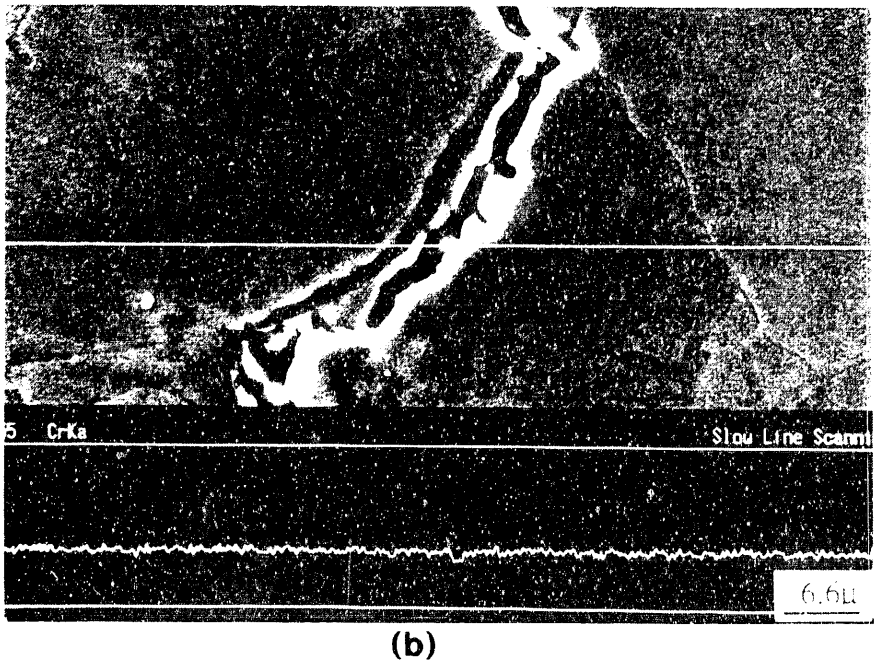

(b)

Figure 25. Element Line Scans Across Liquated Grain Boundary in Heat E. (a) Line Scan for Ni; (b) Line Scan for Cr. (c) Line Scan for Ti; and (d) Line Scan for Nb.

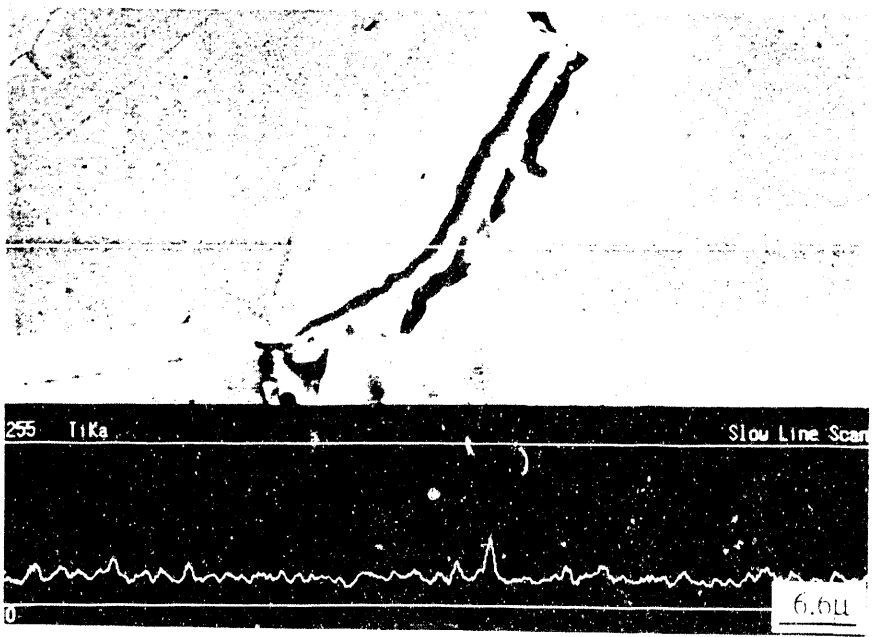

(c)

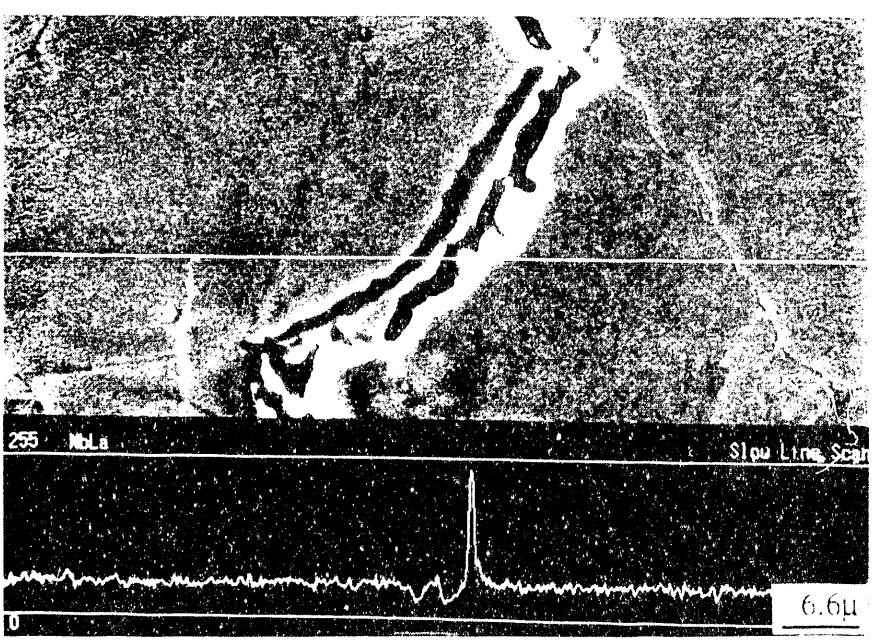

(d)

Figure 25. (Continued)

(a)

(b)

Figure 26. Microstructural Morphology of Liquated Grain Boundaries in HAZ of Heat F. (a) Secondary Electron Imaging; (b) Back-scattering Imaging.

analysis was carried out at locations A, B, C, and D. The EDS results are summarized in Table 4.

Table 4.Composition (wt%) at the locations in Figure 8

	Cr	Ni	Ti	Nb	Si	Al	S	P	W
A	18.84	29.39	1M	0.9M	0.8M	0.8M	0.9M	0.9M	1.3M
B	19.08	29.50	1M	1M	0.9M	0.9M	1M	1M	1M
C	19.54	29.27	M	M	M	M	M	M	M
D	18.90	26.29	13M	2.9M	0.9M	0.9M	1M	1M	1M

*. "M" chemical content in matrix; Contents less than or greater than or equal to the matrix, the "M" is preceded by a multiplier.

It is noted that at the tip of crack (location A in Figure 26) the Si content is higher and the small precipitates along the migrated grain boundary are Ti, Nb and Si rich (location B) and Ti, S, and P rich particles are present along grain boundaries in the HAZ. However, no significant heavy element segregation (such as Nb and Mo) was detected along the liquid grain boundaries in the HAZ. The results of dot mapping agree with the EDS spot results. The element dot mapping results for Mo, Ti, W and Cr are shown in Figure 27.

Examination of the GTA Welded Sample

It is noticed that Heat A and K have basically the same composition, however, a significant difference of their base metal HAZ liquation cracking resistance is exhibited according to the Varestraint test results. Metallographic examinations revealed that a different grain size between two heats may be responsible for their differing HAZ liquation cracking tendencies. Figure 28, a bar graph of the total crack length for all materials studied, indicates the HAZ grain size which was measured adjacent to the fusion zone. It can be seen that the HAZ liquation cracking tendency is

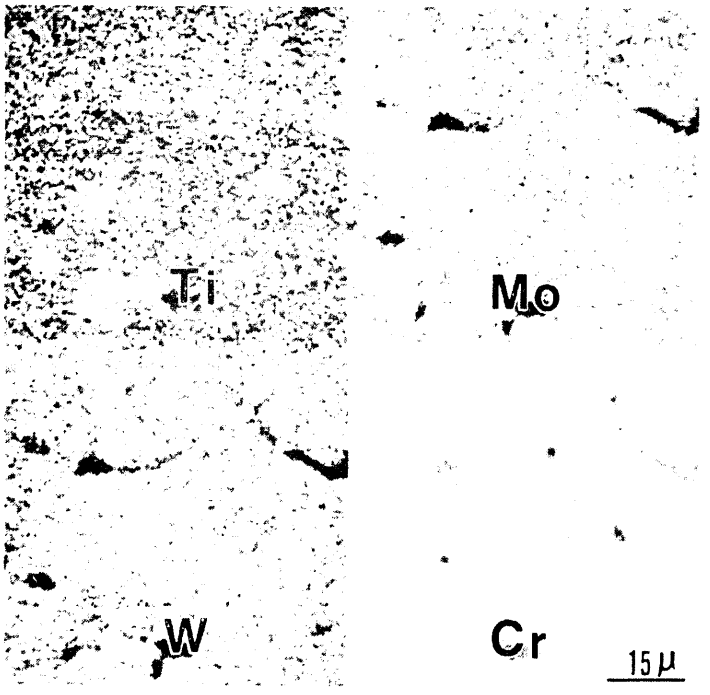

Figure 27. Element Dot Mapping of HAZ Region in Heat F.

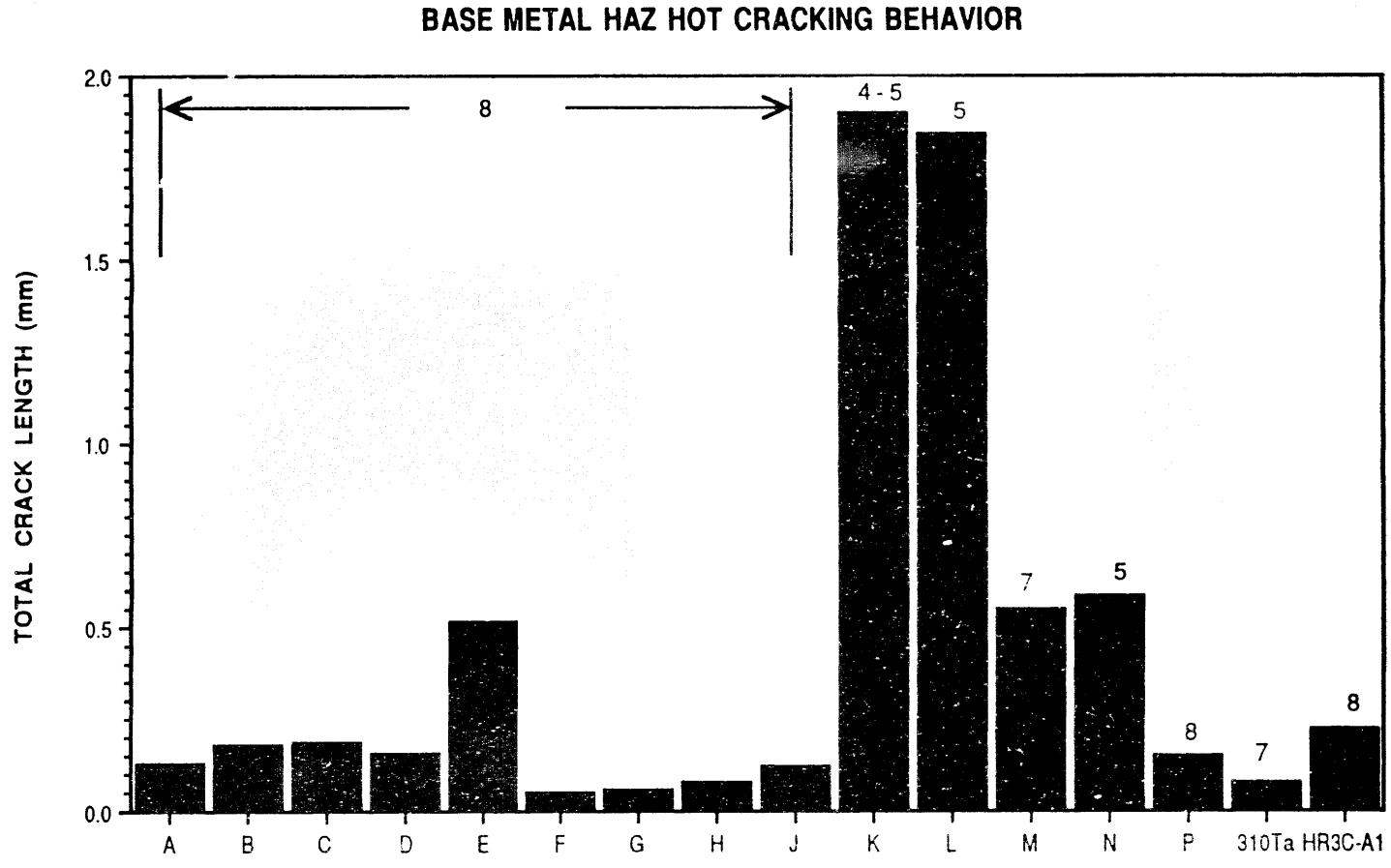

Figure 28. A Bar Figure Depicts the Relationship between Base Metal HAZ Hot Cracking Behavior and Grain Size.

dominantly influenced by the grain size in the HAZ adjacent to fusion zone. Figures 29 and 30 show photomicrographs of the HAZ's of GTA welds in Heats F and K, respectively. It is evident from these figures that grain boundary segregation behavior can be varied by changing the grain size, therefore, HAZ liquation cracking tendency is similarly altered. Few researchers [47] have carefully investigated the influence of grain size on the HAZ liquation cracking tendency in detail although this effect has been recognized for same time. Thompson et al. [47] claimed that the HAZ microfissuring susceptibility in alloy 718 is linearly dependent on the grain size. They explained that the effect of grain size on microfissuring is related to both the liquid distribution and grain boundary sliding. A large grain size would lead to a thicker liquid layer than a small grain size if the same volume of liquid is present in both cases. A larger volume fraction of intergranular liquid could increase the temperature range and time duration during which the liquid wets the grain boundary faces under nonequilibrium freezing conditions. However, the above explanations about the grain size effect on liquation cracking susceptibility can not precisely explain the observations in this study. Therefore, a detailed discussion on a new model of HAZ intergranular liquation is given in the following sections.

HAZ Liquation Behavior in Modified 800H Materials (Examination of Electric Resistance Spot Welded Samples)

In order to study the relationship between HAZ hot cracking susceptibility and HAZ liquation behavior in the modified 800H alloys it was considered necessary to take an advantage of rapid heating and cooling cycles characteristic of electric resistance spot welding.

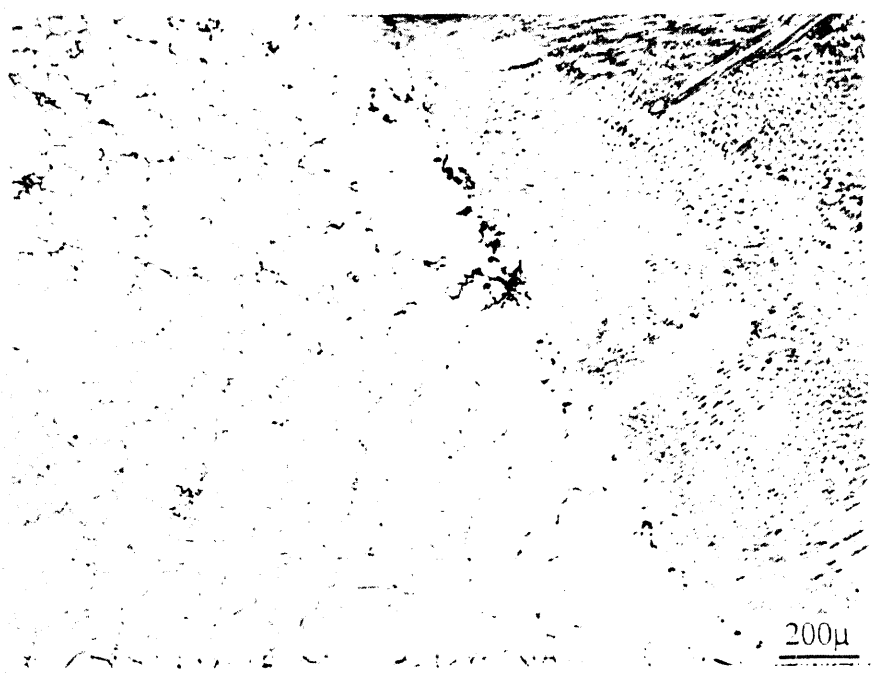

Figure 29. A General Microstructural Morphology of the HAZ in Modified 800H (Heat K).

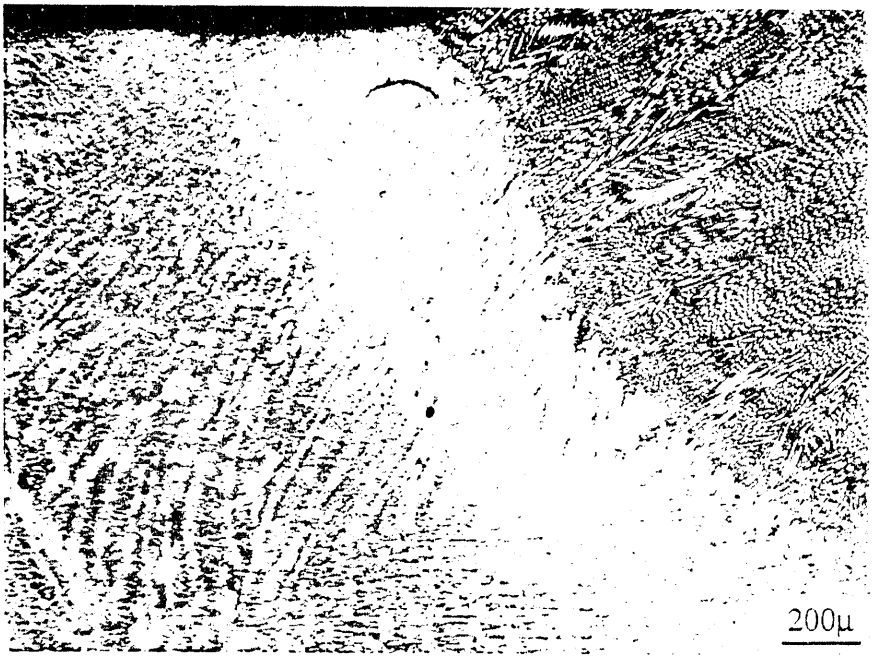

Figure 30. A General Microstructural Morphology of the HAZ in Modified 800H (Heat F).

Careful metallographic examinations were undertaken for all the modified 800H alloys, 310Ta and HR3C-A1. Liquation in the HAZ of conventional and super austenitic stainless steels can be classified into following categories:

1) Intragranular liquation, includes

   i. Liquation caused by segregation,

   ii. Liquation caused by reactions between a secondary phase and the matrix (constitutional liquation);

2) Intergranular grain boundary liquation, includes four basic types

   i. Isolated grain boundary liquation without the occurrence of an eutectic reaction. The materials which show this type of liquation have the lowest HAZ liquation cracking susceptibility. The liquid is always located at the corners and/or edges of grain boundaries (wetting between the liquid and grain matrix along the boundary is minimal).

   ii. Nonuniformly distributed grain boundary liquation. Eutectic reactions are often involved during liquid formation. The eutectic reactions occur between the matrix and a grain boundary which exhibits segregation of certain alloying or trace elements and/or the existence of secondary phase particles. The width of the grain boundary is depended on the local chemical composition distribution and distance to the fusion zone since eutectic reaction occurrence is dependent on both the chemical composition and the temperature distribution. The materials which show this type of grain boundary liquation during welding have a intermediate HAZ liquation cracking tendencies since "healing" is usually involved.

iii. Uniformly distributed grain boundary liquation. This type of liquation usually surrounds the entire grain in the partially melted HAZ. In most cases evidence of diffusion can be observed. Diffusion along grain boundaries and in the matrix occurs, however, no eutectic type reaction appears. Materials which show this type of liquation exhibit a high HAZ liquation cracking tendency. (In this case, liquation cracking increase with an increase in the thickness of the liquid along the grain boundaries.)

iv. Thin film type grain boundary liquation. This type of grain boundary liquation usually does not result in extensive films surrounding entire grains. For this case, the liquated grain boundary length is short, however, once a crack is initiated it will remain without healing (if the cracks are not directly connected to the fusion zone). Liquation evidence can be only observed at higher magnification for enhanced resolution. The materials with this type of grain boundary liquation in the HAZ during welding show the highest HAZ liquation cracking tendency.

Figure 31 schematically shows the classifications of HAZ grain boundary liquation in the conventional austenitic stainless steels and super austenitic stainless steels. In addition to the above definition another parameter is proposed for evaluating HAZ liquation/liquation cracking tendency. The concept is schematically illustrated in Figure 32. The maximum length of a liquated grain boundary (MLLGB), measured parallel to the temperature gradient, is correlated with the embrittlement temperature range (ETR). However, measurement of the MLLGB is dependent on technique related accuracy defining the extent of a liquated grain boundary.

The darkened areas in this figure are liquated at elevated temperature

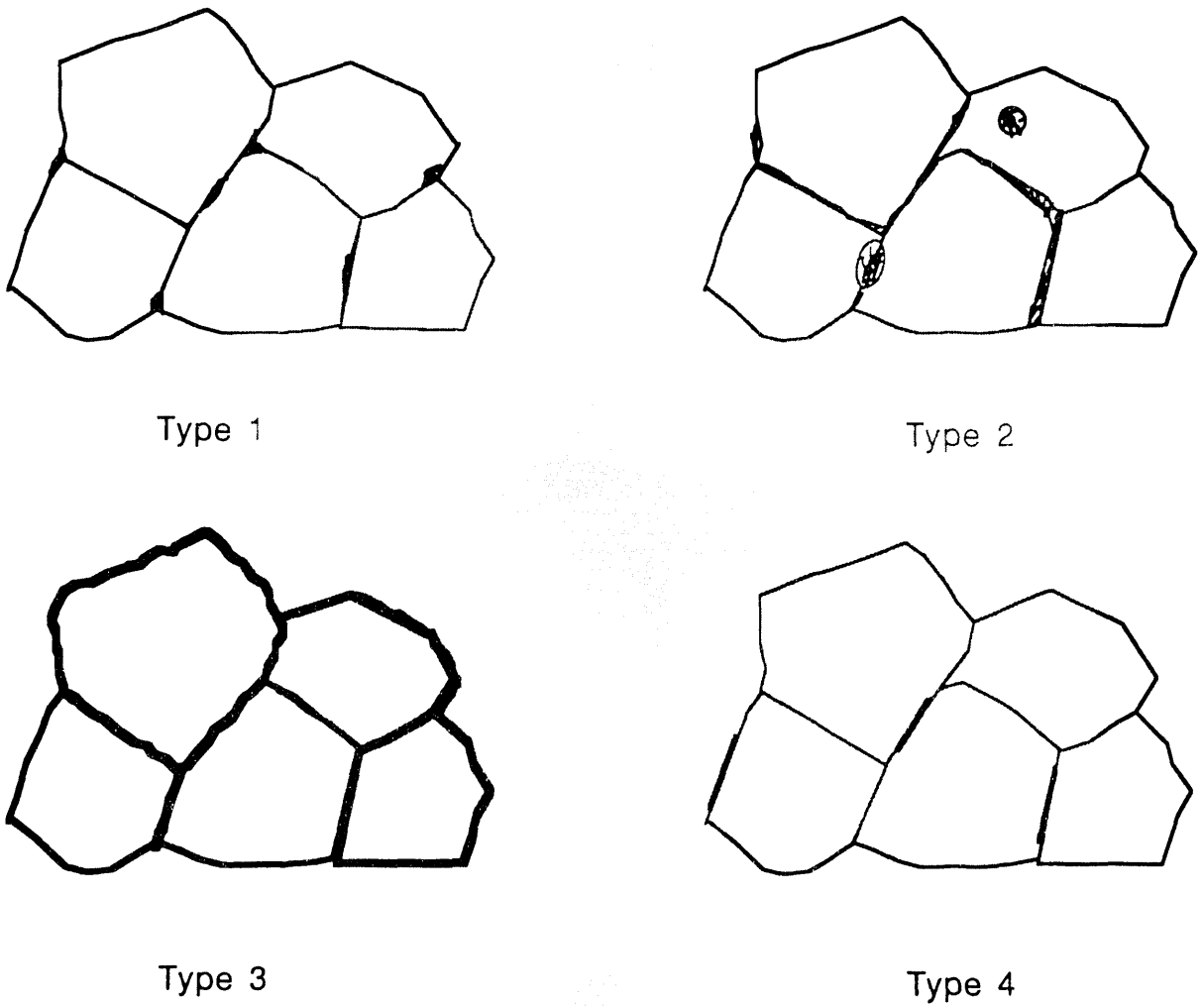

Figure 31. Schematic Illustration of the HAZ Grain Boundary Liquation Type.

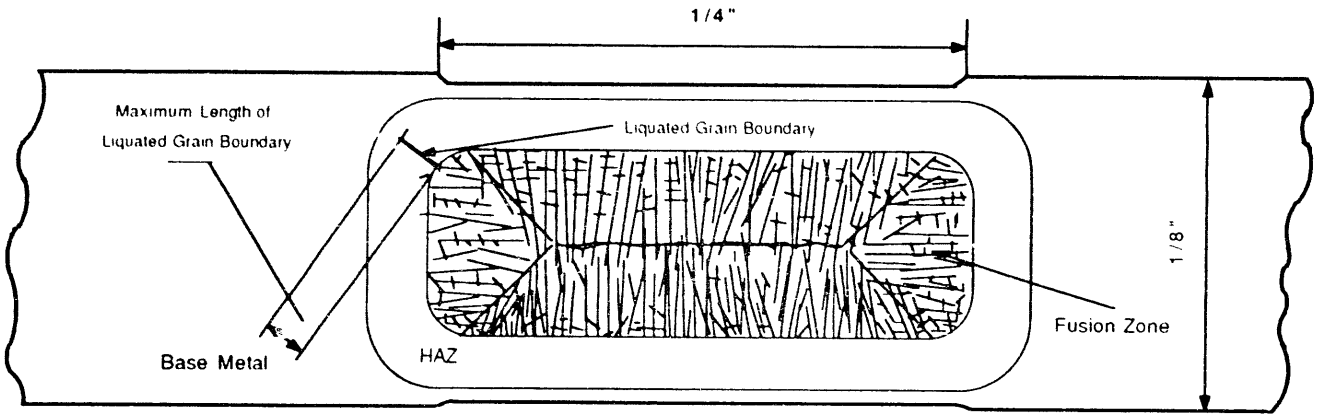

Figure 32. Schematic Illustration of the Concept of Maximum Length of Liquated Grain Boundary.

Therefore, this concept can be only used as a semi-quantitative criterion. To precisely interpret the HAZ liquation cracking resistance, a Varestraint hot cracking test should be performed since MLLGB is an indirect cracking evaluation method (predicting cracking susceptibility from liquation behavior). For resistance welds it is to be noticed that the locations which have the shallowest temperature gradient are at the "corners" of the fused nugget. Therefore, the MLLGB is usually obtained at these locations. All fifteen heats of the alloys were used in this study. The aim of the study was to generate information on, 1) relationship between chemical composition and the HAZ liquation type; 2) liquation type and HAZ liquation cracking susceptibility, 3) grain size influence on liquation cracking susceptibility, and 4) assessment of the MLLGB in the HAZs. With exception of the first goal all tasks were completed. A summary of HAZ liquation behavior is tabulated in Table 5.

Figures 33 to 36 show examples of the four typical types of HAZ liquated grain boundaries in modified 800H alloys (isolated grain boundary liquation, nonuniformly distributed grain boundary liquation (always with an eutectic reaction between the grain boundary and matrix), uniformly distributed grain boundary liquation and thin film type grain boundary liquation, respectively).

When the TCL, MCL and CHL (the Varestraint test criteria) were compared with the MLLGB (electric resistance spot weld liquation study criterion), no clear correlation was found. However, when a coefficient for the MLLGB (the values of the coefficient depended on the type of grain boundary liquation) is applied then, a clear relationship between the HAZ resistance spot welding criterion (MLLGB index) and Varestraint hot cracking testing criteria (MCL and CHL) is evident. The relation between the MLLGB index and CHL is shown in Figure 37. To precisely obtain the values of

Table 5. Summary of Results of HAZ Liquated Grain Boundary Examination.

Heats	Type of HAZ liquation	Maximum length of liquated grain boundary (MLLGB) (mm)	MLLGB Index
A	2	0.22	0.44
B	2	0.10	0.20
C	2	0.12	0.24
D	2	0.35	0.70
E	3	0.20	0.60
F	1	0.42	0.42
G	1	0.20	0.20
H	1	0.02	0.02
J	1	0.05	0.05
K (CE3891)	3	0.52	1.56
L (BW5480)	3	0.25	0.75
M (V988-1)	4	0.40	1.60
N (V988-1)	4	0.16	0.64
P	2	0.11	0.22
310Ta	1	0.11	0.11
HR3C-A1	2	0.07	0.14

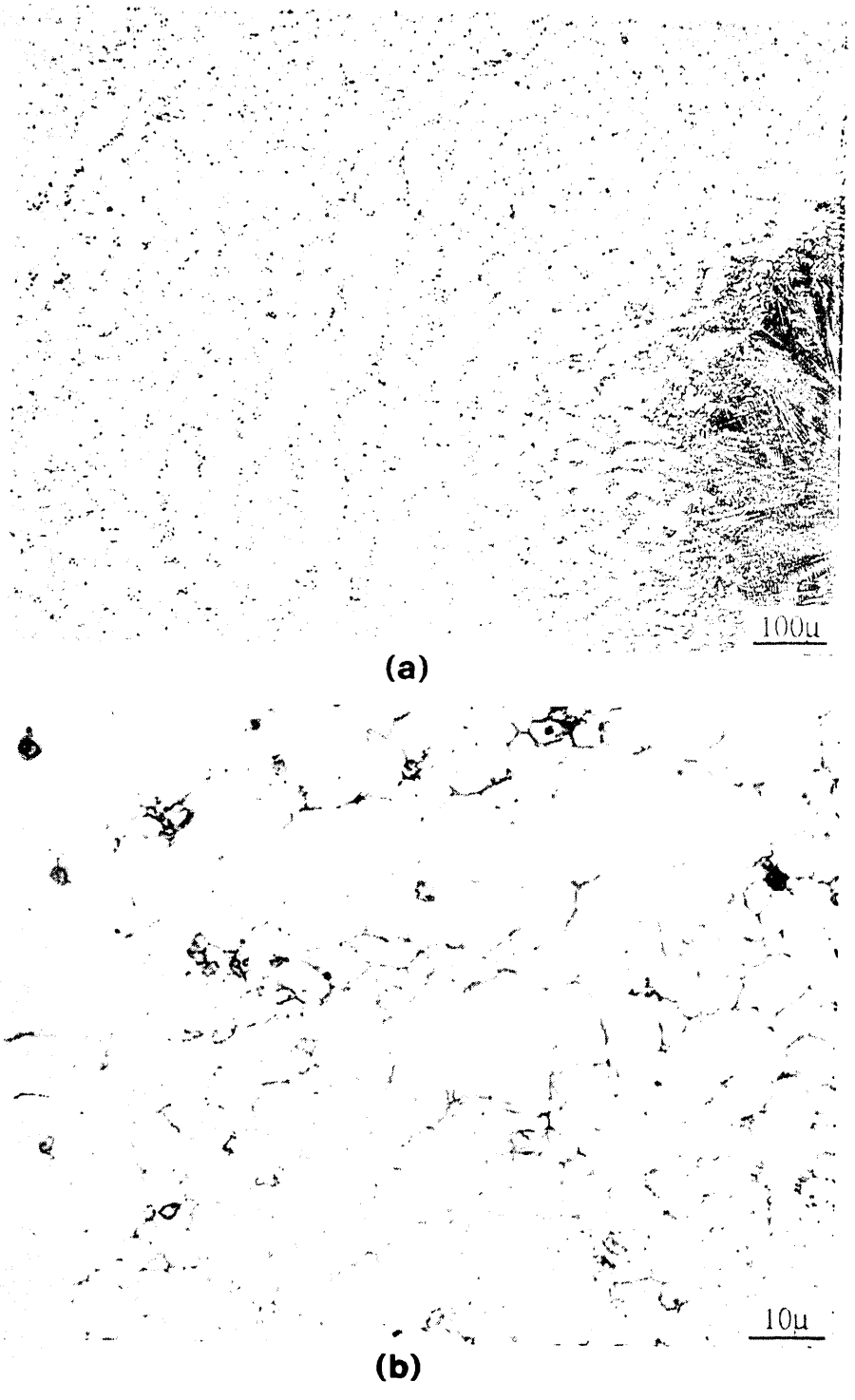

Figure 33. A Photomicrograph Shows the Type I Grain Boundary Liquation.

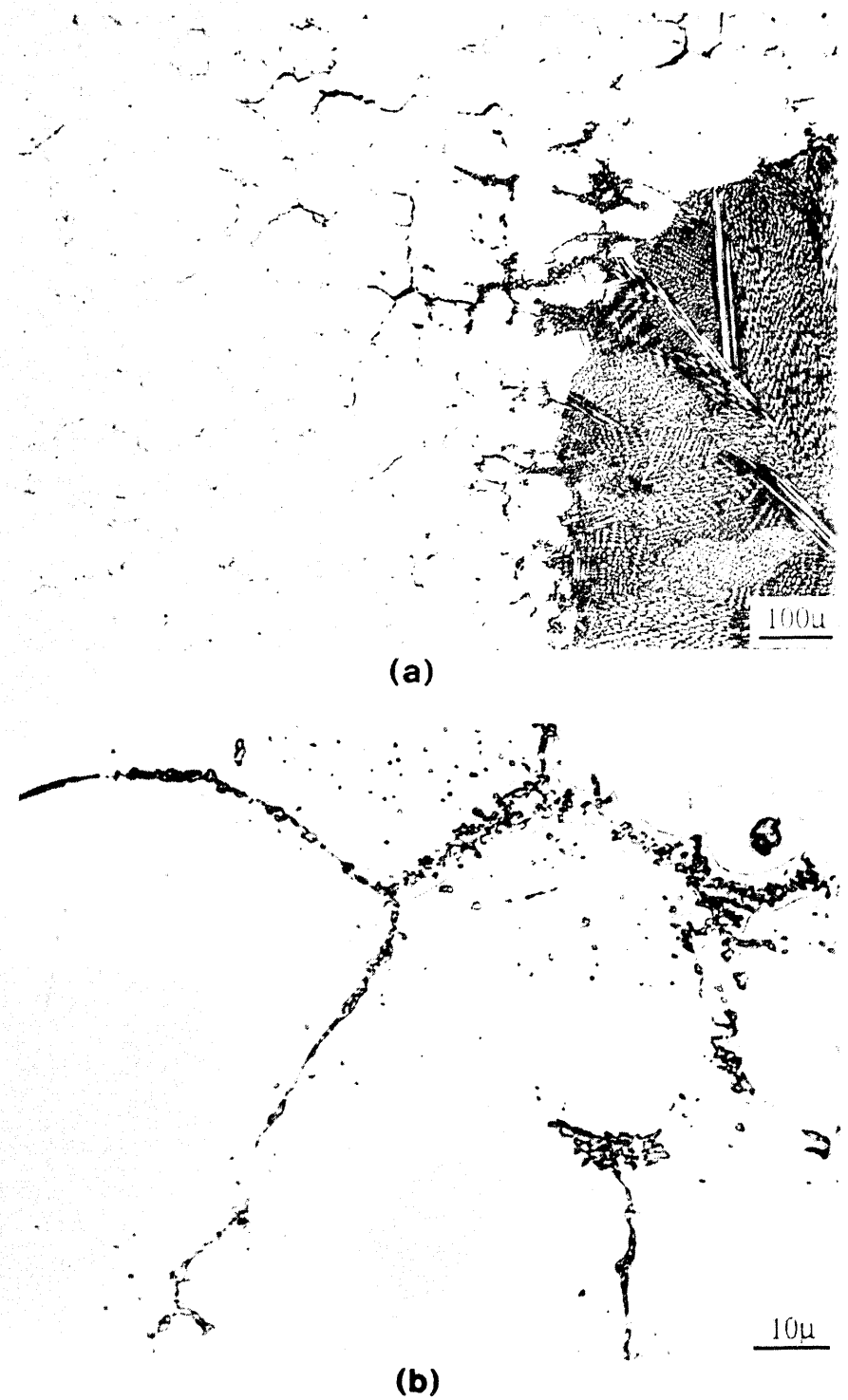

Figure 34. A Photomicrograph Shows the Type II Grain Boundary Liquation.

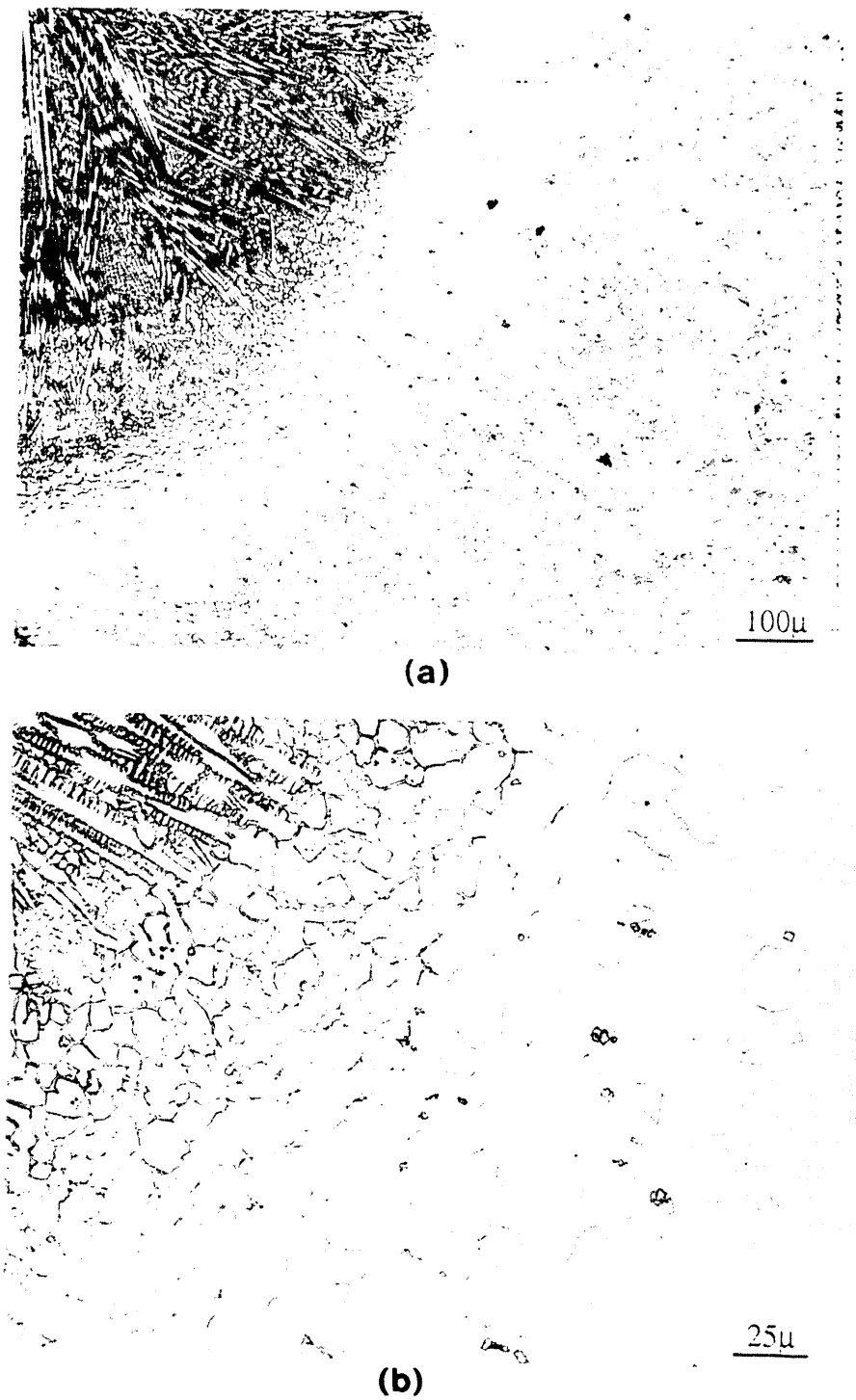

Figure 35. A Photomicrograph Shows the Type III Grain Boundary Liquation.

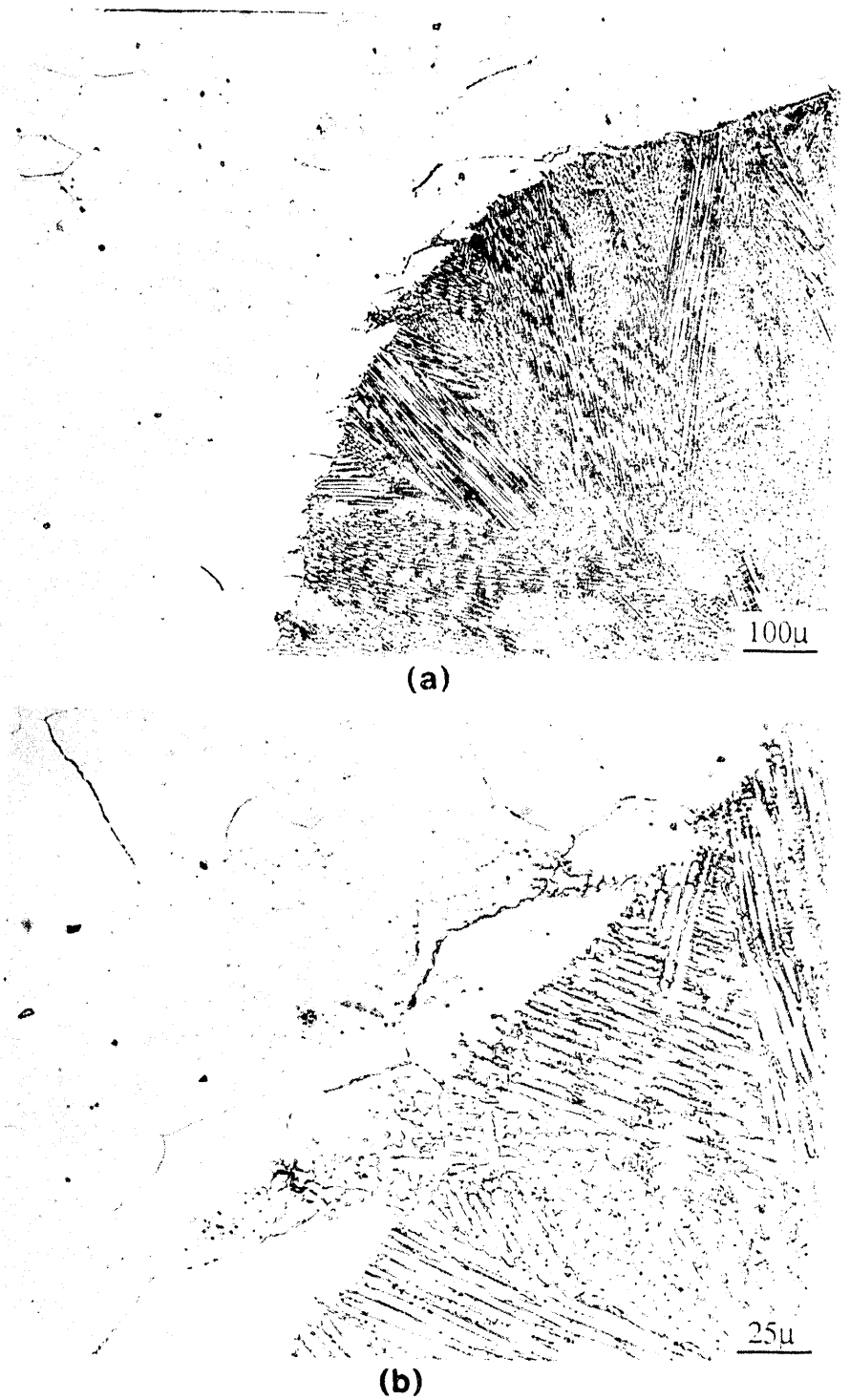

Figure 36. A Photomicrograph Shows the Type IV Grain Boundary Liquation.

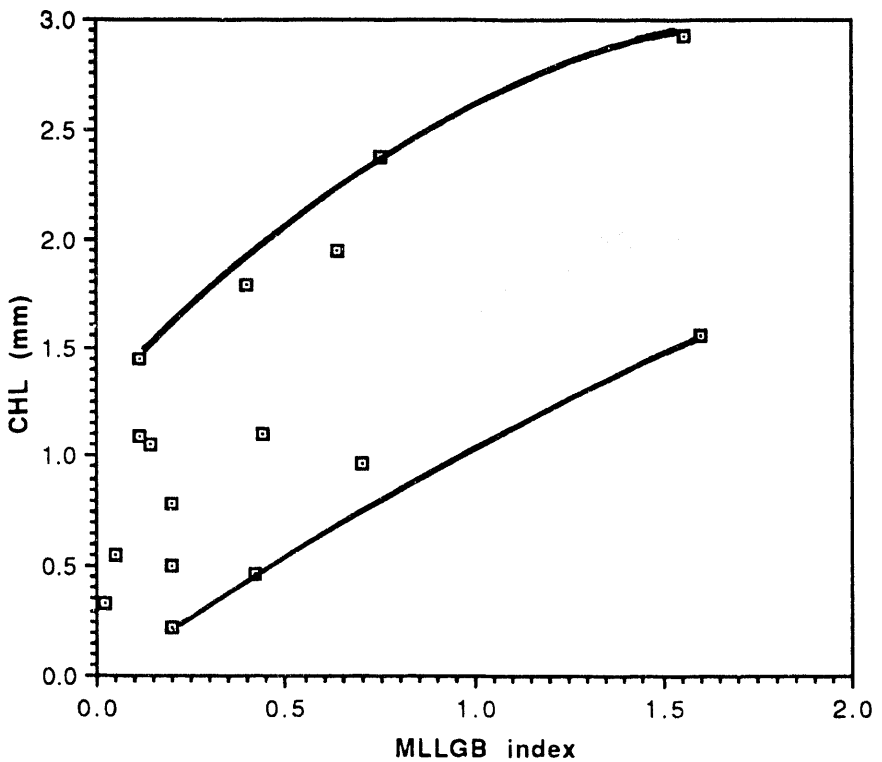

Figure 37. Relationship Between Varestraint Hot Cracking Test Parameter CHL and HAZ Grain Boundary Liquation Parameter MLLGB Index.

the coefficients, the multi-linear regression method is needed. Since only limited data is available, the coefficients cited are based on experience. The MLLGB index should be a useful criterion for semi-quantitative evaluation of HAZ liquation cracking tendency. The major advantages of this method are speed and limited metallographic investigation.

Another advantage of using spot welding techniques in the determination of HAZ liquation behavior is the enhanced study of the liquation mechanism (to reveal the liquation cracking mechanisms and assess liquation cracking tendency). Investigations of HAZ liquation grain boundary behavior of modified 316 were conducted by Lundin et al. [61]. The analysis of the liquated grain boundaries in HAZ of modified 316 can be adapted to give a general explanation although a more sophisticated theory should be evolved in order to fully define the liquated grain boundary models proposed in this study.

HAZ Softening Behavior Investigation

Microhardness Evaluations

HAZ softening behavior was evaluated using microhardness traverses across the weld fusion zone/HAZ/base metal. Six GTA welds with heat inputs of 20, 22, 28, 41, 45, and 120 kJ/in, and a GTA weld with HD556 filler were made in modified 800H tubing (Heat V988-1). Evaluations were performed for all weld heat inputs and aging conditions (as welded, aged 1, 10, 100, 1,000 hours at 700°C). HAZ softening behavior was revealed in all welds. In general, the width of "soft zone" increases with increasing heat input, and the minimum hardness in the "soft zone" reduces with increasing the aging time. The OLM observation showed that HAZ softening is

related to precipitate dissolution and grain growth in the HAZ adjacent to fusion zone during welding. Typical hardness traverses for as-welded samples with 28 and 45 kJ/in heat inputs, are shown in Figures 38 to 39. The hardness traverses of the weld made at 28 kJ/in and aged for 1, 10, 100, and 1,000 hours at 700°C are indicated in Figures 40 to 43. It is evident that the "soft zone" shown in the as-welded conditions virtually disappears after ageing for 100 hours at 700°C. Hardness recovery is a function of ageing time and temperature. However, complete recovery is impossible since the base materials are cold worked.

Knoop hardness testing was also utilized for further examination because of its enhanced resolution. The results of Knoop hardness testing are summarized in Table 6. It is evident that Knoop microhardness testing results agree with the results attained from Vickers hardness. In order to simplify designation of samples, the form of X/Y was utilized to define the samples in the table. Here, X is a number which represents weld heat input in kJ/in; Y is a number which represents aging time in hours. For instance, 28/1 is a weld with a heat input of 28 kJ/in and aged one hour at 700°C.

Heat-affected Zone Microstructural Investigations

Figures 44 and 45 show the microstructures of the GTA weld HAZs of modified 800H with two different heat inputs, 28 kJ/in and 45 kJ/in, respectively. As indicated in the figure, recrystallization and grain growth occurred in the HAZs. The width of the HAZ and the width of coarse grained zone are dependent on heat input. The higher the heat input the greater the width of the HAZ and coarse grained zone. At higher magnification particle dissolution in the coarse

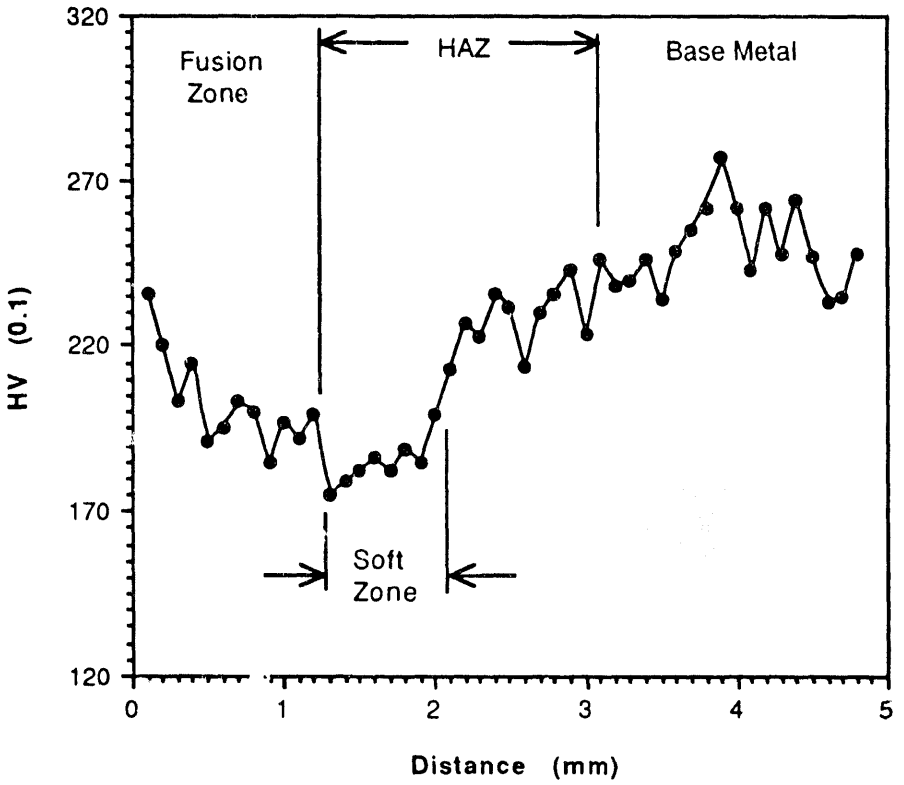

Figure 38. Microhardness Traverse Across the GTA Weld with An As-welded Condition (Heat Input 28 kJ/In).

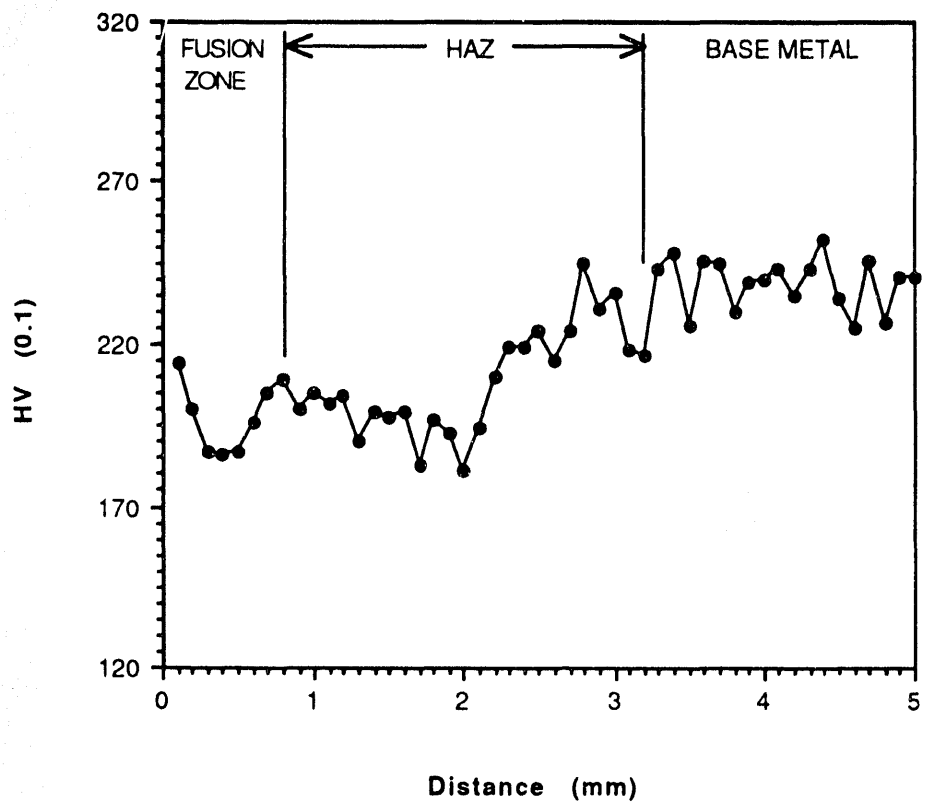

Figure 39. Microhardness Traverse Across the GTA Weld With an As-welded Condition (Heat Input 45 kJ/In).

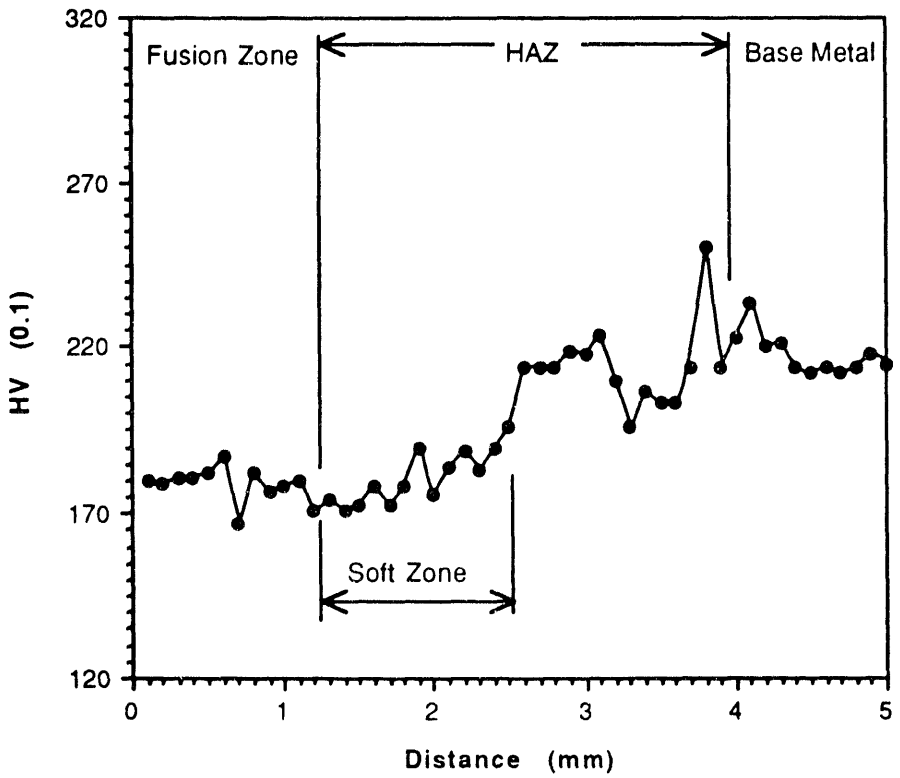

Figure 40. Microhardness Traverse Across the GTA Weld Aged for One hour at 700°C (Heat Input 28 kJ/In).

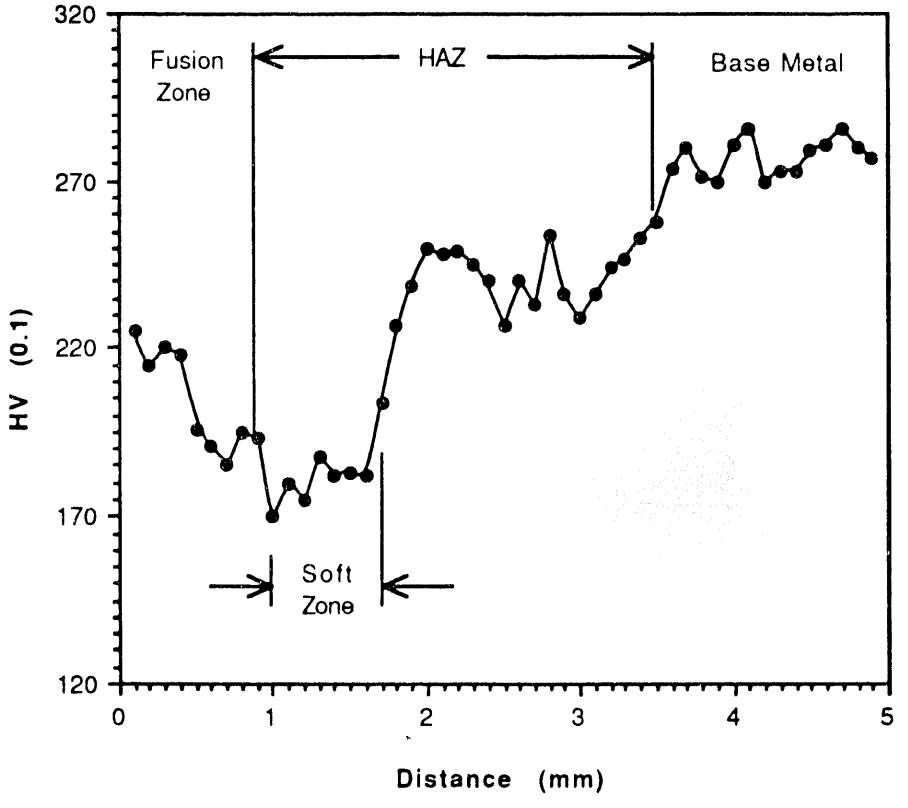

Figure 41. Microhardness Traverse Across the GTA Weld Aged for Ten hours at 700°C (Heat Input 28 kJ/In).

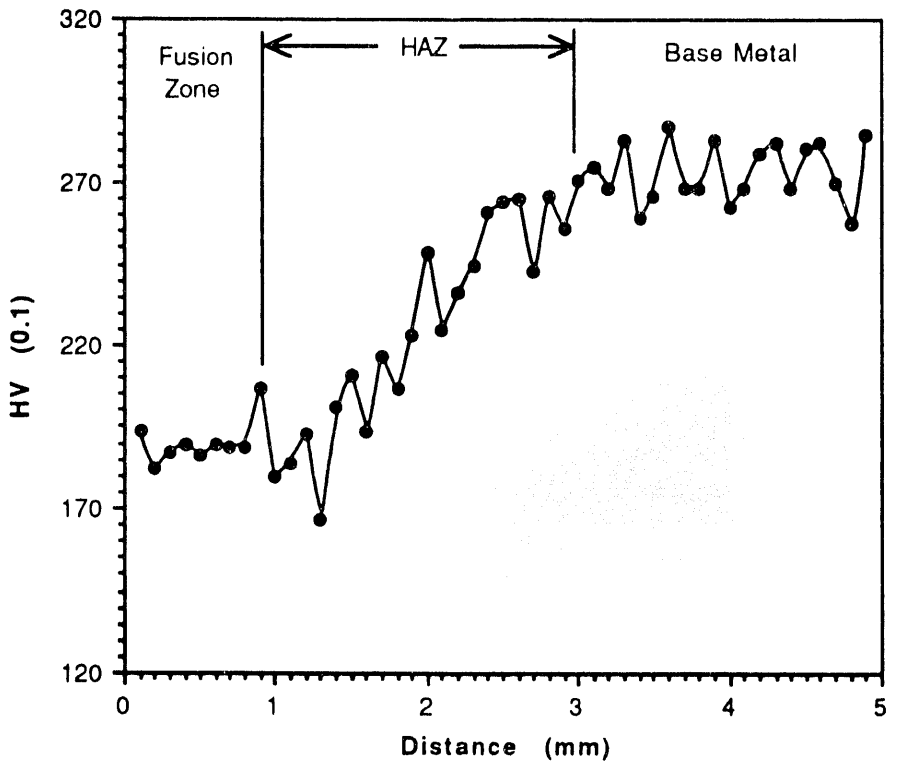

Figure 42. Microhardness Traverse Across the GTA Weld Aged for One Hundred hours at 700°C (Heat Input 28 kJ/In).

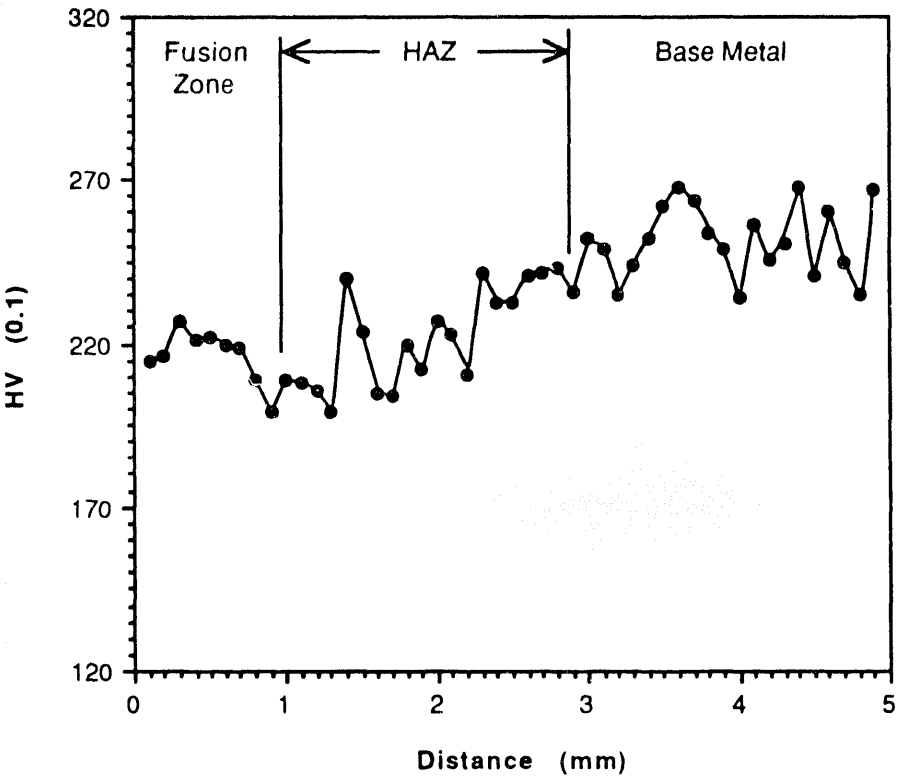

Figure 43. Microhardness Traverse Across the GTA Weld Aged for One Thousand hours at 700°C (Heat Input 28 kJ/In).

Table 6. Summary of the Knoop Hardness Measurements.

CONDITION	SAMPLE (ENERGY INPUT/TIME)	FUSION ZONE	HAZ	BASE METAL
AS-WELDED	20/0	258	226	256
	22/0	197	183	
	28/0	158	166	
	41/0	194	183	
	45/0	174	148	
	120/0	194	175	
1 HOUR AGED AT 700°C	20/1	209	188	
	22/1	221	211	
	28/1	235	202	
	41/1	219	202	
	45/1	214	192	
	120/1	169	152	
10 HOURS AGED AT 700°C	20/10	217	207	
	22/10	211	187	
	28/10	177	160	
	41/10	224	210	
	45/10	198	179	
	120/10	215	198	
100 HOURS AGED AT 700°C	20/100	242	229	
	22/100	223	207	
	28/100	220	231	
	41/100	206	206	
	45/100	232	201	
	120/100	214	209	
1,000 HOURS AGED AT 700°C	20/1,000	234	237	
	22/1,000	229	219	
	28/1,000	222	216	
	41/1,000	225	203	
	45/1,000	199	205	
	120/1,000	227	217	
CONDITION TIME/TEMPERATURE	MULTIPASS GTA AGEING TIME	FUSION ZONE	HAZ	
0 HOUR/700°C	0	228	193	
1 HOUR/700°C	1	239	209	
10 HOURS/700°C	10	230	195	
100 HOURS/700°C	100	252	208	
1,000 HOURS/700°C	1,000	299	247	

Figure 44. A General Morphology of HAZ in Heat V988-1 With a Heat Input 28 kJ/in.

Figure 45. A General Morphology of HAZ in Heat V988-1 With a Heat Input 45 kJ/in.

grained HAZ can be clearly observed (Figure 46). It is evident that more extensive precipitate dissolution occurred in the HAZs of a higher heat input weld than that of lower heat input (comparing Figures 44 to 45). It is also noticed that with long term ageing (such as 1,000 hours at 700°C) more precipitates were observed as compared to the samples in the as-welded condition (Figure 47). This result indicates that the "soft" zone can be minimized by a postweld heat treatments or at elevated temperature during service. However, the hardness dip can not be completely restored. This is due to the fact that the initial cold work structure can not be restored by ageing. However, reduction in HAZ softening by proper control the welding processes is still important to ensure good weldment mechanical properties. Figures 48 and 49 show the HAZ microstructural morphologies from the carbon replica samples. Figure 48 exhibits a region where remaining carbides and nitrides grow and are distributed intergranularly and intragranularly while Figure 49 emphasizes the dendritic type carbide morphology (growth during the weld thermal cycling).

Ageing Studies of Base Metal and HAZ's

The commercial tubing heat of modified 800H (V988-1) was employed in the conduct of the aging studies. Determination of the evolution of precipitates is beneficial to understanding the behavior of base metal under aging conditions as well as for the HAZ. Figure 50 shows a photomicrograph of the microstructure if the as-received base metal of modified 800H (a) Heat V988-1; and (b) Heat F. It is clear that the grains are slightly elongated along the rolling direction in heat V988-1. Fine particles are distributed relatively homogeneous intra- and intergranularly. As compared to heat V988-1, heat F has a

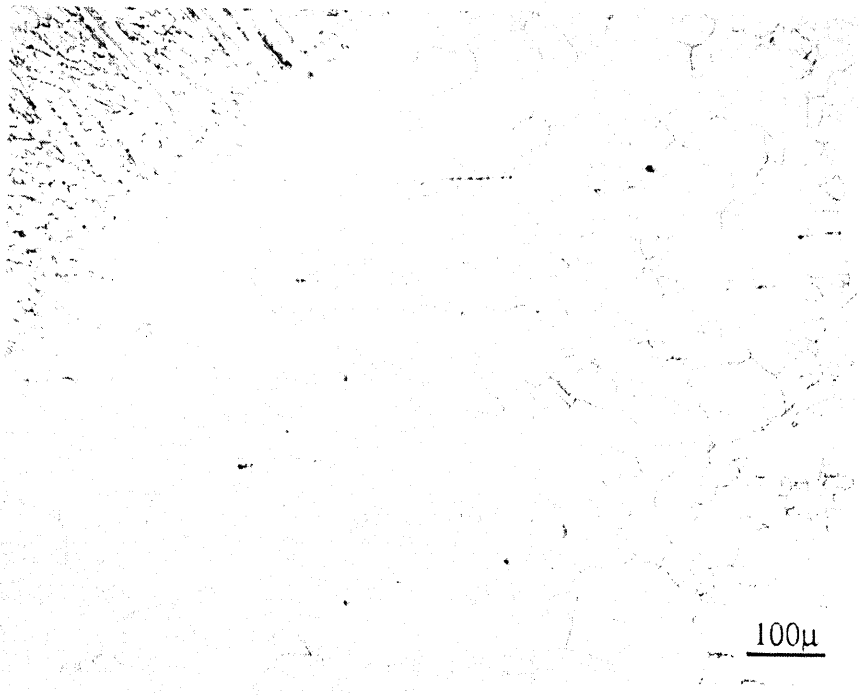

Figure 46. A Higher Magnification Morphology of the HAZ Microstructure for Heat V988-1 with a Heat Input 45 kJ/in.

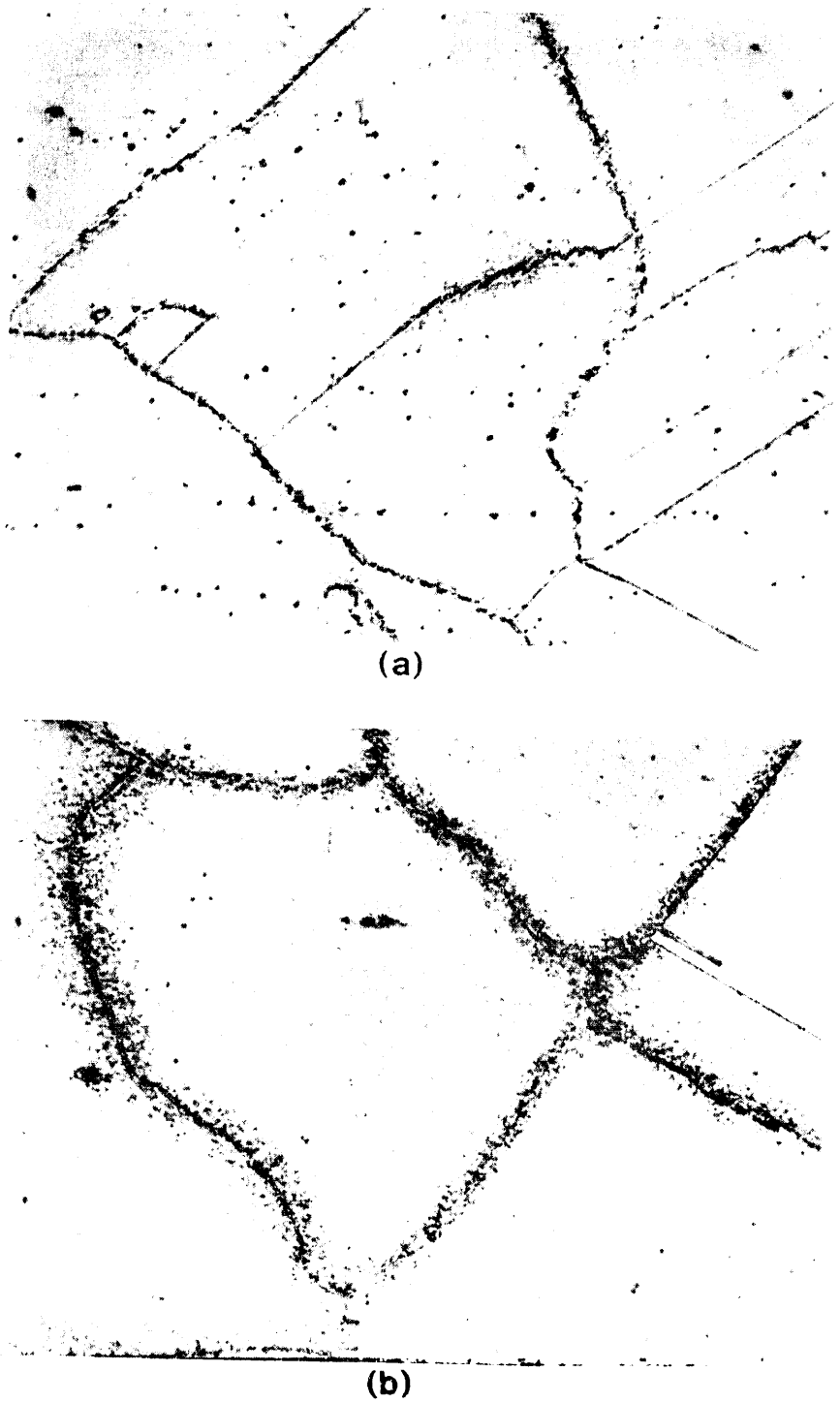

Figure 47. Microstructure of the HAZ in Heat V988-1 (a) as-welded condition; (b) Aged for one thousand Hours at 700°C.

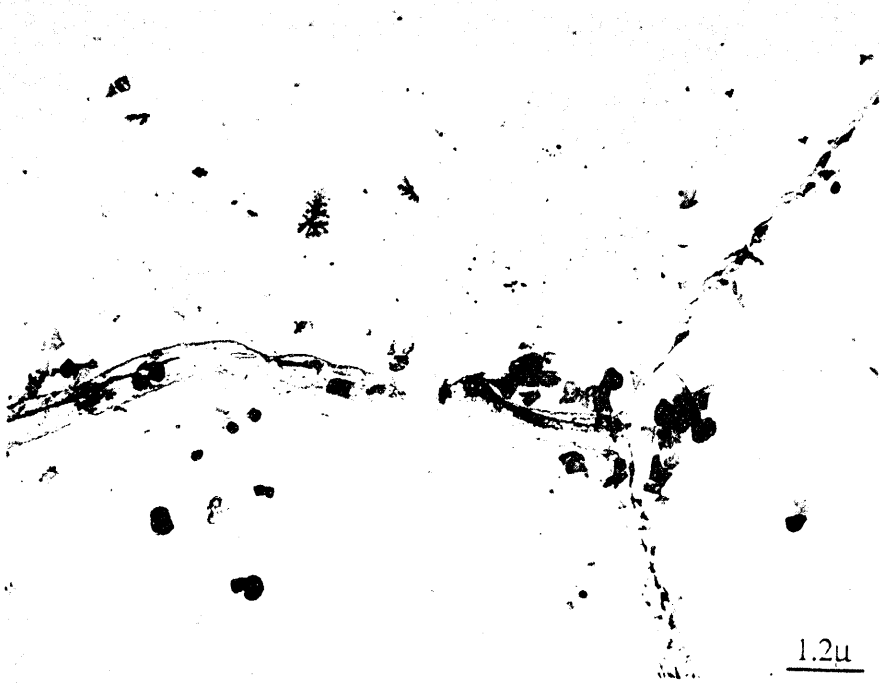

Figure 48. Carbides Distribution and Morphologies in the HAZ With an As-welded Condition.

Figure 49. Carbides Distribution and Morphologies in the HAZ With an As-welded Condition.

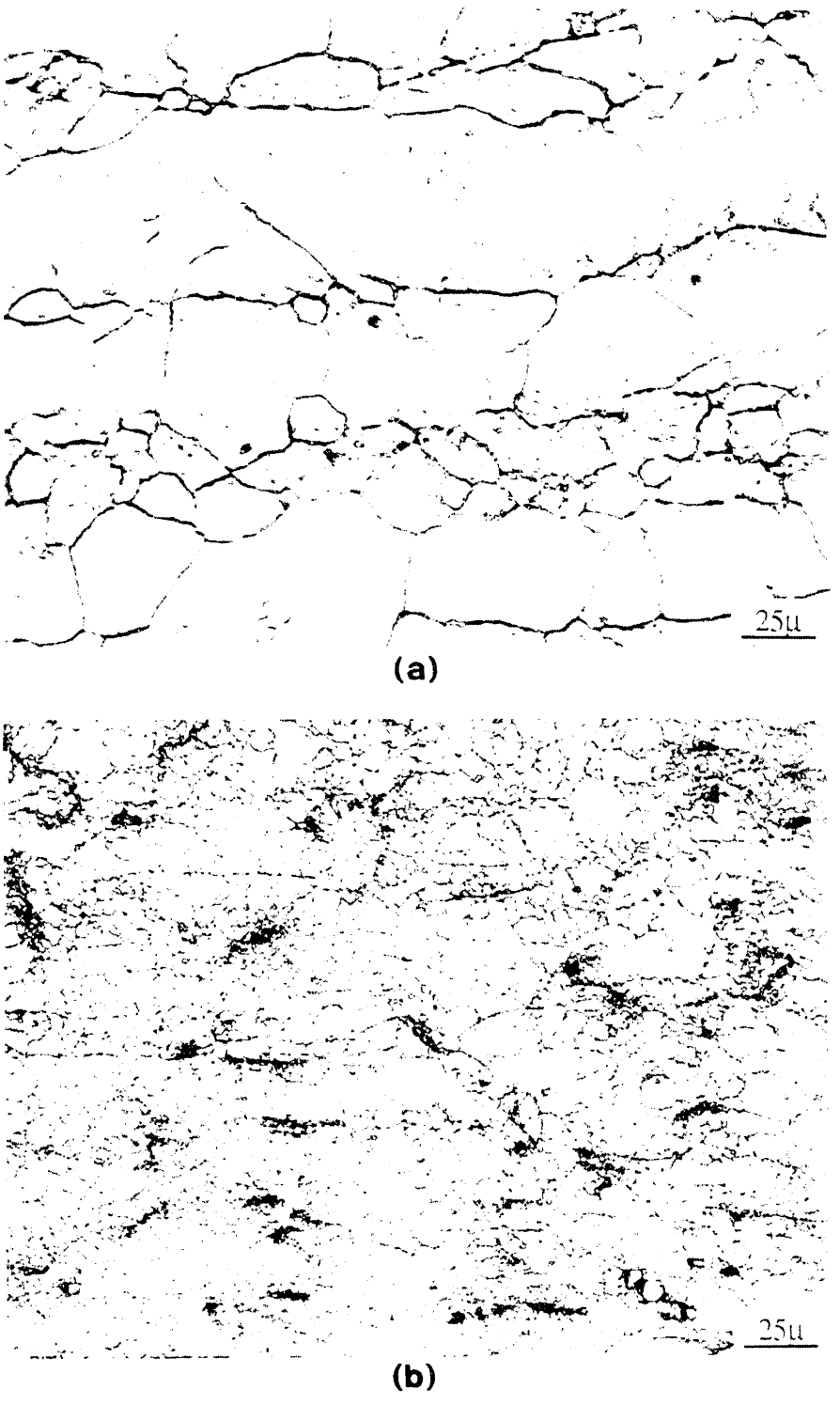

Figure 50. Microstructure of the Base Metal With an As-Received Condition in Modified 800H. (a) Heat V988-1; and (b) Heat F.

much smaller grain size. A carbon replica sample from the as-received base metal (Heat V988-1) is shown in Figure 51. Basically, two different particle shapes exist. The results from electron diffraction and EDS analysis indicate that most of the small round particles are Ti or Nb rich MC type carbides while the most of the large, irregularly shaped particles along the grain boundaries are $M_{23}C_6$ type carbides. Figure 52 shows the base metal microstructure after 100 hours ageing at 700°C. An evident increase of the amount of particles and the size of the particles, especially, along the grain boundaries can be identified in this sample as contrasted to the base metal in the as-received condition. Figure 53 shows the microstructures of samples with ageing times of 1,000 hours at 700°C. It is clear that no significant difference is observed between the sample with 100 hours and 1,000 hours ageing. Figure 54 shows the microstructures of the base metal for as-received and aged 1,000 hours at 700°C. More precipitates exist not only along the grain boundaries but also at the annealing twin boundaries in the aged sample as compared to the sample in the as received condition. Again, most particles in both samples are identified as MC and $M_{23}C_6$ type carbides.

Evaluations of the Secondary Phases in the Base Metal and HAZ

As mentioned above, the HAZ liquation cracking tendency and HAZ softening behavior are significantly related to the secondary phase dissolution and re-precipitation processes. Therefore, the investigation of the precipitate distribution and dissolution/reprecipitation behavior in HAZ becomes significant for precisely illustrating both the HAZ liquation cracking propensity and HAZ softening behavior.

Figure 51. Carbides Distribution and Morphologies in the Base Metal With an As-received Condition of Heat V988-1.

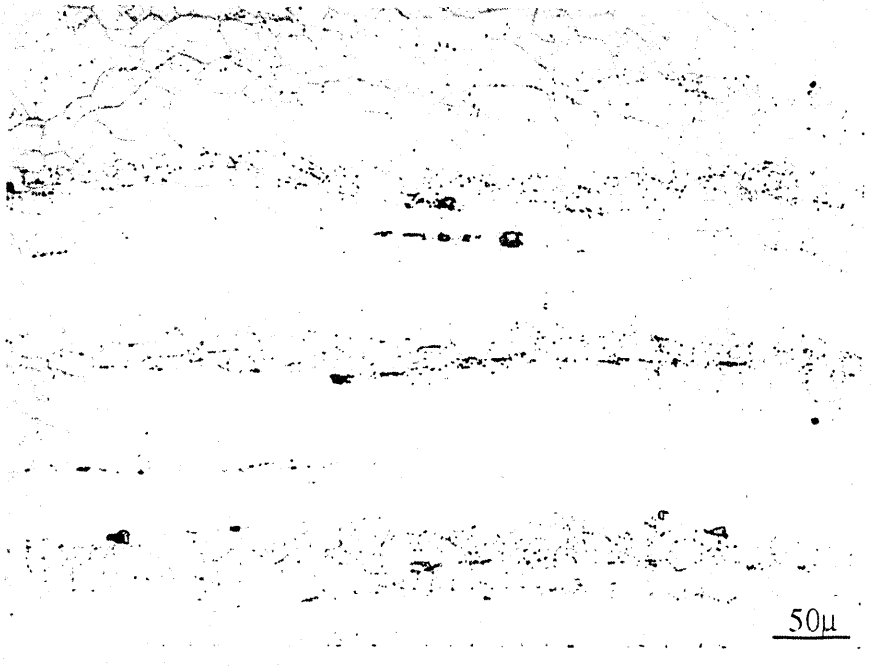

Figure 52. Microstructure of Base Metal in Heat V988-1 Aged One Hundred Hours at 700°C.

Figure 53. Microstructure of Base Metal in Heat V988-1 Aged One Thousand Hours at 700°C.

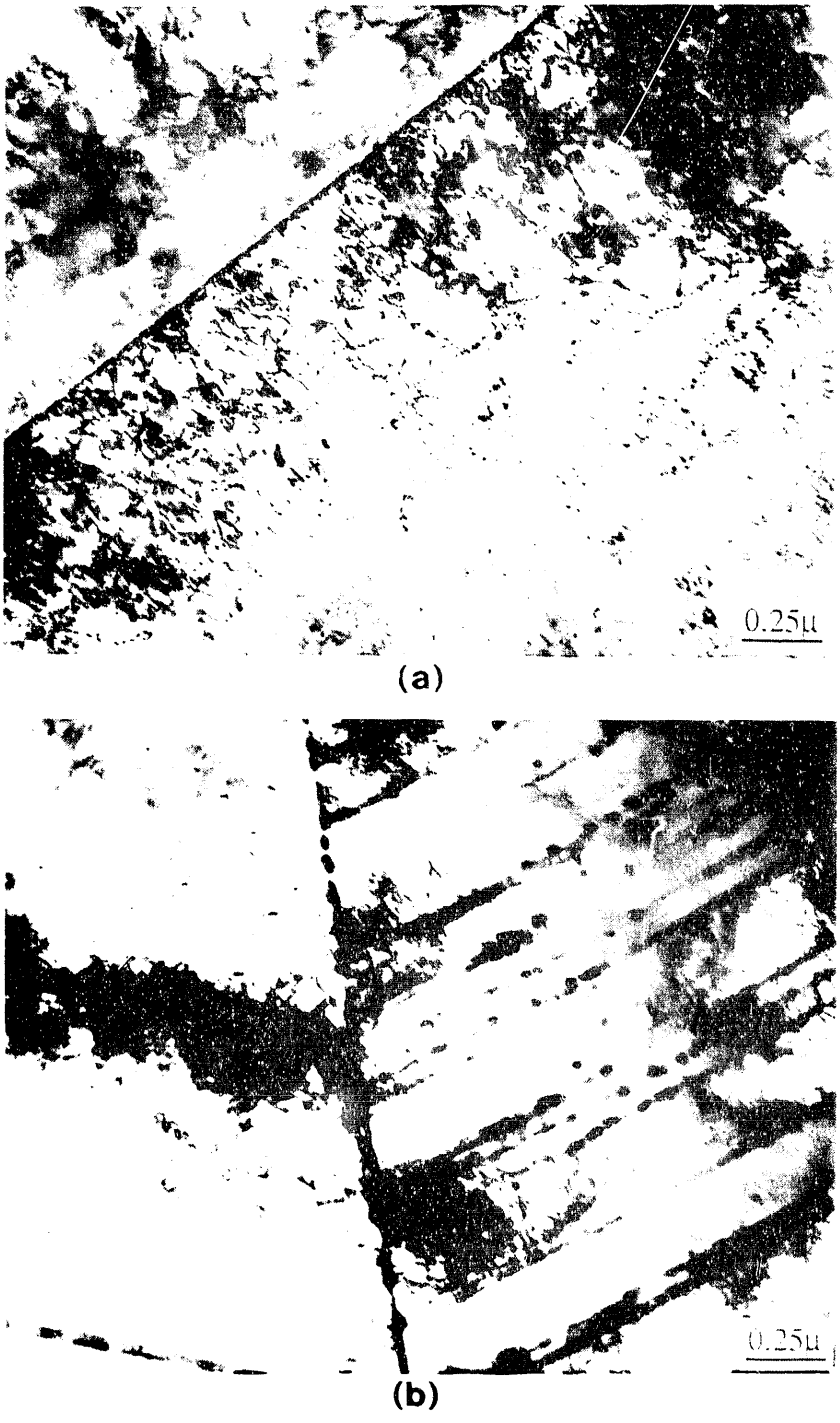

Figure 54. TEM Microstructural Morphologies of the Base Metal in Heat V988-1. (a) As-received Condition; (b) Aged for One Thousand Hours at 700°C.

Metallographic Examinations and EDS Analysis

An electrolytic precipitate extraction technique was employed to obtain the precipitates from the base metal and the simulated HAZs with different peak temperatures. The electrolytic precipitate extraction results for the base metal and the simulated HAZs are summarized in Table 7. Figure 55 shows the relationship between the weight percent of precipitate and the peak temperature. It is evident that a significant dissolution of the precipitates at and above a peak temperature of 1300°C has taken place. Therefore, particle dissolution is one major reason and is responsible for the HAZ softening and subsequent precipitate redistribution due to reprecipitation (preferentially, along the grain boundaries in the HAZ of modified 800H). These processes can significantly enhances the HAZ liquation cracking tendency.

Table 7. Summary of the Electrolytic Extraction Results

Simulating Condition Peak Temperature	Percentage of Precipitate (wt.%)
base metal (25°C)	0.24
1001°C	0.17
1090°C	0.16
1145°C	0.14
1200°C	0.28
1260°C	0.25
1290°C	0.33
1320°C	0.11

The shape of the curve reflects the dissolution and re-precipitation behavior with different peak temperatures and

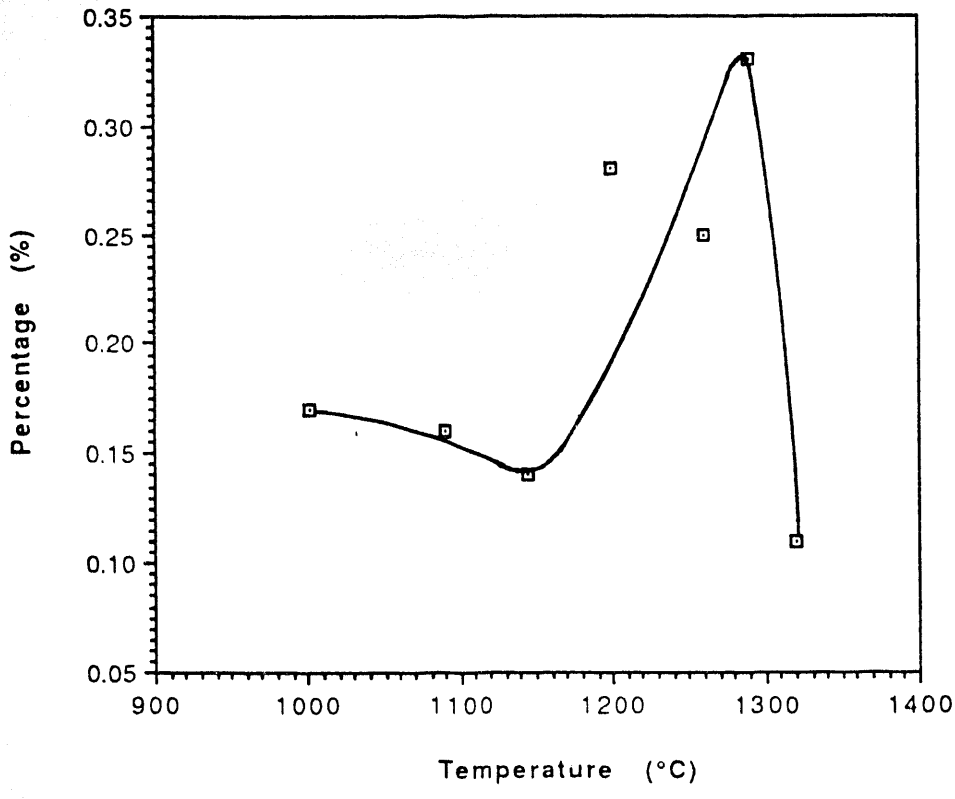

Figure 55. Percentage of Electrolytical Extracted Particles as a Function of the Peak Temperature.

Figure 56. SEM Morphology Showing the Typical Particles Existed in Base Metal of Modified 800H (Heat V988-1).

therefore, various distances from the fusion boundary. However, more work must be accomplished in order to precisely explain this behavior. Nevertheless, it is clear that significant particle dissolution occurs at the peak temperatures above 1290°C. This is the region adjacent to the fusion zone which exhibit the maximum decrease in hardness.

Extracted particles were examined in the SEM and characterized by EDS. Figure 56 shows two typical particles (A and B) which frequently appeared in the samples. The EDS spectrum for particles A and B are shown in Figures 57 and 58, respectively. Based upon the morphology of the particle, data analysis, and the reference spectrums in the literature [46], it is concluded that particle A is an MC type and particle B is an $M_{23}C_6$ type carbide.

CONCLUSIONS

1. The results of Varestraint hot crack testing indicate that the base metal liquation cracking tendency of the small heats of modified 800H with controlled HAZ grain sizes is minimal.

2. Metallographic examination suggests that a smaller HAZ grain size may significantly enhance base metal HAZ liquation cracking resistance.

3. Ti and/or Nb rich carbides in the HAZ enhance the liquation cracking tendency due to dissolution and subsequent redistribution of Ti and Nb along the grain boundaries.

4. EDS evaluation of the hot cracked regions reveals that S and P segregation along the grain boundaries is major factor affecting HAZ liquation cracking.

5. "Soft" zones were found in the HAZs of all welds. Hardness decreases in the softened regions occurred during thermal ageing.

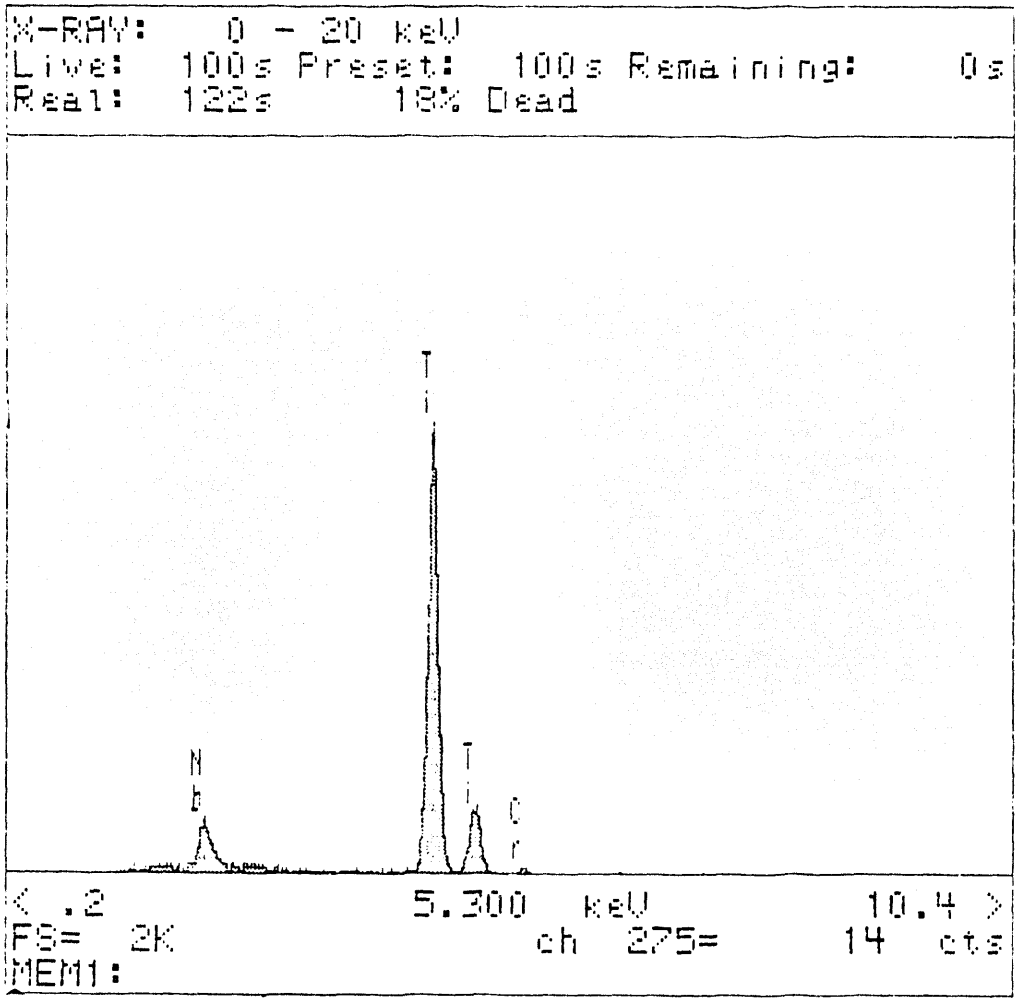

Figure 57. EDS Spectrum of the Particle A in Figure 56.

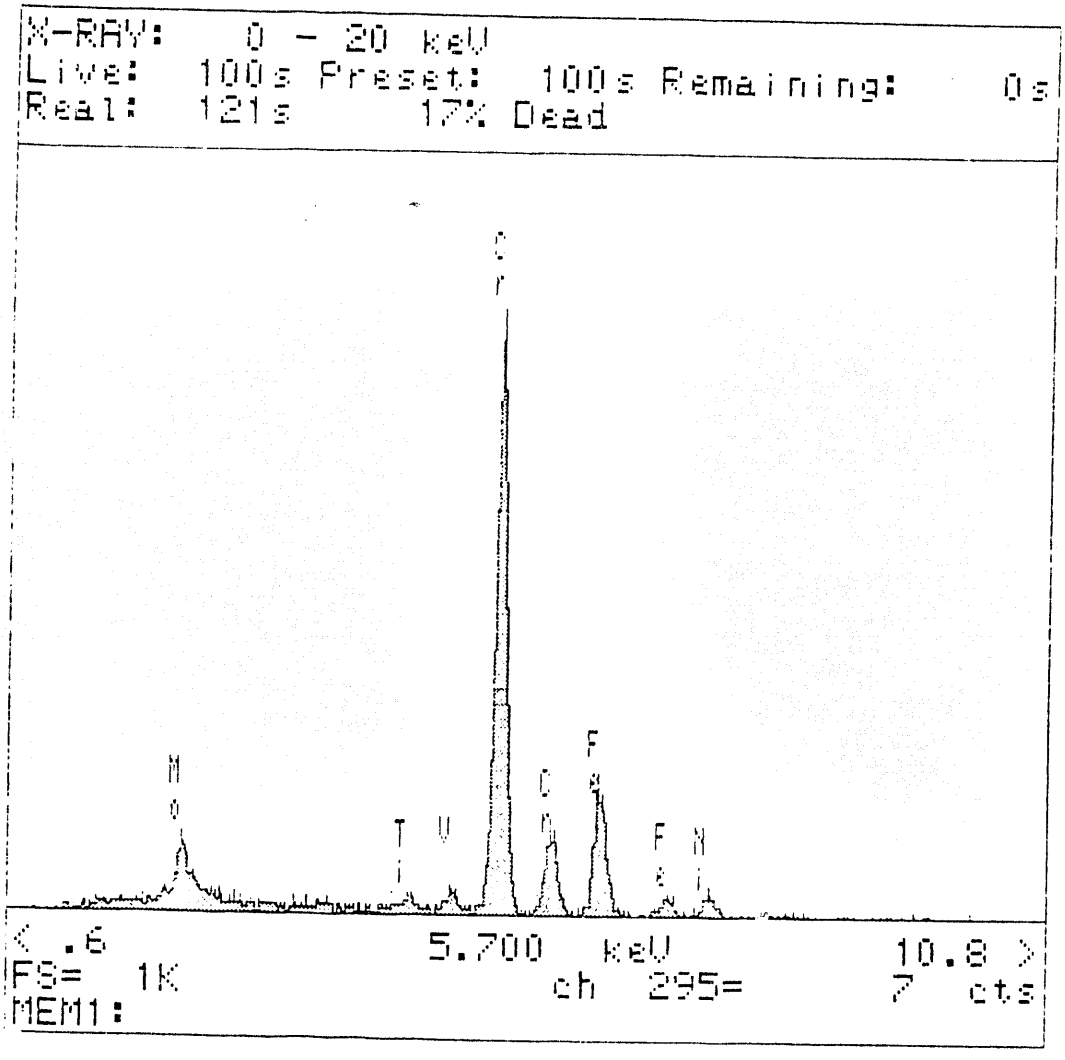

Figure 58. EDS Spectrum of the Particle B in Figure 56.

6. Clear evidence of precipitate changes were observed in the HAZ of the modified 800H materials. The precipitates dissolution during welding is responsible for the HAZ softening and precipitate dissolution and redistribution of dissolved elements in the HAZ adjacent to fusion zone enhances HAZ liquation cracking tendency.

7. Metallographic examinations on the aged samples of the modified 800H materials indicates that the amount of precipitate increases with an increase in ageing time at 700°C. Precipitate growth during ageing, preferentially along the grain boundaries was also observed in the aged base metal samples. After 100 hours at 700°C, further precipitation is minimized.

8. MC type (commonly Ti rich or Nb rich) carbides, nitrides and carbonitrides and $M_{23}C_6$ type carbides are the major secondary phases in modified 800H. However, the MC type carbides, nitrides and carbonitrides are relatively stable during ageing as contrasted to the $M_{23}C_6$ type.

REFERENCES

1. Swindeman, R.W., and Maziasz, "Evaluation of Advanced Austenitic Alloys Relative to Alloy Design Criteria for Steam Service - Part 2 - 20 to 30 % Chromium Alloys," Technical Report, ORNL-6629/P2, June 1991.

2. Lundin, C.D., Qiao, C.Y.P., Kikuchi, Y., Shi, C., and Gill T.P.S., "Investigation of Joining Techniques for Advanced Alloys," DOE Report, ORNL/Sub/88-07585/02, May 1991.

3. Pumphrey, W.I., and Jennings, P.H., "A Consideration of the Nature of Brittleness at Temperature above the Solidus in Casting and Welds in Aluminum Alloys," Journal of Institute of Metals, 75, pp. 235-256, 1948.

4. Pellini, W.S., "Strain Theory of Hot Tearing," The Foundry, 80(11), pp. 125-133, 1952.

5. Puzak, P.P., Apblett, W.R, and Pellini, W.S., "Hot Cracking of Stainless Steel Weldments," Welding Journal, 35(1), pp. 9s-17s, 1956.

6. Borland, J.C., "Generalized Theory of Super-Solidus Cracking in Welds (and Casting)," British Welding Journal, 7(8), pp. 508-512, 1960.

7. Borland, J.C., "Suggested Explanation of Hot Cracking in Mild and Low Alloy Steel Welds," British Welding Journal, 8(11), pp. 526-540, 1060.

8. Smith, C.S., "Grains, Phases, and Interface: An Interpretation of Microstructure," Transaction of American Institute of Mining and Metallurgical Engineering, pp. 15-52, Vol., 1948-1949.

9. Kammer, P.A., Masubuchi, K., and Monroe, R.E., "Cracking in High Strength Steel Weldments - A Critical Review," Defense Metals Information Center Report, Battle Memorial Institute, Columbus 1, Ohio.

10. Lundin, C.D., Qiao, C.Y.P., and Lee, C.H., "Weldability and Hot Ductility Behavior of Nuclear Grade Austenitic Stainless Steels," Welding Group Research Report on Group Sponsored Study, The University of Tennessee, December, 1988.

11. Lundin, C.D., and Qiao, C.Y.P., "Weldability of Nuclear Grade Stainless Steels," Proceedings of the International Conference on New Advances in Welding and Allied Processes, Vol. 2, pp. 3-10, May 1991.

12. Brooks, J.A., "Effect of Alloy Modifications on HAZ Cracking of A-286 Stainless Steel," Welding Journal, pp. 517s-523s, November 1974.

13. Hull, F.C., "Effects of Alloying Additions on Hot Cracking of Austenitic Chromium-Nickel Stainless Steels," Proceedings, American Society of Testing Materials Vol. 60, pp. 667-690, 1960.

14. Hull, F.C., "A High-Strength Weldable Stainless Steel for Elevated Temperature Service," pp. 88-89, STP 369, 1965.

15. Thielsch, H., "Alloying Elements in Chromium-Nickel Stainless Steels," Welding Journal, pp. 361s-404s, August 1950.

16. Donati, J.R., Spiteri, P., and Zacharie, G., "Evaluation of Tendency toward Hot Cracking in the Welding Heat-Affected Zone of Austenitic 18-10 Stainless Steels - Discussion of A Cracking Criterion," Memoiries Scientifiques la Revue de Metallurgie, pp. 905-515, December 1974.

17. McKeown D.,"Review on Welding Alloy 800," Proceedings of the Petten International Conference on Alloy 800, pp. 371-339, North-Holland Publishing Company, Amsterdam - New York - Oxford, 1978.

18. Pease, G.R., "The Practical Welding Metallurgy of Nickel and High-Nickel Alloys," Welding Journal, pp. 330s-334s, July 1957.

19. Wolstenholme, D.A., "Weld Crater Cracking in Incoloy 800," Welding and Metals Fabrication, pp. 433-439, 1973.

20. Arata, Y., Matsuda, F., and Katayama, S., "Solidification Crack Susceptibility in Weld Metals of Fully Austenitic Stainless Steels," Transaction of JWRI, pp. 150-116, Vol. 5, No 2, 1976.

21. Rundell, G.R., "Effect of Minor Elements on the Weldability of a Nickel-base Heat-resistant Alloy," Conference Proceedings of of a WRC Symposium on Effects of Minor Elements on the Weldability of High Nickel Alloys, pp. 36-46, July 1969.

22. Kihlgren, T.E., and Lacy, C.E., "The Control of Weld Hot Cracking in Nickel-Chromium-Iron Alloy," Welding Journal, pp. 769s-775s, November 1946.

23. Polgary, S., "The influence of Silicon Content on Cracking in Austenitic Stainless Steel Weld Metal with Particular Reference to 18Cr-8Ni Steel," Svetsaren, pp. 8-13, Vol. 6, 1970.

24. Morishige, N., Kuribayashi, M., and Okabashi, H., IHI Engineering Review, pp. 1-6, 1982.

25. Homeycombe, J., and Gooch, T.G., "Microcracking in Fully Austenitic Stainless Steel Weld Metal," The Welding Institute Report, M39/3/69, February 1970.

26. Savage, W.F., Nippes, E.F., and Miller, T.W., "Microsegregation in Partially Melted Regions of 70Cu-30Ni Weldments," Welding Journal, pp. 181s-187s, July 1976.

27. Matsuda, F., Nakagawa, H., and Katayama, S., Compilation of the Reports Published on "Solidification Crack Susceptibility and Its Improvement in Fully Austenitic Stainless Steel Weld Metals," Welding Research Institute of Osaka University, Osaka, Japan, June 1984.

28. Lundin, C.D., and Qiao, C.Y.P., "Improvement on Weldability of Modified 316 Stainless Steel," Non-published Research Work, The University of Tennessee, Knoxville 1992.

29. Canonico, D.A., Savage, W.F., Werner, W.J., And Goodwin, G.M., "Effects of Minor Additions on Weldability of Incoloy 800,"Conference Proceedings of of a WRC Symposium on Effects of Minor Elements on the Weldability of High Nickel Alloys, pp. 68-92, July 1969.

30. Miura, M., "Weldability of Austenitic Stainless Steel Tubes," Translation of Journal of Sumitomo Metal, Vol. 34, No. 1, Sumitomo Metal Industries, Ltd., Japan, 1981.

31. Sadowshi, E.P., "Modification of Cast 25Cr-20Ni for Improved Crack Resistance," Welding Journal, pp.49s-58s, February 1974.

32. Yoshikuni, N., and Shinozaki, K., "Hot Cracking in Ni-base Superalloys," 9th Comm. of Special Mat. Welding Research, Osaka University, Japan, May 1985.

33. Lippold, J,C., "An Investigation of Weld Cracking in Alloy 800" Welding Journal, pp. 91s-103s, March, 1984.

34. Cullen, T.M., and Freeman, J.W., "Metallurgical Factors influencing Hot Ductility of Austenitic Steel Piping at Weld Heat-Affected Zone Temperatures," Journal of Engineering for Power (Transaction of the ASME), pp. 151-164, April 1963.

35. Rundell, G.R., and Rauderaugh, R.J., "The Effect of Phosphorus on the Elevated Temperature Strength and Weldability of Some Low-Carbon Austenitic Stainless Steels," Presented at Forty-Second Annual Convention of the ASM, October 1960.

36. Lundin, C.D., Qiao, C.Y.P., Goodwin, G.M., and Swindeman, R.W., "HAZ Liquation Cracking Behavior in Newly Developed Lean 316 Stainless Steels," Proceedings of the Conference on Fossil Energy Materials, pp. 155-163, May 1990.

37. Lundin, C.D., Lee, C.H., Menon, R., and Osorio, V., "Weldability Evaluations of Modified 316 and 347 Austenitic Stainless Steel: Part I-Preliminary Results," Welding Journal, pp. 35s-46s, February 1988.

38. Lundin, C.D., Qiao, C.Y.P., and Shi. C., "Investigation of the Weldability of Modified 800H Alloys," The Proceedings for fifth Fossil Energy Materials Conference, May 1992.

39. Honeycombe, J., and Gooch, T.G., "Metallurgy Effects of Microcracks on Mechanical Properties of Austenitic Stainless Steel Weld-Metals," Metal Construction and British Welding Journal, pp. 140-147, April 1973.

40. Owczarski, W.A., "Some Minor Element Effects on Weldability of Heat Resistant Nickel-base Superalloys," Conference Proceedings of of a WRC Symposium on Effects of Minor Elements on the Weldability of High Nickel Alloys, pp. 6-23, July 1969.

41. Valdez, P.L., "Effect of Composition and Thermal Treatments on the Weldability of Nickel-Base 718 Alloy," Conference Proceedings of of a WRC Symposium on Effects of Minor Elements on the Weldability of High Nickel Alloys, pp. 93-147, July 1969.

42. Apblett, W.R., and Pellini, W.S., "Factors Which Influence Weld Hot Cracking," Welding Journal, pp. 83s-94s, February 1954.

43. Ohmori, Y., and Maehara, Y., "Precipitation of NbC and Hot Ductility of Austenitic Stainless Steels," Transactions of the Japan Institute of Metals, Vol. 25, No. 3, pp. 160-167, 1984.

44. Ogawa, K., Miura, M., and Minami, T., "Carbide Precipitation and Corrosion Resistance in HAZ of 15Cr-75Ni Alloy," IIW Doc. IX-1411-86, July 1986.

45. Savage, W.F., and Krantz, B.M., "An Investigation of Hot Cracking in Hastelloy X," Welding Journal, pp. 13s-25s, January 1966.

46. Marshall, P., Austenitic Stainless Steels - Microstructure and Mechanical Properties, Elsevier Applied Science Publishers LTD, London and New York, 1984.

47. Thompson, R.G., Cassimus, J.J., Mayo, D.E., and Dobbs, J.R., "The Relationship Between Grain Size and Microfissuring in Alloy 718," Welding Journal, pp. 91s-96s, April 1985.

48. Ogawa, T., Tsunetomi, E., "Hot Cracking Susceptibility of Austenitic Stainless Steels," Welding Journal, pp. 82s-93s, March 1982.

49. Borland, J.C., and Younger, R.N., "Some Aspects of Cracking in Welded Cr-Ni Austenitic Steels," British Welding Journal, pp. 22-59, July 1960.

50. Kujanpaa, V.P., David, S.A., and White, C.L., "Formation of Hot Cracks in Austenitic Stainless Steels - Solidification Cracking," Welding Journal, pp. 203-212, August 1986.

51. Matsuda, F., Nakagawa, H., and Katayama, S., "Effect of Alloying Elements on Solidification Crack Resistance of Austenitic Stainless Steel Weld Metals," IIW Doc. IX 1315.84, 1984.

52. Cieslak, J., and Savage, W.F., "Weldability and Solidification Phenomena of Cast Stainless Steel" Welding Journal, pp. 136s-146s, May 1980.

53. Baeslack III, W.A., Lata, W.P., and West, S.L., "A Study of Heat-Affected Zone and Weld Metal Liquation Cracking in Alloy 903," pp. 77s-87s, April 1988.

54. McCoy, H.E., and King, J.F., "Mechanical Properties of Inconel 617 and 618," ORNL/TM-9337, February 1985.

55. Swindeman, R.W., Goodwin, G.M., King, J.F., Lundin, C.D., and Qiao, C.Y.P., "Evaluation of Filler Metals for High-Strength Lean Stainless Steels," Proceedings of Third International conference on Improved Coal Fired Power Plants (ICPP), April 1991.

56. Savage, W.F., and Lundin, C.D., "The Varestraint Test," Welding Journal, pp.433s-442s, October 1965.

57. Savage, W.F., and Lundin, C.D., "Application of the Varestraint Technique to Study of Weldability," Welding Journal, pp. 497s-530s, November 1966.

58. Lundin, C.D., Qiao, C.Y.P., and Lee, C.H., and Goodwin, G.M., "Evaluation of Hot Cracking Susceptibility of Nuclear Grade Austenitic Stainless Steels by Four Hot Cracking Test Methods," Conference Proceedings on Recent Trends in Welding Science and Technology, pp. 699-705, May 1989.

59. Lundin, C.D., Lingenfelter, A.C., Grotke, G.E., Lessmann, G.G., and Matthews, S.J., "The Varestraint Test," WRC, Bulletin 280, pp. 1-19, August 1982.

60. Pepe, J.J., and Savage, W.F., "Effects of Constitutional Liquation in 18Ni Maraging Steel Weldments," Welding Journal, pp. 411s-420s, September 1967.

61. Lundin, C.D., Qiao, C.Y.P. and Swindeman, R.W., "Microstructural Investigation of the Heat-Affected Zones in Newly Developed Advanced Austenitic Stainless Steels, Will be published in Microstructural Science, Vol. 19, International Metallographic Society.

62. Ogawa, T., Suzuki, K., and Zaizen, T., "The Weldability of Nitrogen-containing Austenitic Stainless Steel: Part II - Porosity, Cracking and Creep Properties," Welding Journal, pp. 213s-223s, July 1984.

63. Sumitomo Metal Industries, Ltd Report, "Characteristics of a New Steel Tube (HR3C) with High Elevated Temperature Strength and High Corrosion Resistance for Boiler," December 1987.

END

DATE FILMED

2/2/93